DOCTORAL THESIS

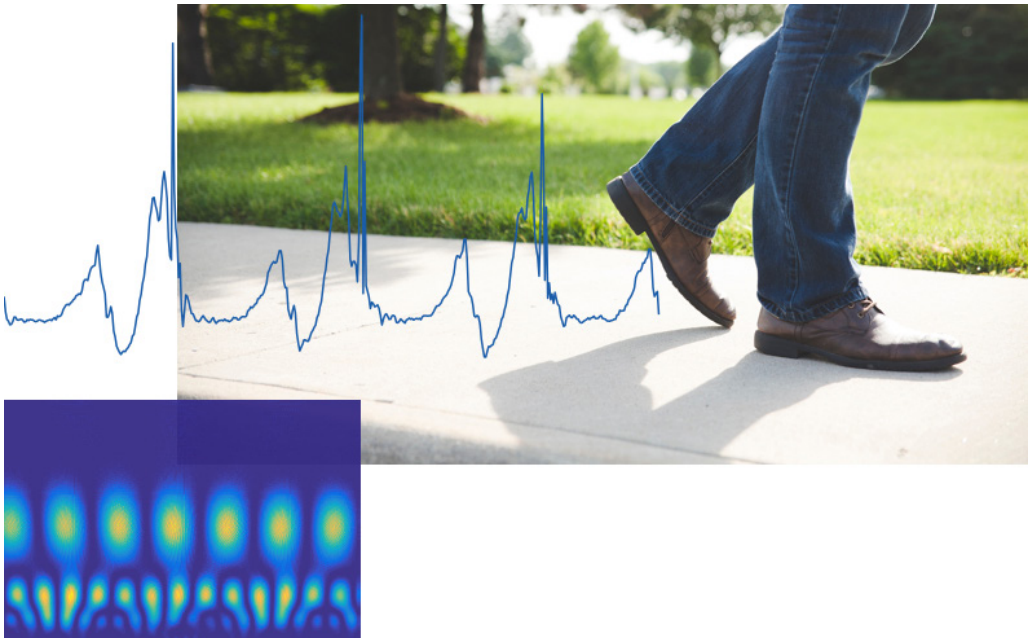

Gait Event Detection in the Real World

Siddhartha Khandelwal

Halmstad University | School of Information Technology
Doctoral Thesis | Halmstad University Dissertations no. 42

Gait Event Detection in the Real World

Siddhartha Khandelwal

Supervisors:
Nicholas Wickström
Thorsteinn Rögnvaldsson

DOCTORAL THESIS | Halmstad University Dissertations no. 42

Gait Event Detection in the Real World

Halmstad University Dissertations no. 42
ISBN 978-91-87045-86-8 (printed)
ISBN 978-91-87045-87-5 (pdf)
Publisher: Halmstad University Press, 2018 | www.hh.se/hup
Printer: Media-Tryck, Lund

Abstract

Healthy gait requires a balance between various neuro-physiological systems and is considered an important indicator of a subject's physical and cognitive health status. As such, health-related applications would immensely benefit by performing long-term or continuous monitoring of subjects' gait in their natural environment and everyday lives. In contrast to stationary sensors such as motion capture systems and force plates, inertial sensors provide a good alternative for such gait analysis applications as they are miniature, cheap, mobile and can be easily integrated into wearable systems.

This thesis focuses on improving overall gait analysis using inertial sensors by providing a methodology for detecting gait events in real-world settings. Although the experimental protocols for such analysis have been restricted to only highly-controlled lab-like indoor settings; this thesis presents a new gait database that consists of data from gait activities carried out in both, indoor and outdoor environments. The thesis shows how domain knowledge about gait could be formulated and utilized to develop methods that are robust and can tackle real-world challenges. It also shows how the proposed approach can be generalized to estimate gait events from multiple body locations. Another aspect of this thesis is to demonstrate that the traditionally used temporal error metrics are not enough for presenting the overall performance of gait event detection methods. The thesis introduces how non-parametric tests can be used to complement them and provide a better overview.

The results of comparing the proposed methodology to state-of-the-art methods showed that the approach of incorporating domain knowledge into the time-frequency analysis of the signal was robust across different real-world scenarios and outperformed other methods, especially for the scenario involving variable gait speeds in outdoor settings. The methodology was also benchmarked on publicly available gait databases yielding good performance for estimating events from different body locations. To conclude, this thesis presents a road map for the development of gait analysis systems in real-world settings.

Acknowledgments

“Do you want to work with robots the rest of your life, or do you think you can rise up to the level of humans? ”- Denni (Thorsteinn Rögnvaldsson)

“PhD is the journey from being a dependent researcher to becoming an independent researcher”- Nicholas Wickström

“I am always here to help you”- Eva Nestius

do you have some time by any chance? I need to ask some questions... “Yes, sure! Go ahead ”- Josef Bigun, Eric Järpe, Antanas Verikas

“Hahahaha! Haahahaaaa...”- Anna, Saeed, Gaurav, Wagner, Alina, Deycy, Essayas, Asif, Suleyman, Joao and all of HRSS

rough weather today... “Its ok. It could be worse! ”- the spirit of IS Lab

“You should take a moment and think. What is it that you really want to be known for? ”- Misha Pavel & Holly Jimison

“We are also your family and friends! ”- Olaf, Elke, Kristina, Mats, Nicolina, Olle, Durga, Survi

“Te quiero mucho ”- Inma

“To live with others, first you have to learn how to live with yourself ”- Roberto

“If you ever fall back, you wont touch the ground. Because I will be there in between ”- Stefano

“When I was 15, I read the novel called ‘Siddhartha’...and then I came to meet you ”- Helon

“Let’s do it, Jani! ”- Udaya

“Life will teach you many lessons. Be open and learn ”- Nanaji, Naniji (Ramesh Chandra Gupta, Keshar Gupta)

within the neurons... “Whatever you do, I will do better ”..out loud..“Just kidding! You are my idol ”- Shalini

“I hope I can put sunshine in your heart with this delicious breakfast! Bisous”- Your breakfast girl (Ioana)

“Life is built one brick at a time ”- Dad

“If you think good, good things will happen ”- Mom

This thesis is a compilation of strong beliefs, immense love and unwavering support of some amazing human beings who have shaped my thoughts and directed my life. I thank you all from the deepest corners of my heart and stand humbled by the thought of having interacted and received invaluable lessons from some of the greats of this era. Writing this thesis has been a journey within and now, I dare to look beyond...

To Nanaji, Mom and Ioana...

Contents

List of Figures

List of Tables

Chapter 1
Introduction

1.1 Motivation

Healthy gait requires a balance between various interacting neuronal systems and consists of three primary components [67]:

- locomotion, including initiation and maintenance of rhythmic stepping,
- balance, and
- the ability to adapt to the environment.

As such, healthy gait is considered an important indicator for quality of life and deviations from normal walking behavior may be an indication of improper coordination or dysfunction in any of the involved neuro-physiological systems. This drives the need for gait analysis which can be used to help diagnose and assess the severity of neuro-physiological disorders, monitor the rate of recovery during rehabilitation and be further utilized in wide variety of applications such as sports science, limb prosthetics, functional electrical stimulation (FES) systems and more. Many of these applications would immensely benefit if the analysis could be carried out continuously or over longer periods of time in patients' everyday lives with minimum intrusion. This would potentially initiate newer interventions and improve existing decision-support systems.

The present state of practice is to perform clinical gait analysis in sophisticated gait labs equipped with stationary motion capture systems and force places that enable videotape examination, kinetic and kinematic analysis of walking [71, 72]. Although they provide rich and accurate information, they are inadequate for use in daily living as they are very expensive, require high operational competence and are fixed to the environment such as lab or smart-home. Moreover, the walking data is generally collected under highly controlled conditions and many countries do not have access to such facilities.

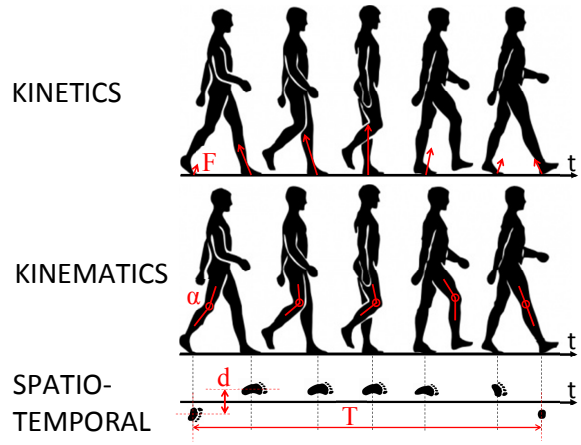

Figure 1.1: The figure illustrates the kinetic, kinematic and spatio-temporal aspects of gait. Kinetics is the study of forces involved in producing the movements while kinematics is the study of the movement of body through space. The spatio-temporal aspect consists of spatial parameters such as step length and temporal parameters such as stride time. Image adopted from [59].

On the other hand, wearable systems and in particular, inertial sensors i.e. accelerometers and gyroscopes, are gaining momentum as they provide a cost-effective, low-power, small and unobtrusive alternative for conducting long-term and continuous monitoring of gait in everyday life. The information collected from these inertial measurement units or IMUs can be used to estimate kinematic and spatio-temporal parameters of gait or fused using filtering techniques to re-construct the trajectory of gait. However, a major drawback with using inertial sensors is that they suffer heavily from noise and require robust methods to handle the noisy signals to extract clinically relevant information.

An essential constituent of objective gait assessment is to study the spatio-temporal parameters (refer Figure 1.1) and use them to develop objective measures that can characterize a person's gait. These parameters can be studied from stride-to-stride of a given leg over longer periods of time, or compared between the left and right leg, or evaluated how much they deviate from the parameters of a reference population group with no gait pathology. Thus, in order to compute many of these spatio-temporal parameters, the gait cycle is divided into different walking phases, as shown in Figure 1.2. These phases are defined and segmented using two primary events that occur during a gait cycle: (1) when the heel of the foot strikes the ground, referred to as Heel-Strike (HS) or Initial Contact (IC), and (2) when the toe of the foot leaves the ground, referred to as Toe-Off (TO) or Final Contact (FC). Hence, accurately

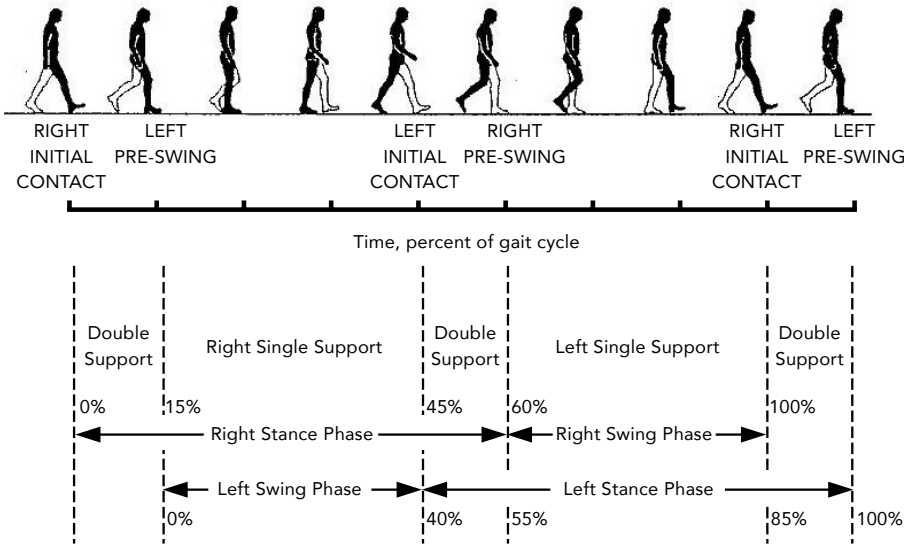

Figure 1.2: This figure illustrates the different gait phases within a complete gait cycle. Identification of these gait phases and the estimation of other gait parameters depends on the accurate detection of the gait events of Heel-Strike (HS) or Initial Contact (IC) and Toe-Off (TO) or Final Contact (FC). Image adopted from [19].

identifying these gait events from inertial sensor signals is essential for many gait analysis applications [81, 45, 56, 84, 21, 83, 28] and towards this goal, numerous gait event detection (GED) algorithms have been developed over the years.

However, although the major argument of using inertial sensors over fixed sensing modalities is that they can be worn continuously in everyday life; most authors have restricted the experiments to either gait labs or flat indoor corridors. Generally, the experiments are designed in a way that imposes strict constraints on the sensor location and its alignment with respect to the body, and instructs the subject to walk in straight line with pre-defined walking speeds. While having high control over the experiments may be necessary such that any changes in the signal waveform can be attributed to visual observations or to validate the algorithm's accuracy with ground truth reference systems (normally taken to be force plates or mocap systems); these well-structured environments and highly controlled conditions are quite in contrast to real-world situations. Gait in everyday life may involve walking with varying gait speeds, taking turns and navigating around obstacles, walking on different surfaces and surface inclinations, etc. Hence, these real-world conditions may be quite different and difficult to simulate inside labs and corridors.

This thesis is motivated by the research questions:

- How do the existing GED methods perform in actual real-world conditions?
- How to develop GED methods that are robust and accurate in real-world scenarios?

Many of the existing GED methods that have been developed using inertial sensors are purely data-driven approaches that apply implicit or explicit thresholds and contain many tuning parameters. Some methods use supervised machine learning techniques where the model parameters are dependent on labeled training data and it is not clear whether and how often they would require re-training with different real-life settings. Hence such methods may not generalize well across different subjects and environments. Furthermore, since the intermediate data representations and transformations resemble a 'black-box', the underlying steps maybe be difficult to interpret by users such as clinicians. Few efforts have been made to include expert or domain knowledge about gait into the data analysis to develop robust GED methods. Additionally, such knowledge may be easier to understand by medical personnel and help in creating intermediate data representations that are perhaps more comprehensible.

This thesis addresses the questions:

- How can domain knowledge about gait be formulated and used to drive the analysis of gait signals?
- Can the use of domain knowledge help in improving robustness of the method?

Another disparity that exists between controlled laboratory experiments and real-world situations is that of sensor placement. In the lab experiments, the IMU is generally fixed to a body location such that the sensor axis is aligned with some pre-defined limb axis and it is assumed that the sensor shall stay static in this configuration throughout the walking trails. Next, using the collected data, a GED method is developed that is designed specifically for that particular body location and sensor alignment. Although the subjects follow these instructions during the experiment, such restrictions would be hard to follow in everyday life situations, especially for applications that may require wearing the sensors for longer periods of time. It is quite likely that due to comfort or other practical issues, the patients may re-adjust the sensor disturbing the original configuration or even move them to a different body position. Such real-world challenges require methods to be robust to changes in axis alignment and generalize to different body locations.

This thesis hypothesizes that domain knowledge could be used to help tackle some of these real-world challenges and addresses the question:

- Can the of use of domain knowledge help in generalizing the approach to multiple body locations and be invariant to axis-alignment?

1.2 Contributions

The main contributions of this thesis can be summarized as follows:

- The first step was to create a gait database that is more representative of different real-world scenarios in contrast to data collected only from controlled indoor experiments. Paper II presents a new gait database called MAREA: Movement Analysis in Real-world Environments using Accelerometers that consists of walking and running data collected from 20 subjects with accelerometers positioned on waist, wrist and both ankles. The data was collected in various environments such as treadmill, indoor flat space and an outdoor street. The protocol consisted of both, controlled and semi-controlled experiments with fixed and variable sensor alignment, varying speeds, different walking surfaces, varying surface inclinations and regular turns, among others. In addition to accelerometers, the shoes were instrumented with Force Sensitive Resistors to provide an external reference for validation.

- A novel GED method was developed and presented in Paper I by incorporating domain knowledge about gait into time-frequency analysis. The hypothesis was that prior knowledge about the fundamental principles of gait could be used to help guide the data analysis in order to achieve greater robustness and accuracy in estimating gait events. The paper exhibits how domain knowledge could be formulated and the results show that the presented method not only outperforms the existing methods but also demonstrates consistently good performance across different environments and scenarios.

- In parallel, state-of-the-art GED algorithms were evaluated in different real-world scenarios using the MAREA Gait Database and it was assessed whether their performance was consistent across different environments. Paper II evaluates six existing GED methods and the results reveal that the performance of these algorithms is inconsistent and varies with changing environments and gait speeds. All algorithms demonstrated good performance for the scenario of steady walking in a controlled indoor environment but exhibited significantly decreased performance when evaluated in other lesser controlled scenarios such as an outdoor street. The results underline the importance of testing GED

algorithms developed for potential real-world applications in actual real-world situations. It was also shown that the traditional and widely used Mean Absolute Error metric is not enough to assess the overall accuracy and consistency of a GED algorithm and that non-parametric statistical tests could be used in conjunction to present a more comprehensive view of their performance in different scenarios.

- Finally, Paper III presents a methodology to estimate initial contact events from accelerometers attached to different body locations such as legs, waist, chest and hands. The idea of utilizing domain knowledge about gait to guide the time-frequency analysis is extended to other body parts as the body movements are co-ordinated and periodic during normal gait. The presented methodology is shown to be robust and is benchmarked on four publicly available gait databases.

1.3 Publications

Appended Publications

Table 1.1 lists the three selected publications included in this thesis.

Table 1.1: List of appended publications.

Paper I	S. Khandelwal and N. Wickström, Gait Event Detection in Real-World Environment for Long-Term Applications: Incorporating Domain Knowledge Into Time-Frequency Analysis, in IEEE Transactions on Neural Systems and Rehabilitation Engineering, vol. 24, no. 12, pp. 1363-1372, Dec. 2016. doi: 10.1109/TNSRE.2016.2536278
Paper II	S. Khandelwal and N. Wickström, Evaluation of the performance of accelerometer-based gait event detection algorithms in different real-world scenarios using the MAREA gait database, in Gait & Posture, vol. 51, pp 84-90, Jan. 2017. doi: 10.1016/j.gaitpost.2016.09.023
Paper III	S. Khandelwal, N. Wickström, Novel methodology for estimating Initial Contact events from accelerometers positioned at different body locations, in Gait & Posture, vol. 59, pp 278-285, Jan. 2018. doi: 10.1016/j.gaitpost.2017.07.030

Other Publications

Table 1.2 presents a list of other publications that are not explicitly included in thesis as they form smaller parts of the appended publications or have been written outside the scope of this thesis.

Table 1.2: List of other publications.

J. Bentes, S. Khandelwal, H. Carlsson, M. Kärrman, Tim Svensson, Nicholas Wickström, Novel System Architecture for Online Gait Analysis, at The 39th Annual International Conference of the IEEE Engineering in Medicine and Biology Society (EMBC), Jeju, South Korea, July 2017
S. Khandelwal, N. Wickström, Detecting Gait Events from Outdoor Accelerometer Data for Long-term and Continuous Monitoring Applications, at 13th International Symposium on 3D Analysis of Human Movement (3D-AHM), Lausanne, Switzerland, July 2014.
S. Khandelwal, Nicholas Wickström, Identification of Gait Events using Expert Knowledge and Continuous Wavelet Transform Analysis, at 7th International Conference on Bio-inspired Systems and Signal Processing (BIOSIGNALS), Angers, France, March 2014.
S. Khandelwal, C. Chevallereau, Estimation of the Trunk Attitude of a Humanoid by Data Fusion of Inertial Sensors and Joint Encoders, at The 16th International Conference on Climbing and Walking Robots and the Support Technologies for Mobile Machines (CLAWAR), Sydney, Australia, July 2013. (received Highly Commendable Paper Award)

1.4 Outline

The outline of this thesis is as follows. Chapter 2 presents a brief overview of different sensing modalities used to develop GED methods. It also presents different methodological aspects of state-of-the-art GED methods developed using inertial sensors. Chapter 3 presents how domain knowledge is formulated and used in reasoning around the chosen methodological steps. It also introduces the reader to time-frequency analysis using continuous wavelet transforms and explains how non-parametric statistical tests can be used to evaluate the accuracy of a GED algorithm. This is followed by Chapter 4 which provides a summary of the appended papers. Chapter 5 offers a discussion on the thesis and finally, Chapter 6 concludes this thesis.

Chapter 2
Related Work

2.1 Gait Analysis

Human motion analysis refers to the study of human movements using sensors and is generally focused towards two main goals: (1) classifying the movement patterns in order to figure out what activity is being performed, and (2) characterizing the movement patterns to assess how (or how well) a given activity being performed [23, 59]. Low levels of physical activity have been associated with increased risk of chronic diseases and thus knowing which activities a person preforms during a day gives insights into their overall health status [8, 79]. As such, numerous works have been dedicated to classifying daily-living activities using wearable sensors [6, 44].

On the other hand, characterizing an activity and in particular gait, provides detailed information about the subject's physical and cognitive condition [2, 21, 28]. Many studies have been dedicated to characterize gait and have developed quantifiable gait measures associated with one or more gait disorders [17]. While some of these gait measures are more basic spatio-temporal measures such as: cadence or step frequency, stance time, swing time and double support time; others are more higher-level measures such as: gait variability which relates to a subject's stride-to-stride fluctuations over time [12, 43, 73]; gait symmetry which is a measure of the parallels between the two lower limbs [53, 60, 58]; and gait normality which relates to the deviation of a patient's gait parameters from a reference population group exhibiting no gait pathology [61, 62, 7]. Gait events enable the computation of various temporal gait parameters, and in turn facilitate the computation of many of the aforementioned gait measures. As such, developing methods for detecting gait events using various sensing modalities has been an active area of research for many years.

The rest of this chapter is organized as follows. First, various sensing modalities used in gait event detection (GED) methods are presented. Next, different methodological aspects such as experimental design and algorithmic techniques of state-of-the-art inertial sensor-based GED methods are presented.

2.2 Sensing Modalities

Gait is usually investigated from three aspects: kinetic, kinematic and spatio-temporal as shown in Figure 1.1 [14, 80]. Kinetics examines the forces that act upon the body causing it to move. As such, kinetic analysis provides information about how the movement is produced and maintained. Kinematics is concerned with the motion of the body and examines this from a spatial and temporal perspective. Spatio-temporal parameters are based on spatial variables such as stride length or step width and temporal variables such as step time or stride time. Hence, to examine these aspects of gait, different sensors or a combination of sensors are employed [49].

Camera-based systems

A sensing modality used for kinematic analysis is the motion capture system which consists of fixed high-speed video cameras that track movement with the help of reflective markers attached to the body. Then, marker trajectories are constructed using biomechanical models and the position of the heel or toe marker is tracked through multiple frames to identify the gait events by visual inspection. Otherwise, threshold-based peak detection algorithms are applied to the velocity or acceleration curves of these markers in order to estimate gait events from them [86, 20, 51, 10, 66, 27].

Force-based Systems

Another sensing modality is the use of force-based sensors which can be fixed or mobile and the only possible position for these sensors is between the foot and the ground. Force plates and pressure-sensitive mats allow kinetic analysis as they measure the ground reaction forces exerted by the foot sole on the ground. Other force-based sensors include foot switches or force sensitive resistors (FSRs) attached to the heel and toe to detect gait events. Also, an alternative is to use pressure insoles that consists of a matrix of sensors covering the entire sole. As HS and TO produce larger impact forces compared to the rest of gait cycle, usually thresholds such as 5, 10 or 20N are applied to the vertical ground reaction force to detect gait events [26, 51, 37, 78, 48, 65].

Motion capture systems and force plates are commonly used together in gait labs for comprehensive gait analysis and are generally considered as the

ground truth reference or 'gold-standard' for evaluating the accuracy of event detection algorithms.

Inertial Sensor Systems

Although camera and force-based systems provide rich and accurate information, these sensing modalities are not well suited for out-of-clinic applications that require long-term or continuous monitoring of gait in everyday life. For such applications, inertial sensors developed using MEMS (Micro-Electric Mechanical Systems) technology provide a good trade-off between a variety of factors such as size, weight, ease of use and comfort, cost, mobility, battery-life, sensor positioning and cosmetic acceptance. Due to the these factors, the literature on using inertial sensors for gait analysis is huge and is being constantly reviewed [23, 33, 64, 11, 49, 17, 77]. On the other hand, the major drawback of using MEMS-based inertial sensors is their susceptibility to noise which may be caused by calibration errors, constant bias, thermo-mechanical noise, temperature effects, etc. (usually stated in the respective datasheets) and hence require robust algorithms to analyze inertial sensor signals [82].

The use of accelerometers or gyroscopes is application-dependent and are generally commercially available packaged into a single Inertial Measurement Unit (IMU) [55]. While accelerometry can be used to provide temporal gait parameters, gyroscopes can be used to estimate joint rotation angles. As such, many studies are aimed at obtaining reliable spatio-temporal gait parameters and using them for further gait assessment. Both sensors have been widely used for developing GED algorithms [57], and recent studies have used them for biometric gait recognition [69].

2.3 Gait Event Detection Methods

Experimental Design

Numerous GED methods have been developed using inertial sensors. A closer inspection of their experimental design reveals that they involve many different protocols with variations in environment, floor type or walking surface, surface inclinations, instructions for gait speed, sensor locations and other specific conditions and constraints.

Almost all experimental set-ups consist of a highly-structured environment such a laboratory or a hospital corridor. A recent study reviewed 78 papers based on using IMUs as a tool for pathological gait assessment and reported that approximately 86% were set in a lab or hospital only, 11% in patients' home environment only and the rest 3% in both [77]. With few exceptions which have included walking slopes [52, 5, 32] or considered included indoor

and outdoor free walking in their experiments [52, 70]; there is a considerable lack of studies which have developed and tested GED methods with protocols involving free-living settings.

Most GED methods are designed for a particular body location by fixing the sensor at a pre-defined position such as around the foot [52, 56, 31, 32], ankle [5, 34, 74, 60], shank [24, 9, 4, 40, 25, 25], just below the knee [63, 81, 74], thigh [4], waist (front or back) [85, 88, 46] and ear [30]. Once a body location is chosen, usually the sensor axes is aligned with the limb/body axes with the assumption that the sensor shall remain in this configuration throughout the experiment. Such restrictions may be impractical and hard to follow in real-life settings, especially for long-term and continuous monitoring applications where the original sensor location and alignment are quite likely to get disturbed due to practical issues and unforseen circumstances. Hence, there is a need for algorithms which are invariant to axis-alignment [56, 60, 34] and generalize to multiple body locations [36].

In terms of gait speed, most protocols either instruct subject to walk in a straight line at their preferred walking speed [24, 46, 60, 81, 74] or simulate different speeds by asking them to walk at slow, normal and fast pace [25, 40, 4, 85, 88, 63, 9]. However, since the walking distance is often in the range of 5 to 30 meters, this results in reporting performance by considering only a couple of steps. Hence, some studies have additionally used treadmill to test their methods on a range of walking speeds [52, 4, 88, 74, 34].

From the aforementioned factors, it can be noted that not only is there a lack of standardized protocols but most studies carry out experiments only in well-structured and highly-controlled lab-like conditions. As the primary motivation of using IMUs over fixed sensors is that they be easily employed for health-related applications in daily living, the validity of such methods in free and uncontrolled real-world settings is unknown and needs further investigation. In this regard, publicly available gait databases can help as different algorithms can be objectively compared and benchmarked using them [35, 87, 50, 42].

Algorithmic Design

A number of algorithms developed using inertial sensors either directly apply spatial or temporal thresholds to filtered sensor signals or use them at some intermediate stage after signal transformation, to perform peak detection for identifying gait events [25, 85, 74, 39]. Some algorithms investigate the zero-crossing of the signal obtained from a particular axis, i.e. when the signal magnitude changes its sign, to set temporal windows and detect gait events [24, 88]. Other methods use a state machine-based approach by defining different gait phases as states and then determining state transitions by using pre-defined rules or applying adaptive thresholds on intermediate signals [56, 52, 9]. A factor common to all these methods is the use of many thresholds and other

tuning parameters. As such, their performance is dependent on the choice of these tunables which makes it difficult to generalize them.

Other approaches include the use of machine learning techniques such as artificial neural network or clustering [81, 5, 47]. However, there are pros and cons as on one hand they can easily handle large amounts of gait data, on the other hand the model parameters are dependent on labeled training data which may not generalize to real-world settings; especially given the lack of abundant training data [16]. Moreover, since they resemble a 'black-box', the results may be difficult to interpret by medical personnel who need to understand the reasoning behind a decision before validating it [59].

In recent years, wavelet transforms have been used in gait analysis and in developing GED algorithms using time-frequency analysis [4, 5, 22, 24, 68, 46, 32]. For example in [4], wavelet transform was applied to decompose the shank angular velocity into low-frequency approximation signals and high-frequency detail signals using the Coiflet wavelet. Next, peak detection was applied on the approximation signals to set temporal windows (with pre-defined thresholds), and search for gait events within each window. A common issue in the use of wavelet transform for biosignal processing is the choice of appropriate mother wavelet function as there are insufficient guidelines [54]. Different mother wavelets have been used in GED methods for time-frequency analysis either using Discrete Wavelet Transform: coiflet [4], bior [22], symmlet2 [24], daubechies6 (db6) and db10 [68], db1 and db2 [32]; or Continuous Wavelet Transform: db2 [5], Mexican hat [46]. While some studies report that the choice of mother wavelet was based on visual similarity between the wavelet waveform and the sensor signal [4, 22, 32], others do not provide any reasoning or explanation and the selection is more ad hoc [68, 24, 5, 46].

Very few methods have considered the approach of formulating and incorporating domain or expert knowledge into their algorithmic design to achieve greater robustness in detecting gait events. In [52], expert knowledge is implicitly used to reason around the motion of the foot during different gait phases and how it would result in different FSR (force sensitive resistors) values, placed below the feet. In [60], the use of expert knowledge is more explicit where the original acceleration signal is transformed into a cyclic sequence of symbols and organized into all possible pairs to determine which symbols are associated with HS and TO. Next, domain knowledge about gait phases is used to formulate different hypothesis and choose the most likely symbol pair as HS and TO.

This thesis exhibits the formulation and use of domain knowledge to logically reason around the algorithmic steps in order to detect gait events from sensor signals. It also shows how it can be utilized to generalize the method such that it can be adapted to real-world settings involving different environments, gait speeds and sensor positioning, among others. The use of domain knowledge also helps in making the system more transparent, thus potentially increasing the acceptance of such an approach by health-care professionals.

Chapter 3
Methodology

This chapter introduces the reader to how domain knowledge about gait is formulated and used to guide the methodological steps taken to develop a robust GED method that can tackle challenges such as changes in axis-alignment, different sensor locations and varying gait speeds. Next, the reader is introduced to time-frequency representation of the sensor signal using continuous wavelet transform (CWT) by choosing an appropriate mother wavelet. The last section of this chapter explains why traditionally used metrics such as Mean Absolute Error (MAE) are not sufficient and shows how non-parametric tests can be used to complement the MAE in providing an overview of the accuracy and performance of a GED method.

3.1 Domain Knowledge

Invariance to axis-alignment

As mentioned before, most algorithms analyze signals obtained from individual accelerometer axis by positioning the sensor in a specific pre-defined orientation [81, 45, 63, 31, 74, 5, 85] with the assumption that the accelerometer shall stay statically positioned throughout the experiment. However, it is quite likely that external factors might disturb the original configuration during long-term analysis [85], and thus either the axis alignment should be checked and readjusted frequently or the exact orientation of the accelerometer must be known throughout, to compensate for the misalignment of the axes. Hence, a preprocessing step is utilized to make the algorithm invariant to any changes in axis alignment at the expense of losing information about the directional vectors of each individual axis. This is done by computing the magnitude of the resultant acceleration signal, i.e. $\mathtt{Acc}_\mathtt{r} = \sqrt{\mathtt{acc}_\mathtt{x}{}^2 + \mathtt{acc}_\mathtt{y}{}^2 + \mathtt{acc}_z{}^2}$ where

acc_x, acc_y, acc_z are the signals obtained from each individual axis of the 3-axes accelerometer; and then using it for further analysis.

Spectral relationships present in normal gait

A major challenge is to design an algorithm that can effectively tackle varying gait speeds in real-world scenarios. It is known that normal gait is rhythmic in nature and involves a series of co-ordinated body movements. Hence, the principles or underlying fundamental gait relationships involved in walking also remains consistent throughout different gait speeds. For example, one such underlying gait principle is the frequency relationship that is present between gait event and gait cycle. In every gait cycle, there are two gait events, namely HS and TO. Hence the frequency of the event (HS and TO) is twice that of the cycle.

In a similar manner, such logical reasoning can be extended to other parts of the body in order to develop a common methodology for estimating gait events from accelerometers located at different body locations. An accelerometer placed at any body location captures accelerations from the local movement of the respective body part and the global movement of the body, in a given direction. As these co-ordinated body movements are periodic in nature during normal gait, the underlying frequencies associated with these movements are also co-related. For example, arm swing is a natural motion where each arm swings with the motion of the opposite leg. Thus, the wrist accelerometer captures a combination of the local acceleration forces due to the arm swing and the global acceleration forces due to the forward movement of the body. An accelerometer positioned in the central body such as chest or waist captures a combination of forces generated periodically, consisting of the gait events from both legs and local movements of the body part such as pelvic movements in the transverse and frontal plane [29]. As such, the major frequency in the central body acceleration signal is a combination of the gait cycles of the two legs, which is twice the frequency of the gait cycle of an individual leg.

As these spectral relationships remain consistent with varying gait speeds, incorporating them into the algorithmic design minimizes the use of thresholds and tuning parameters; thus making it more robust across different subjects and real-world scenarios.

CWT and choice of mother wavelet

It is important to find a representation that allows to capture the aforementioned spectral relationships in gait, localized in time such that they can be effectively utilized. Thus, continuous wavelet transform (CWT) is used as it provides a simultaneous time-frequency decomposition of the acceleration signal. However, there are insufficient guidelines on the selection of wavelet basis function for gait signals and choosing the most appropriate mother wavelet

is a challenge [15, 54]. As explained later in the following section, domain knowledge is used to logically reason around the choice of mother wavelet for computing the CWT of the acceleration signal.

3.2 Time-frequency representation

In order to exploit the aforementioned spectral relationships present in gait and capture local variations in the temporal gait acceleration signal, a signal representation is needed that allows to study or inspect these frequencies localized in time.

Fourier Transform

Fourier Transform (FT) has been the classical way of studying the frequency content of a signal by computing the inner product of the signal $x(t)$ with sine and cosine basis functions, given as:

$$F(\omega) = \int_{-\infty}^{\infty} x(t)\, e^{-j\omega t}\, dt \tag{3.1}$$

However, as FT assumes that the frequency content of the signal is constant throughout the entire signal, it is not possible to localize on frequency variations in time [3].

Short-Time Fourier Transform

An option is to use short-time Fourier Transform (STFT) which takes a window of finite length and slides it over the temporal signal. By performing FT in each of the overlapping windows, we can plot a time-frequency diagram, also known as spectrogram, that shows the power spectrum for each time region. However, since the window size is fixed, the time-frequency resolution will be the same throughout the region. Hence, a challenge is to specify the appropriate window size as a short window length will yield good time resolution but poor frequency resolution as shown in Figure 3.1. This is due to the fact that a short window length can capture high frequencies but there will be a limit to the low frequencies it can capture within the window. Similarly, choosing a large window length will allow to analyze low frequencies but then will result in a poor time resolution due to the big window length.

Continuous Wavelet Transform

An alternative is to use Continuous Wavelet Transform (CWT) which allows to analyze the signal using variable window width, with different frequencies. As

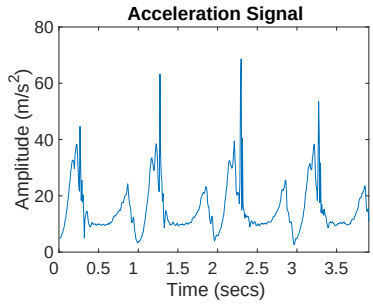

(a) Example of composite acceleration signal, computed as, $\mathrm{Acc_r} = \sqrt{\mathrm{acc_x}^2 + \mathrm{acc_y}^2 + \mathrm{acc_z}^2}$, obtained from the 3-axis accelerometer attached to the right ankle. The figure contains four gait cycles.

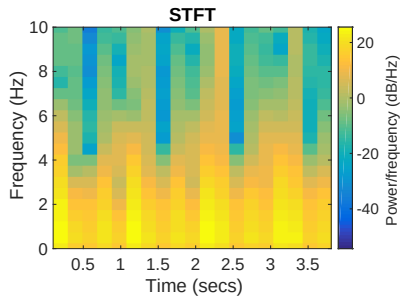

(b) Spectrogram of $\mathrm{Acc_r}$ using a window length of 50 samples with 50% overlap. As the window size is fixed in STFT, the time-frequency resolution is same throughout the region.

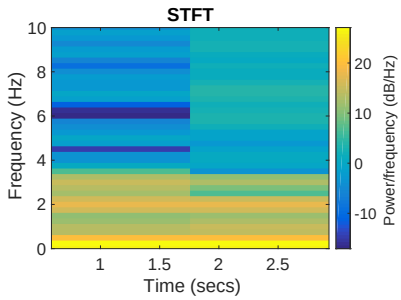

(c) Spectrogram of $\mathrm{Acc_r}$ using a window length of 300 samples with 50% overlap. Due to a larger window size, this spectrogram gives better frequency resolution but poorer time resolution in comparison to the previous figure (Fig. 3.1b) with a smaller window size.

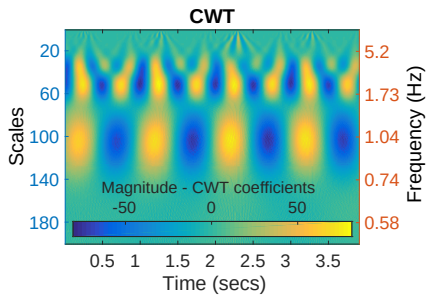

(d) Continuous Wavelet Transform (CWT) of $\mathrm{Acc_r}$ using the Morlet wavelet. CWT produces a time-frequency decomposition where both, short-duration high frequency and long-duration low frequency information can be captured simultaneously.

Figure 3.1

such, it is designed to give good time resolution and poor frequency resolution at high frequencies (small or finer scales); and good frequency resolution and poor time resolution at low frequencies (large or coarser scales) as shown in Figure 3.1. Another advantage is that CWT is not limited to using sinusoidal analyzing functions and a large selection of basis functions, known as wavelets, can be employed that satisfy predefined mathematical criterion [3].

The CWT is a convolution of the signal $x(t)$ with scaled and translated versions of the wavelet function $\psi^*_{a,b}$, also called the mother wavelet, and is expressed as:

$$\begin{aligned} CWT(a,b) &= \int_{-\infty}^{\infty} x(t)\, \psi^*_{a,b}\, dt \\ &= \int_{-\infty}^{\infty} x(t)\, \frac{1}{\sqrt{a}} \psi^* \left(\frac{t-b}{a} \right) dt \end{aligned}$$

where a and b are the scaling and position or translation parameters [3]. The normalization factor $1/\sqrt{a}$ is to ensure that the norm for any translated or scaled version of the mother wavelet is same as the mother wavelet itself, i.e. $\|\psi_{a,b}(t)\| = \|\psi(t)\|$. For its practical implementation, the CWT involves a numerical approximation of the transform integral, i.e. a summation computed on a discrete grid of a scales and b locations. The CWT of a discrete time signal $x_n (n = 0, .., N-1)$, with equal time spacing δ_t, is defined as the convolution of x_n with a scaled and translated mother wavelet:

$$W_n(s) = \sum_{n'=0}^{N-1} x_{n'} \left(\frac{\delta_t}{s} \right)^{1/2} \psi^* \left[\frac{(n'-n)\delta_t}{s} \right] \tag{3.2}$$

where s is the wavelet scaling factor and n is the localized time index. Thus, for a discrete time signal, the wavelet is resampled at a sampling interval of δ_t/s to obtain the wavelet transform at scale a. The transform coefficients produced by this process are a measure of how similar that wavelet function is to the signal, at that scale and position in time. As such, wavelet transforms have been applied to wide variety of biosignals such as EMG, EEG, respiratory patterns, gait and ECG [1].

In the context of this thesis, CWT was chosen in analyzing gait signals as it could capture subtle signal variations generated by the movement of the legs such as fast changes in gait speed, localized in time. Furthermore, it gives a smooth and redundant time-frequency representation of the signal that is easily comprehensible and interpretable. Fig. 3.2 shows an example of the CWT of a composite acceleration signal obtained from an accelerometer positioned at the ankle during walking and running on a treadmill. The speed transitions captured by CWT can be easily identified and visualized which makes it easier to interpret and explain to medical experts such as clinicians.

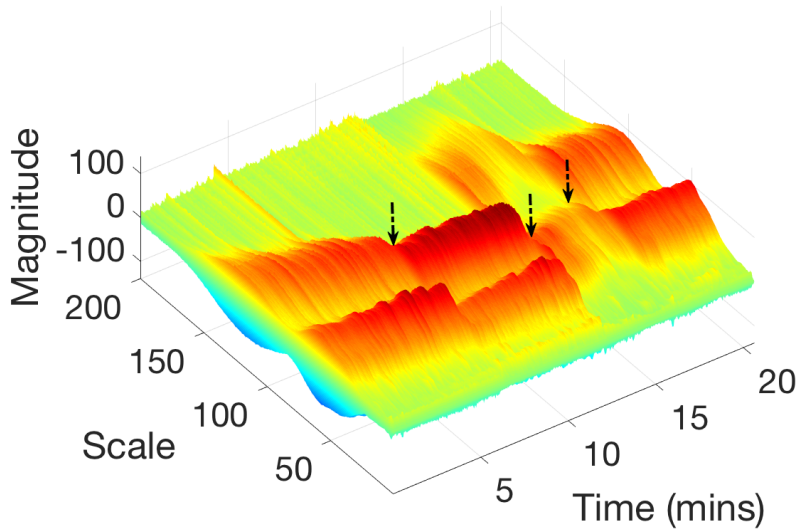

Figure 3.2: The CWT, using the Morlet wavelet, of a composite acceleration signal obtained from an accelerometer positioned at the ankle during walking and running on a treadmill.
The protocol consisted of the following activities:
1. Walking from 4km/hr to 7.4km/hr increasing in steps of 0.4km/hr
2. Running from 7.4km/hr to 10km/hr increasing in steps of 0.4km/hr
3. Walking at preferred walking speed with the treadmill set to 10°inclination
4. Walking at preferred walking speed
The figure shows the ability of CWT to capture non-stationary signal features and yield a representation that is easily interpretable. Low or fine scales correspond to high frequencies and high or coarse scales correspond to low frequencies. The dotted arrows mark the switch between the activities.

Choice of Wavelet Function

There is a wide variety of wavelet basis functions available with different properties, sometime referred to as wavelet families. If no prior knowledge is available, generally some factors may be considered while choosing a particular mother wavelet, such as whether the wavelet is orthogonal or non-orthogonal, complex or real, width and shape of the wavelet [75].

Based on the formulated domain knowledge, a wavelet basis was desired that would facilitate investigating or studying the gait event and gait cycle spectral relationships, in time. In other words, a wavelet function which would correlate very well with both, the gait event (HS and TO) and gait cycle regions in the composite acceleration signal and clearly distinguish between these frequencies in the spectral domain. Another, desirable property was that the wavelet should be symmetric and thus avoid any skewness in the spectral domain. This would facilitate in defining clear spectral-temporal boundaries to localize the gait event region and also define the gait cycle.

Two widely used non-orthogonal and symmetric wavelets for the CWT of biosignals are the Mexian hat wavelet and the Morlet wavelet [1]. The Mexian hat wavelet, which is the second derivative of a Gaussian function, correlates well with the events regions in the composite acceleration signal but does not correlates well with the gait cycle. In contrast, the Morlet wavelet which has multiple oscillations in its waveform clearly distinguishes between event and cycle frequencies, and hence was chosen as the mother wavelet. Figure 3.3 illustrates the result of taking the CWT of the composite acceleration signal with Mexican hat and Morlet wavelet. It shows the effect of using the non-symmetric db44 wavelet, suggested for the use of biosignals in a recent study [54], which leads to skewness in the spectral domain and makes it difficult to define both, gait event and gait cycle boundaries.

As shown in Figure 3.4a, the Morlet wavelet is a complex sinusoid within a Gaussian envelope and is defined as:

$$\psi_0(t) = \pi^{-1/4}\, e^{i\omega_0 t}\, e^{-t^2/2} \tag{3.3}$$

where ω_0 is the central frequency of the mother wavelet and its value determines the number of 'effective' sinusoidal oscillations contained within the Gaussian envelope. The $\pi^{-1/4}$ term is a normalization factor which ensures that the wavelet has unit energy. To satisfy the admissibility criteria, ω_0 is generally chosen to be greater than 5.

The wavelet scale a and its equivalent Fourier frequency f are inversely proportional to each other, i.e. $a \propto 1/f$. For the Morlet wavelet, this relationship can be derived analytically and is given as [75, 13]:

$$\frac{1}{f} = \frac{4\pi\, a}{\omega_0 + \sqrt{2 + \omega_0^2}} \tag{3.4}$$

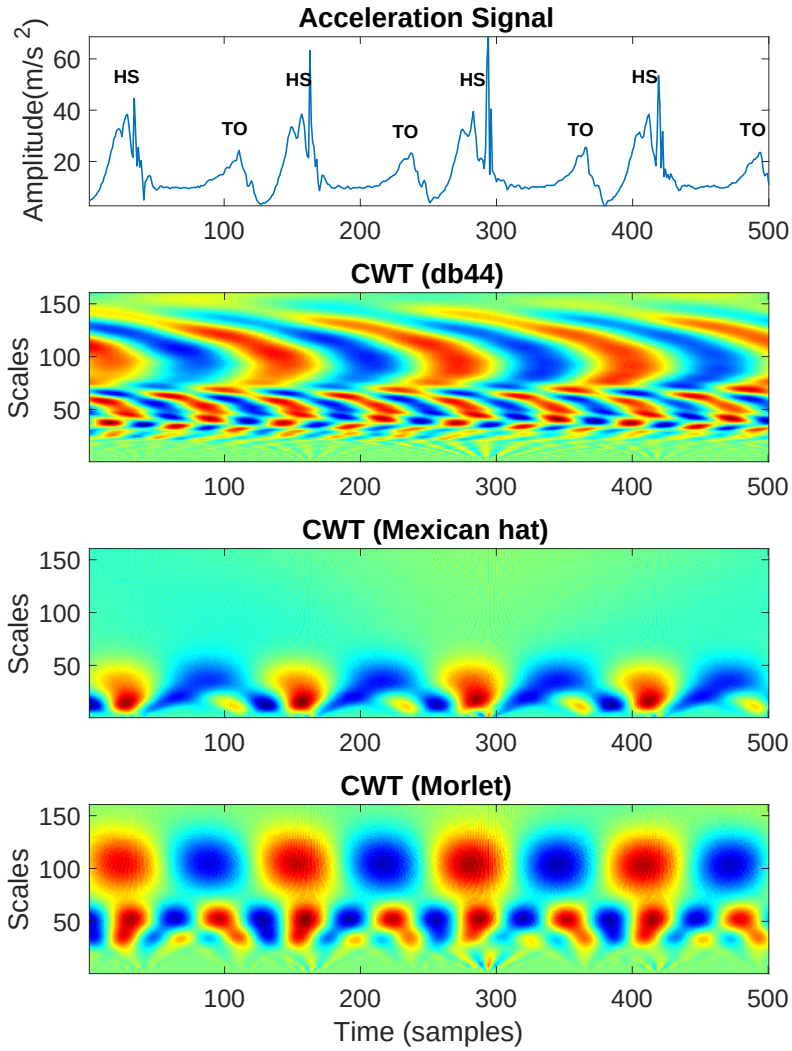

Figure 3.3: The CWT of a composite acceleration signal using different wavelet functions, namely, db44, Mexican hat and Morlet wavelet. db44 is an asymmetric wavelet and causes skewness in the spectral domain. Mexican hat is a symmetric wavelet but does not distinguish between the gait event and cycle frequencies, in time. The Morlet wavelet is symmetric and clearly distinguishes between the event and cycle frequencies, in time. As such, the Morlet wavelet was chosen as the mother wavelet.

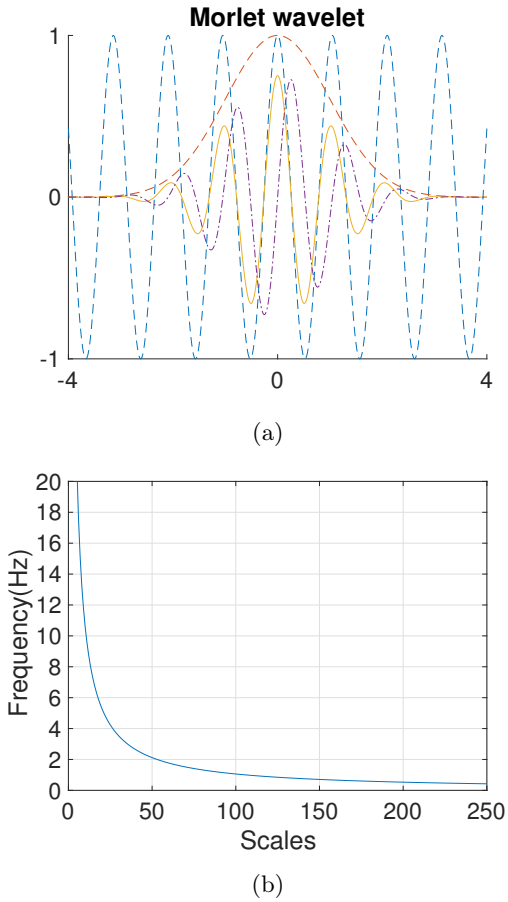

(a)

(b)

Figure 3.4: (a) An example of Morlet wavelet which is a complex sinusoid within a Gaussian envelope ($\omega_0 = 6$ rad/s, $\mathtt{f_o} = 0.954$Hz). (b) Scale-frequency relationship of the Morlet wavelet by taking $\omega_0 = 5.105$ rad/s or $\mathtt{f_o} = 0.812$Hz.

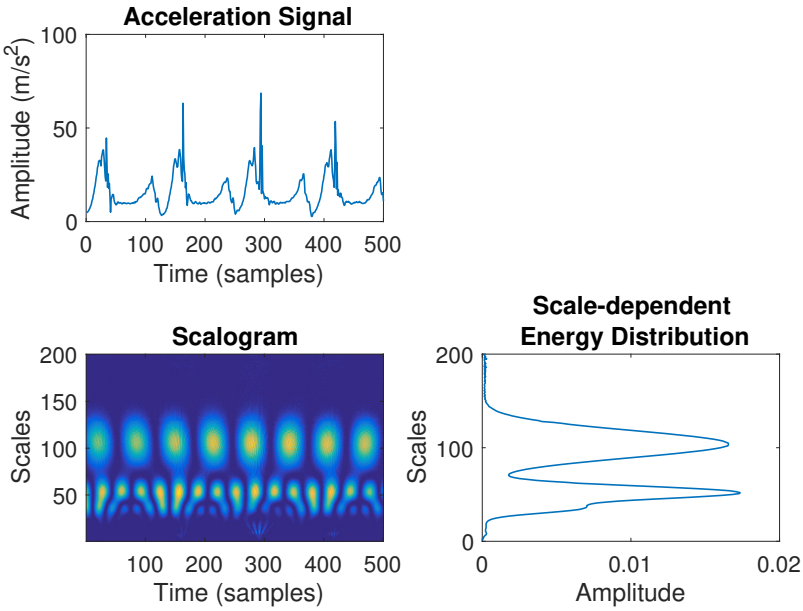

Figure 3.5: An example of the scalogram of the composite acceleration signal and the corresponding scale-dependent energy distribution.

where ω_0 is the center frequency of the Morlet. Figure 3.4b shows this scale-frequency relationship of the Morlet.

Scale-dependent Energy Distribution

The relative contribution to the total energy contained within the signal x_n at a specific scale a is given by the scale-dependent energy distribution:

$$E(a) = \sum_{n=0}^{N-1} |W_n(a)|^2 \tag{3.5}$$

where $|W_n(a)|^2$ is the two-dimensional wavelet energy density spectrum, also known as scalogram. Peaks in $E(a)$ highlight the dominant energetic scales within the signal. For example, as shown in Figure 3.5, peaks in the scale-dependent energy density spectrum of the composite acceleration signal highlight the dominant scales that correspond to the frequency of gait events and gait cycle.

3.3 Using non-parametric tests for evaluating performance

Various statistical measures are used in the literature to indicate the performance of a GED algorithm, i.e. how well is the algorithm able to detect gait events. One of the most popular ways used to present the performance of an algorithm is by reporting it's temporal detection accuracy, sometimes referred to as True Error [76, 41, 66, 88, 63]. It is computed by taking mean of the temporal difference between the estimated gait events by the algorithm and the corresponding ground truth (GT) events, given as:

$$\mathsf{TE} = \frac{1}{n} \sum_{i=1}^{n} (\mathrm{Algo}_i - \mathrm{GT}_i)$$

Another similar temporal accuracy measure often reported in literature is the Mean Absolute Error [60, 5, 46, 34], given as:

$$\mathsf{MAE} = \frac{1}{n} \sum_{i=1}^{n} |\mathrm{Algo}_i - \mathrm{GT}_i|$$

Although they indicate the ability of a GED method to detect events accurately in time, they standalone do not provide an overview of the algorithmic performance as only the true positive events estimated by the method are used to compute these measures. Figure 3.6 shows an example of applying two methods, namely Method 1 and Method 2, on a part of the left foot composite acceleration signal of a subject from the Outdoor Walk & Run dataset in the MAREA Gait Database [35]. The magenta triangles are the HSs estimated by the two methods where true positive events have been circled in black and the green dots show the corresponding GT events. Although both methods have very similar TE and MAE values, it is evident from the figure that Method 2 performs better than Method 1. As such, these error measures by themselves are not enough to indicate the performance of a GED algorithm. Consequently, many authors have complemented the temporal error measures with other statistical scores such as Sensitivity, Specificity, F1 score or providing the Bland-Altman analysis for showing the agreement between the estimated events and GT [56, 63, 5, 85].

In this thesis, it is shown that an alternate way of assessing the performance of a GED algorithm can be done by comparing the shape of the two stride time distributions obtained from the method and ground truth. Stride time is defined as the time between two consecutive HSs or TOs. If all estimated gait events exactly matched the corresponding GT events, then this would lead to identical stride time distributions and indicate high temporal accuracy and performance of the method. However, occurrence of any false positives or false negatives would lead to shorter or longer stride time durations, which in

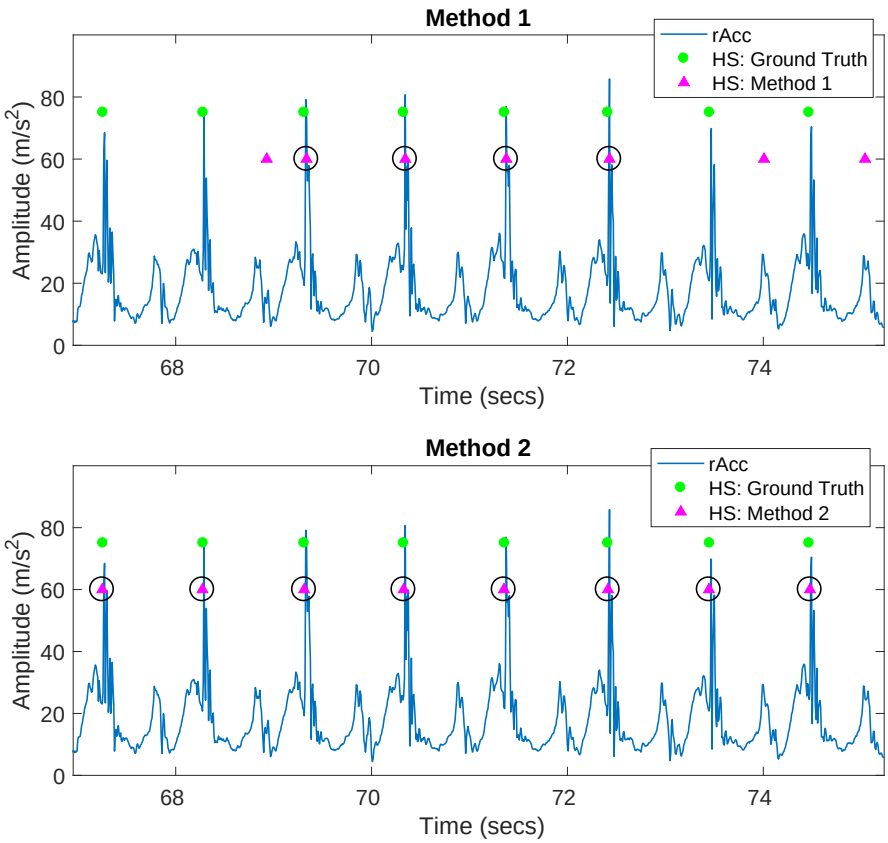

Figure 3.6: This figures shows the result of applying two GED methods, namely Method 1 and Method 2, on the left foot acceleration signal (Subject 15) taken from the Outdoor WalknRun dataset of MAREA Gait Database. The estimated HSs by the respective methods are shown as magenta triangles and the ground truth (GT) HSs are shown as green circles. The true positive events (taking a temporal tolerance of GT $\pm$ 5 samples) detected by the respective algorithms have been circled in black. The TEs obtained for Method 1 and 2 are -0.0031s and 0.0029s respectively, and the MAEs are 0.003s and 0.004s. Although it is evident from the figure that Method 1 has occurrence of false positives and false negatives, both methods have very similar TE and MAE values.

turn would be reflected in the shape of the resulting stride time distribution and would be dissimilar compared to the corresponding one obtained from GT. The same logic can be extended to comparing the step time distributions where step time is defined as the time between the gait event of one leg and corresponding event of the other leg.

Since daily life walking involves varying gait speeds, it is difficult make any assumptions on the underlying form of the resulting stride or step time distributions. As such, non-parametric statistical tests such as Kolmogorov-Smirnov (KS) test and the Mann-Whitney U (MWU) test can be employed to test the similarity of two stride or step time distributions [18].

Kolmogorov-Smirnov Test

The Kolmogorov-Smirnov (KS) test is used to compare two data distributions by comparing their empirical cumulative distribution functions (CDFs), given as $F_n(a) = \frac{1}{n} \sum_i \mathbb{I}(x_i < a)$ where n is the observed data points and $\mathbb{I}$ is a function that returns 1 when its argument is true and 0 when it is false. The top row in Figure 3.7 shows the histogram of the stride time distributions obtained by applying Method 1 and 2, along with corresponding GT, on an Outdoor WalknRun dataset in the MAREA Gait Database. The bottom row shows the corresponding empirical CDFs of the respective methods along with the stride time CDF computed from GT events. Thus if we have two samples of size n and m with corresponding empirical CDFs $F_n(x)$ and $G_m(x)$, and we want to test:

$$H_0 : F = G \qquad \text{vs} \qquad H_1 : F \neq G$$

then the KS statistic D_{nm} is given as:

$$D_{nm} = \max_x |F_n(x) - G_m(x)|$$

The null hypothesis is rejected if $D_{nm} > c(\alpha) \left(\frac{m+n}{mn}\right)^{1/2}$ where $c(\alpha)$ is the critical value at α level of significance (for example, $c(\alpha)$ is 1.36 for $\alpha = 0.05$).

Applying the KS test to the stride time distributions obtained from Method 1 and GT leads to a KS statistic: $D = 0.22$. This is shown using the dotted magenta line in the bottom-left subfigure of Figure 3.7. Hence the test rejects the null hypothesis as D is greater than the critical value, i.e. $D > 0.09$ (for $\alpha = 0.05$). Similarly, applying the KS test to Method 2 and GT leads to a KS statistic $D = 0.028$ and hence the test does not reject the null hypothesis indicating that the stride time distribution of Method 2 is more similar to GT as compared to Method 1. In other words, two distributions are more similar if the KS statistic is closer to 0 and more dissimilar if it is closer to 1.

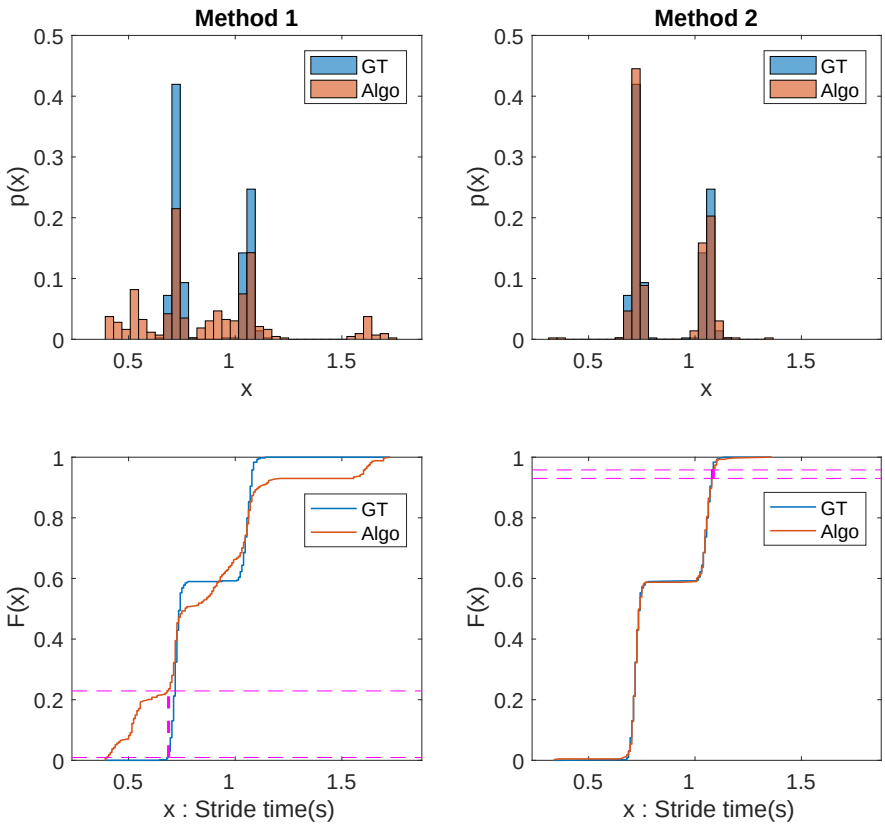

Figure 3.7: The top row shows the stride time histograms of applying two GED methods, namely Method 1 and Method 2, on the left foot acceleration signal (Subject 17) taken from the Outdoor WalknRun dataset of MAREA Gait Database. The stride time computed from ground truth (GT) HS events is also shown. The bottom row shows the empirical cdfs of the above stride time histograms. The KS test is utilized to compare the cdf of a method and the GT and the corresponding KS statistic is shown using dotted magenta lines.

Mann-Whitney U Test

The Mann-Whitney U (MWU) test is another non-parametric test that can be employed to test the null hypothesis that two groups have the same distribution while the alternate hypothesis is that one group has larger (or smaller) values than the other. The test statistic for MWU is computed as:

1. Combine all data points and rank them.
2. Add up the ranks for data points in the first group and call this R_1. Compute $U_1 = R_1 - n_1(n_1+1)/2$ where n_1 is the number of data points in this group. Similarly, compute U_2 for the second group.
3. The test statistic is defined as $U = min(U_1, U_2)$.

If both the sample sizes are large (>10), then U is approximately normally distributed in which case the p-value can be obtained from a z-test computed as $z = (U - m_U)/\sigma_U$, where $m_U = n_1(n_1 + n_2 + 1)/2$ and $\sigma_U = \sqrt{m_U n_2/6}$ [38].

Taking the same example in Figure 3.7, applying the MWU test to compare the stride time distributions computed from Method 1 and GT events leads to $z = 2.02$ and results in a p-value of 0.043. As this is less than the level of significance $\alpha = 0.05$, the MWU test rejects the null hypothesis that the two samples have the same distribution. Similarly, when comparing the stride time distributions computed from Method 2 and GT events, the MWU test yields a p-value of 0.956 and the test does not reject the null hypothesis. In other words, it is a test of equality of medians and tests whether both samples come from distributions with the same shape.

Chapter 4
Summary of Appended Papers

This section introduces the motivation, objectives and results of each individual paper and how they relate to the overall objectives of this thesis.

4.1 Paper I - Gait Event Detection in Real-World Environment for Long-Term Applications: Incorporating Domain Knowledge Into Time-Frequency Analysis

Gait analysis can be used to help diagnose and assess the severity of neurophysiological disorders such as Parkinson's Disease, multiple sclerosis, cerebral palsy, dementia, etc [77, 21]. Moreover it could be used to assess the rate of recovery of a patient during rehabilitation after stroke, hip replacement or lower limb injuries [17]. These applications would immensely benefit from long term and continuous monitoring of gait in patients' natural ecology. In contrast to fixed sensors such as motion capture systems and force places found in gait labs; inertial sensors can be used for gait analysis in daily life as they are unobtrusive, cheap, miniature and wearable.

The goal of Paper I was to propose a new method that can detect gait events from accelerometer signals. The method was shown to be robust and effectively tackle real-world challenges such as varying gait speeds, different walking surfaces and surface inclinations, and changes in sensor axes orientation. The gait event detection results were compared to two state-of-the-art methods for experiments conducted in different environments such as indoor flat space, treadmill and outdoor street. Two 3-axes Shimmer3 accelerometers were positioned at the ankles of each subject and force sensitive resistors

(FSRs) were embedded in the shoes to simultaneously collect ground truth information.

The proposed method was based on utilizing domain knowledge in the form of fundamental spectral relationships present in gait to drive time-frequency analysis of the acceleration signals. Domain knowledge was used to logically reason around choosing the Morlet wavelet to compute the continuous wavelet transform (CWT) and represent the acceleration signal simultaneously in both, time & frequency. A running window was taken across the CWT coefficients and the energy density spectrum was computed in every window to highlight the major frequencies associated with gait event and cycle. As the energy density spectrum profile shifts along the spectral axis in response to different gait speeds, a tracking procedure was designed to track these major frequencies varying in time. The information extracted from the tracking procedure was used to define a spectral-temporal search space within which the gait event was estimated.

The results showed that the proposed method performed well when compared to gait events detected using FSRs. It demonstrated good performance as other methods for the activity of steady walking in an indoor flat space, but outperformed other methods when the gait speeds were varied; especially for walking and running in an outdoor street. This was probably due to the fact that there is larger variation in the acceleration signals collected from walking and running in an unstructured environment such as an outdoor street in comparison to steady walking in a well-structured indoor corridor. As such, while the proposed method utilized spectral relationships in gait that remain unchanged; the other methods are unable to adapt as they are purely data driven with numerous tuning parameters.

Paper I contributed to this thesis by presenting a robust gait event detection method that helps in enabling long-term and continuous gait analysis in everyday life. It also illustrates how domain knowledge about gait could be formulated and used to guide the signal analysis. Additionally, the paper shows how domain knowledge is used to logically reason around choosing a mother wavelet to compute the CWT of the acceleration signal.

4.2 Paper II - Evaluation of the performance of accelerometer-based gait event detection algorithms in different real-world scenarios using the MAREA gait database

Although the major argument of using inertial sensors over fixed sensors such as high-speed cameras and force plates is that they can be easily used in

everyday life, almost all existing gait event detection methods have been developed and assessed using data collected in well-structured and highly controlled indoor conditions with pre-defined paths and walking speeds. Thus, it is presently unclear and remains to be seen how these methods perform in other environments and lesser controlled conditions [67]. Moreover, there is a lack of publicly-available gait databases that consist of data collected outside indoor corridors and other real-world settings.

The objective of Paper II was to present a new gait database called MAREA (Movement Analysis in Real-world Environments using Accelerometers) and benchmark the performance of six state-of-the-art gait event detection algorithms in different scenarios constructed using the database. The selected methods were developed from accelerometers positioned on the lower leg, such as forefoot, ankle and shank. It was also shown that non-parametric statistical tests could be used to provide an overview of the detection accuracy of a method and that the traditionally used Mean Absolute Error is not enough to indicate the overall performance of a method.

The database consisted of walking and running activities done by 20 healthy subjects in indoor flat space, treadmill and outdoor street, with accelerometers positioned on waist, wrist and both ankles. From this five different scenarios were constructed to reflect varying real-world situations on which the state-of-the-art methods were evaluated. In addition to presenting the absolute temporal accuracy of each method, the F1 score was computed and two non-parametric statistical tests (Kolmogorov-Smirnov test and Mann-Whitney U test) were employed to compare the shape of stride time distributions obtained from each method and corresponding ground truth datasets.

The results reveal that the performance of these algorithms is inconsistent and varies with changing environments and gait speeds. All algorithms demonstrated good performance for the scenario of steady walking in a controlled indoor environment but exhibited significantly decreased performance when evaluated in other lesser controlled scenarios such as walking and running in an outdoor street. This is probably due to the use of many tuning parameters and spatial or temporal thresholds in the algorithmic design which renders them unable to adapt to large variations such as differences in gait speeds. Additionally, it may be attributed to fact that many methods process individual axis signals obtained from pre-defined axes alignment fixed relative to the limb with the assumption that they shall remain static throughout the experiment. However, deviations from original configuration are likely to occur in uncontrolled scenarios and everyday life conditions.

Paper II contributed to this thesis by showing that methods developed and previously assessed in highly controlled indoor conditions with the argument of use in daily living, demonstrate significantly lower performance in lesser controlled and structured conditions such as an outdoor street. Additionally, the paper shows how non-parametric statistical tests could be used to assess the overall detection accuracy of a method.

4.3 Paper III - Novel Methodology for Estimating Initial Contact Events from Accelerometers positioned at Different Body Locations

Most gait event detection algorithms are designed for a specific body location such as ankle, shank, waist, chest, arm, etc [57]. Although choosing a position is application-dependent, it restricts the patient to wear the sensor at that pre-defined location throughout the study. This can be problematic, especially for long-term or continuous monitoring of gait during daily life, where either the patient may not comply and change the original sensor location or take-off and re-attach the sensor, thus disturbing the original alignment. Hence there is a need for robust algorithms that can detect gait events with high accuracy from different body locations.

The objective of Paper III was to present a methodology called DK-TiFA (Domain Knowledge in Time-Frequency Analysis) that can detect Initial Contact events from different body locations. In order to assess the performance, DK-TiFA was benchmarked on four large publicly available gait databases consisting of total seven unique body locations [35, 87, 50, 42]. It was shown that the proposed methodology demonstrated high accuracy and robustness for estimating Initial Contact events from data consisting of different accelerometer specifications, varying gait speeds and different environments.

The proposed methodology builds on the approach presented in Paper I by extending the domain knowledge about spectral relationships present in gait (previously formulated for the ankles), to other parts of the body. For each location, a running window was taken along the CWT coefficients of the acceleration signal and the energy density spectrum was computed in every window to highlight the dominant spectral frequencies (or scales). Next, a tracking procedure was designed to consistently track the most dominant spectral energy scale in every window. This information was used to obtain a distinct temporal signal where the local maxima points in the signal corresponded to the estimated Initial Contact events.

The results showed that the proposed methodology performed well when applied to different gait databases. Non-parametric statistical tests and Bland-Altman analysis were used to assess the accuracy and overall performance of applying the method to acceleration signals collected from different body locations. However, it was observed that the proposed methodology demonstrated lower performance for estimating events from placements on the arm such as wrist and upper arm. This was due to the fact that the tracking procedure was unable to effectively tackle rapid changes in arm swing behaviour of the subjects.

Paper III contributed to this thesis by presenting a methodology that is capable of estimating Initial Contact events from different body locations. This

helps in enabling gait analysis in daily life by overcoming patient compliance and other practical sensor location issues, likely to occur in real-life settings.

Chapter 5
Discussion

The goal of the work presented in this thesis was to develop methods that could detect gait events in real-world conditions from inertial sensor signals. This requires the methods to be robust to changes in original sensor configuration, different environments, variations in gait speeds and adapt to multiple body locations. While this thesis addresses many of these issues, there are other practical and application-based requirements which may arise when implementing the proposed methodology in real-world situations. Moreover, there are some methodological limitations which may restrict its direct use in various applications and require future work.

One such requirement may be that the method should be online or fast enough to be executed in near real-time. Currently, the proposed method is offline as it requires temporal windowing of the CWT coefficients to extract relevant information from every window which is then compiled together in a later step. One approach, to render it online would be to parse the sensor signal in chunks of some size and run the algorithm over each such chunk of data. The windowing is necessary to adapt the method to varying gait speeds and as such could be avoided for studies where the gait speeds remain fairly constant, such as walking with preferred walking speed. Also, currently the method is implemented in MATLAB® v8.5 (MathWorks, USA) with in-built functions and routines. The execution speed may be increased by migrating to a low-level language such as C/C++ and using faster routines for computationally expensive operations; such as calculating the CWT coefficients which is a essentially convolving two signals. Overall, future work is required for figuring out optimal ways of converting the proposed methodology online.

Monitoring a patient over longer periods of time would generate sensor data that consists of activities other than just walking such as sleeping, sitting and other daily living activities. A limitation of the proposed method is that it can be implemented only on walking segments of the sensor signal as it does not distinguish between walking and non-walking tasks. A possible solution may be to integrate an activity recognition algorithm that can extract walk-

ing segments from the raw data and then parse it to the proposed method. Additionally, as the method avoids thresholds and uses little tuning parameters, the sampling frequency may be varied depending on the activity. Thus for non-walking tasks the data could be sampled at lower rates to save energy and increase battery-life and switched to higher sampling rates during walking to obtain better detection accuracies.

The algorithms designed in Paper I and Paper III take a temporal window along the CWT coefficients to track the varying gait speeds. However, the algorithms are unable to adapt to very fast transitions in gait speeds as they cause large shifts in local signal energy. Thus, depending on the window size, this leads to an energy density spectrum profile which is a combination of two very different gait speeds with overlapping event and cycle regions from the CWT coefficients corresponding to each speed. For example, this is seen in Paper I where both constraints are not satisfied and curve is fit over the profile which may still not satisfy the set constraints. Another similar example is seen in Paper III where the algorithm is unable to adapt to fast changes in arm swing motion of the subjects.

Choosing a sensor location for an application may depend on numerous aspects such as the body part to be studied, practical issues such comfort and ease of use, aesthetic appeal, number of sensors, etc. Although Paper III aims to present a method that can detect HS from multiple locations, it does not do so autonomously and requires the location information as an input to the algorithm. Also, while Paper I shows how to detect both HS and TO from sensors located at the ankles, future work is required to extend the methodology to detect TOs from upper body locations such as waist. This would be challenging as the TO forces experienced in the upper body parts is much less in magnitude compared to the feet and there may be overlapping forces such as HS of the other foot and local body movements. On the other hand, it would be advantageous as instead of two sensors (placed at the ankles) required to obtain gait events from both legs, only one sensor (placed on the upper body) would be enough.

A current limitation is that the presented algorithms have been tested only on healthy gait. This was because there is lack of any publicly-available pathological gait databases. Although, I believe that in a similar fashion, domain knowledge could be adapted and coupled with time-frequency analysis to tackle issues with pathological gait. But that being said, extremely challenging gait behaviors such as shuffling gait with no well-defined gait events would warrant deeper investigation.

For further development of gait analysis, I believe it is necessary to not only conduct experiments in laboratory settings but also move out and perform experiments in patients' daily lives. This would help in understanding user behaviors such as preferred sensor location, gauging practical requirements such as system specifications, data storage, data privacy, battery-life, feedback to users, and simultaneously drive the development of robust algo-

rithms. Also, with homes and offices now being equipped with various sensors, fusing the information from fixed and wearable sensing modalities would yield much richer raw and contextual information about the patient's movements; leading to newer interventions and improved support systems.

Chapter 6
Conclusions and Future Work

This thesis deals with performing gait analysis, and in particular estimating gait events, using inertial sensors in real-world settings. Traditionally, such analysis is carried out in laboratory or similar settings, imposing a number of assumptions and restrictions on the experimental protocols. Inertial sensors are cheap, durable, low-powered and unobtrusive which makes them convenient for use in daily living and enable long-term health-related applications. However, they yield noisy signals and require robust algorithms for data analysis.

This thesis presents the use of domain knowledge about gait and shows how it can be formulated and applied to guide the analysis of gait signals. Based on domain knowledge, continuous wavelet transform is used by selecting an appropriate mother wavelet which yields an intermediate data representation that is more comprehensible and facilitates further analysis. The thesis also suggests the use of non-parametric statistical tests in addition to traditionally used error metrics to assess the accuracy and performance of gait event detection methods. The presented methodology serves as blueprint for formulating domain knowledge for estimating periodically occurring events from other related biosignals.

A database called MAREA is presented that consists of gait activities performed in different settings such as indoor space, treadmill and outdoor street; with sensors positioned on different body locations (made publicly available at `http://islab.hh.se/mediawiki/Gait_database`). It is shown that existing methods show inconsistent performance across different scenarios constructed using the database. The thesis presents a robust method that is capable of detecting gait events from sensors positioned at the ankles with excellent accuracy in different environments and gait speeds. Domain knowledge is used to extend the method to estimate initial contact events from multiple body locations such as ankle, thigh, waist, chest, upper arm and wrist; and is benchmarked on three other publicly-available gait databases.

The presented methodology has its limitations and requires further work. The designed algorithms are offline and work only on walking segments of the

raw input signals. One way to deal with this would be to integrate existing activity recognition methods in order to segregate walking and non-walking activities from the raw sensor signals. Next, the walking sections would be parsed in batches and the algorithms would be applied on each batch of raw walking data.

Furthermore, the presented methodology has been tested only on healthy gait and future work is required to adapt it to pathological gait. This could potentially open doors to new possibilities by enabling continuous monitoring of neuro-physiological patients (such as Parkinson's Disease) in their natural environment and continually obtain their gait parameters such as step time, stride time, stance and swing time. By studying how these parameters vary over time (such as stride time variability) in response to medicine or interventions could not only provide objective information but also help in observing their effects over different time scales, planning better protocols and developing new tools for assessing disease severity.

References

[1] Paul S Addison, James Walker, and Rodrigo C Guido. Time–frequency analysis of biosignals. IEEE engineering in medicine and biology magazine, 28(5), 2009. (Cited on pages 19 and 21.)

[2] Gilles Allali, Marian Van Der Meulen, and Frédéric Assal. Gait and cognition: the impact of executive function. Schweizer Archiv fur Neurologie und Psychiatrie, 161(6):195–199, 2010. (Cited on page 9.)

[3] B Alsberg. An introduction to wavelet transforms for chemometricians: A time-frequency approach. Chemometrics and Intelligent Laboratory Systems, 37(2):215–239, jun 1997. (Cited on pages 17 and 19.)

[4] Kamiar Aminian, B Najafi, C Büla, P-F Leyvraz, and Ph Robert. Spatio-temporal parameters of gait measured by an ambulatory system using miniature gyroscopes. Journal of biomechanics, 35(5):689–699, 2002. (Cited on pages 12 and 13.)

[5] Min S H Aung, Sibylle B Thies, Laurence P J Kenney, David Howard, Ruud W , Andrew H Findlow, and John Y Goulermas. Automated detection of instantaneous gait events using time frequency analysis and manifold embedding. IEEE transactions on Neural systems and Rehabilitation engineering, 21(6):908–16, Nov 2013. (Cited on pages 11, 12, 13, 15, and 25.)

[6] Akin Avci, Stephan Bosch, Mihai Marin-Perianu, Raluca Marin-Perianu, and Paul Havinga. Activity recognition using inertial sensing for healthcare, wellbeing and sports applications: A survey. In Architecture of computing systems (ARCS), 2010 23rd international conference on, pages 1–10. VDE, 2010. (Cited on page 9.)

[7] Richard Baker, Jennifer L. McGinley, Michael H. Schwartz, Sarah Beynon, Adam Rozumalski, H. Kerr Graham, and Oren Tirosh. The gait profile score and movement analysis profile. Gait & Posture, 30(3):265 – 269, 2009. (Cited on page 9.)

[8] Noël C Barengo, Gang Hu, Timo A Lakka, Heikki Pekkarinen, Aulikki Nissinen, and Jaakko Tuomilehto. Low physical activity as a predictor for total and cardiovascular disease mortality in middle-aged men and women in finland. European Heart Journal, 25(24):2204–2211, 2004. (Cited on page 9.)

[9] Noelia Chia Bejarano, Emilia Ambrosini, Alessandra Pedrocchi, Giancarlo Ferrigno, Marco Monticone, and Simona Ferrante. A novel adaptive, real-time algorithm to detect gait events from wearable sensors. IEEE Transactions on Neural Systems and Rehabilitation Engineering, 23(3):413–422, 2015. (Cited on page 12.)

[10] Dustin A Bruening and Sarah Trager Ridge. Automated event detection algorithms in pathological gait. Gait & posture, 39(1):472–7, 2014. (Cited on page 10.)

[11] Rafael Caldas, Marion Mundt, Wolfgang Potthast, Fernando Buarque de Lima Neto, and Bernd Markert. A systematic review of gait analysis methods based on inertial sensors and adaptive algorithms. Gait & Posture, 57:204 – 210, 2017. (Cited on page 11.)

[12] Michele L Callisaya, Leigh Blizzard, Michael D Schmidt, Jennifer L McGinley, and Velandai K Srikanth. Ageing and gait variability - a population-based study of older people. Age and ageing, page afp250, 2010. (Cited on page 9.)

[13] Bernard Cazelles, Mario Chavez, Dominique Berteaux, Frédéric Ménard, Jon Olav Vik, Stéphanie Jenouvrier, and Nils C Stenseth. Wavelet analysis of ecological time series. Oecologia, 156(2):287–304, May 2008. (Cited on page 21.)

[14] Henry G Chambers and David H Sutherland. A practical guide to gait analysis. Journal of the American Academy of Orthopaedic Surgeons, 10(3):222–231, 2002. (Cited on page 10.)

[15] T Chau. A review of analytical techniques for gait data. part 1: Fuzzy, statistical and fractal methods. Gait & posture, 13(1):49–66, feb 2001. (Cited on page 17.)

[16] T Chau. A review of analytical techniques for gait data. part 2: neural network and wavelet methods. Gait & posture, 13(2):102–20, apr 2001. (Cited on page 13.)

[17] S. Chen, J. Lach, B. Lo, and G. Z. Yang. Toward pervasive gait analysis with wearable sensors: A systematic review. IEEE Journal of Biomedical and Health Informatics, 20(6):1521–1537, Nov 2016. (Cited on pages 9, 11, and 31.)

[18] David Roxbee Cox and David Victor Hinkley. Theoretical statistics. CRC Press, 1979. (Cited on page 27.)

[19] UT Dallas. Walking in Graphs. `http://www.utdallas.edu/atec/midori/Handouts/walkingGraphs.htm`. [Online; accessed 2-Sep-2017]. (Cited on page 3.)

[20] Eric Desailly, Yepremian Daniel, Philippe Sardain, and Patrick Lacouture. Foot contact event detection using kinematic data in cerebral palsy children and normal adults gait. Gait & posture, 29(1):76–80, 2009. (Cited on page 10.)

[21] V Dietz. Neurophysiology of gait disorders: present and future applications. Electroencephalography and clinical neurophysiology, 103(3):333–55, Sep 1997. (Cited on pages 3, 9, and 31.)

[22] Pia M Forsman, Esko M Toppila, and EO Haeggstrom. Wavelet analysis to detect gait events. In Engineering in Medicine and Biology Society, 2009. EMBC 2009. Annual International Conference of the IEEE, pages 424–427. IEEE, 2009. (Cited on page 13.)

[23] A Godfrey, R Conway, D Meagher, and G ÓLaighin. Direct measurement of human movement by accelerometry. Medical engineering & physics, 30(10):1364–1386, 2008. (Cited on pages 9 and 11.)

[24] Darwin Gouwanda and SMN Arosha Senanayake. Application of hybrid multi-resolution wavelet decomposition method in detecting human walking gait events. In Soft Computing and Pattern Recognition, 2009. SOCPAR'09. International Conference of, pages 580–585. IEEE, 2009. (Cited on pages 12 and 13.)

[25] Barry R Greene, Denise McGrath, Ross O'Neill, Karol J O'Donovan, Adrian Burns, and Brian Caulfield. An adaptive gyroscope-based algorithm for temporal gait analysis. Medical & biological engineering & computing, 48(12):1251–1260, 2010. (Cited on page 12.)

[26] Michael Hanlon and Ross Anderson. Real-time gait event detection using wearable sensors. Gait & posture, 30(4):523–527, 2009. (Cited on page 10.)

[27] Brad D. Hendershot, Caitlin E. Mahon, and Alison L. Pruziner. A comparison of kinematic-based gait event detection methods in a self-paced treadmill application. Journal of Biomechanics, 49(16):4146 – 4149, 2016. (Cited on page 10.)

[28] Trienke IJmker and Claudine JC Lamoth. Gait and cognition: the relationship between gait stability and variability with executive function in

persons with and without dementia. Gait & posture, 35(1):126–130, 2012. (Cited on pages 3 and 9.)

[29] Verne T Inman. Human locomotion. Canadian Medical Association Journal, 94(20):1047, 1966. (Cited on page 16.)

[30] Delaram Jarchi, Charence Wong, Richard Mark Kwasnicki, Ben Heller, Garry A Tew, and Guang-Zhong Yang. Gait parameter estimation from a miniaturized ear-worn sensor using singular spectrum analysis and longest common subsequence. Biomedical Engineering, IEEE Transactions on, 61(4):1261–1273, 2014. (Cited on page 12.)

[31] Jan M Jasiewicz, John HJ Allum, James W Middleton, Andrew Barriskill, Peter Condie, Brendan Purcell, and Raymond Che Tin Li. Gait event detection using linear accelerometers or angular velocity transducers in able-bodied and spinal-cord injured individuals. Gait & Posture, 24(4):502–509, 2006. (Cited on pages 12 and 15.)

[32] D. Joshi, B. H. Nakamura, and M. E. Hahn. A novel approach for toe off estimation during locomotion and transitions on ramps and level ground. IEEE Journal of Biomedical and Health Informatics, 20(1):153–157, Jan 2016. (Cited on pages 11, 12, and 13.)

[33] Justin J Kavanagh and Hylton B Menz. Accelerometry: a technique for quantifying movement patterns during walking. Gait & posture, 28(1):1–15, 2008. (Cited on page 11.)

[34] Siddhartha Khandelwal and Nicholas Wickström. Gait event detection in real-world environment for long-term applications: Incorporating domain knowledge into time-frequency analysis. IEEE transactions on neural systems and rehabilitation engineering, 24(12):1363–1372, 2016. (Cited on pages 12 and 25.)

[35] Siddhartha Khandelwal and Nicholas Wickström. Evaluation of the performance of accelerometer-based gait event detection algorithms in different real-world scenarios using the {MAREA} gait database. Gait & Posture, 51:84 – 90, 2017. (Cited on pages 12, 25, and 34.)

[36] Siddhartha Khandelwal and Nicholas Wickström. Novel methodology for estimating initial contact events from accelerometers positioned at different body locations. submitted to Gait & Posture, 2017. (Cited on page 12.)

[37] Rita M. Kiss. Comparison between kinematic and ground reaction force techniques for determining gait events during treadmill walking at different walking speeds. Medical Engineering & Physics, 32(6):662 – 667, 2010. (Cited on page 10.)

[38] Martin Krzywinski and Naomi Altman. Points of significance: Nonparametric tests. Nature methods, 11(5):467–468, 2014. (Cited on page 29.)

[39] H-K Lee, J You, S-P Cho, S-J Hwang, D-R Lee, Y-H Kim, and K-J Lee. Computational methods to detect step events for normal and pathological gait evaluation using accelerometer. Electronics letters, 46(17):1185–1187, 2010. (Cited on page 12.)

[40] Jung Keun Lee and Edward J Park. Quasi real-time gait event detection using shank-attached gyroscopes. Medical & biological engineering & computing, 49(6):707–712, 2011. (Cited on page 12.)

[41] Jessica Leitch, Julie Stebbins, Gabriele Paolini, and Amy B Zavatsky. Identifying gait events without a force plate during running: A comparison of methods. Gait & posture, 33(1):130–132, 2011. (Cited on page 25.)

[42] Heike Leutheuser, Dominik Schuldhaus, and Bjoern M Eskofier. Hierarchical, multi-sensor based classification of daily life activities: comparison with state-of-the-art algorithms using a benchmark dataset. PloS one, 8(10):e75196, 2013. (Cited on pages 12 and 34.)

[43] Sue Lord, Tracey Howe, Julia Greenland, Linda Simpson, and Lynn Rochester. Gait variability in older adults: A structured review of testing protocol and clinimetric properties. Gait & Posture, 34(4):443 – 450, 2011. (Cited on page 9.)

[44] I. H. López-Nava and A. Muñoz-Meléndez. Wearable inertial sensors for human motion analysis: A review. IEEE Sensors Journal, 16(22):7821–7834, Nov 2016. (Cited on page 9.)

[45] Avril Mansfield and Gerard M Lyons. The use of accelerometry to detect heel contact events for use as a sensor in fes assisted walking. Medical engineering & physics, 25(10):879–885, 2003. (Cited on pages 3 and 15.)

[46] John McCamley, Marco Donati, Eleni Grimpampi, and Claudia Mazza. An enhanced estimate of initial contact and final contact instants of time using lower trunk inertial sensor data. Gait & posture, 36(2):316–318, 2012. (Cited on pages 12, 13, and 25.)

[47] Adam Miller. Gait event detection using a multilayer neural network. Gait & posture, 29(4):542–545, 2009. (Cited on page 13.)

[48] Peter M Mills, Rod S Barrett, and Steven Morrison. Agreement between footswitch and ground reaction force techniques for identifying gait events: Inter-session repeatability and the effect of walking speed. Gait & posture, 26(2):323–326, 2007. (Cited on page 10.)

[49] Alvaro Muro-de-la Herran, Begonya Garcia-Zapirain, and Amaia Mendez-Zorrilla. Gait analysis methods: an overview of wearable and non-wearable systems, highlighting clinical applications. Sensors (Basel, Switzerland), 14(2):3362–94, 2014. (Cited on pages 10 and 11.)

[50] Thanh Trung Ngo, Yasushi Makihara, Hajime Nagahara, Yasuhiro Mukaigawa, and Yasushi Yagi. The largest inertial sensor-based gait database and performance evaluation of gait-based personal authentication. Pattern Recognition, 47(1):228–237, 2014. (Cited on pages 12 and 34.)

[51] Ciara M O'Connor, Susannah K Thorpe, Mark J O'Malley, and Christopher L Vaughan. Automatic detection of gait events using kinematic data. Gait & posture, 25(3):469–474, 2007. (Cited on page 10.)

[52] Ion PI Pappas, Milos R Popovic, Thierry Keller, Volker Dietz, and Manfred Morari. A reliable gait phase detection system. Neural Systems and Rehabilitation Engineering, IEEE Transactions on, 9(2):113–125, 2001. (Cited on pages 11, 12, and 13.)

[53] Kara K. Patterson, William H. Gage, Dina Brooks, Sandra E. Black, and William E. McIlroy. Evaluation of gait symmetry after stroke: A comparison of current methods and recommendations for standardization. Gait & Posture, 31(2):241 – 246, 2010. (Cited on page 9.)

[54] J. Rafiee, M. A. Rafiee, N. Prause, and M. P. Schoen. Wavelet basis functions in biomedical signal processing. Expert Systems with Applications, 38(5):6190–6201, 2011. (Cited on pages 13, 17, and 21.)

[55] N. F. Ribeiro and C. P. Santos. Inertial measurement units: A brief state of the art on gait analysis. In 2017 IEEE 5th Portuguese Meeting on Bioengineering (ENBENG), pages 1–4, Feb 2017. (Cited on page 11.)

[56] Jan Rueterbories, Erika G Spaich, and Ole K Andersen. Gait event detection for use in fes rehabilitation by radial and tangential foot accelerations. Medical engineering & physics, 36(4):502–8, Apr 2014. (Cited on pages 3, 12, and 25.)

[57] Jan Rueterbories, Erika G Spaich, Birgit Larsen, and Ole K Andersen. Methods for gait event detection and analysis in ambulatory systems. Medical engineering & physics, 32(6):545–552, 2010. (Cited on pages 11 and 34.)

[58] Heydar Sadeghi, Paul Allard, François Prince, and Hubert Labelle. Symmetry and limb dominance in able-bodied gait: a review. Gait & Posture, 12(1):34 – 45, 2000. (Cited on page 9.)

[59] Anita Sant'Anna. A Symbolic Approach to Human Motion Analysis Using Inertial Sensors : Framework and Gait Analysis Study. PhD thesis, 2012. (Cited on pages 2, 9, and 13.)

[60] Anita Sant'Anna and Nicholas Wickström. A symbol-based approach to gait analysis from acceleration signals: Identification and detection of gait events and a new measure of gait symmetry. Information Technology in Biomedicine, IEEE Transactions on, 14(5):1180–1187, 2010. (Cited on pages 9, 12, 13, and 25.)

[61] L.M. Schutte, U. Narayanan, J.L. Stout, P. Selber, J.R. Gage, and M.H. Schwartz. An index for quantifying deviations from normal gait. Gait & Posture, 11(1):25 – 31, 2000. (Cited on page 9.)

[62] Michael H. Schwartz and Adam Rozumalski. The gait deviation index: A new comprehensive index of gait pathology. Gait & Posture, 28(3):351 – 357, 2008. (Cited on page 9.)

[63] R. W. Selles, M. A. G. Formanoy, J. B. J. Bussmann, P. J. Janssens, and H. J. Stam. Automated estimation of initial and terminal contact timing using accelerometers; development and validation in transtibial amputees and controls. IEEE Transactions on Neural Systems and Rehabilitation Engineering, 13(1):81–88, 2005. (Cited on pages 12, 15, and 25.)

[64] Pete B Shull, Wisit Jirattigalachote, Michael A Hunt, Mark R Cutkosky, and Scott L Delp. Quantified self and human movement: a review on the clinical impact of wearable sensing and feedback for gait analysis and intervention. Gait & posture, 40(1):11–19, 2014. (Cited on page 11.)

[65] B. T. Smith, D. J. Coiro, R. Finson, R. R. Betz, and J. McCarthy. Evaluation of force-sensing resistors for gait event detection to trigger electrical stimulation to improve walking in the child with cerebral palsy. IEEE Transactions on Neural Systems and Rehabilitation Engineering, 10(1):22–29, March 2002. (Cited on page 10.)

[66] Laura Smith, Stephen Preece, Duncan Mason, and Christopher Bramah. A comparison of kinematic algorithms to estimate gait events during overground running. Gait & posture, 41(1):39–43, 2015. (Cited on pages 10 and 25.)

[67] Anke H Snijders, Bart P van de Warrenburg, Nir Giladi, and Bastiaan R Bloem. Neurological gait disorders in elderly people: clinical approach and classification. The Lancet Neurology, 6(1):63–74, Jan 2007. (Cited on pages 1 and 33.)

[68] Rahul Soangra, Thurmon E Lockhart, and Nathalie Van de Berge. An approach for identifying gait events using wavelet denoising technique and

single wireless IMU. In Proceedings of the Human Factors and Ergonomics Society Annual Meeting, volume 55, pages 1990–1994. SAGE Publications Sage CA: Los Angeles, CA, 2011. (Cited on page 13.)

[69] Sebastijan Sprager and Matjaz B. Juric. Inertial sensor-based gait recognition: A review. Sensors, 15(9):22089–22127, 2015. (Cited on page 11.)

[70] Fabio A. Storm, Christopher J. Buckley, and Claudia Mazzà. Gait event detection in laboratory and real life settings: Accuracy of ankle and waist sensor based methods. Gait & Posture, 50:42 – 46, 2016. (Cited on page 12.)

[71] D.H. Sutherland. The evolution of clinical gait analysis: Part II kinematics. Gait & Posture, 16(2):159 – 179, 2002. (Cited on page 1.)

[72] D.H. Sutherland. The evolution of clinical gait analysis: Part III kinetics and energy assessment. Gait & Posture, 21(4):447 – 461, 2005. (Cited on page 1.)

[73] Qu Tian, Nathalie Chastan, Woei-Nan Bair, Susan M. Resnick, Luigi Ferrucci, and Stephanie A. Studenski. The brain map of gait variability in aging, cognitive impairment and dementiaŮa systematic review. Neuroscience & Biobehavioral Reviews, 74:149 – 162, 2017. (Cited on page 9.)

[74] RR Torrealba, J Cappelletto, L Fermın-Leoın, JC Grieco, and G Fernández-López. Statistics-based technique for automated detection of gait events from accelerometer signals. Electronics letters, 46(22):1483–1485, 2010. (Cited on pages 12 and 15.)

[75] Christopher Torrence and Gilbert P Compo. A practical guide to wavelet analysis. Bulletin of the American Meteorological society, 79(1):61–78, 1998. (Cited on page 21.)

[76] Diana Trojaniello, Andrea Cereatti, and Ugo Della Croce. Accuracy, sensitivity and robustness of five different methods for the estimation of gait temporal parameters using a single inertial sensor mounted on the lower trunk. Gait & posture, 40(4):487–492, 2014. (Cited on page 25.)

[77] Aliénor Vienne, Rémi P. Barrois, Stéphane Buffat, Damien Ricard, and Pierre-Paul Vidal. Inertial sensors to assess gait quality in patients with neurological disorders: A systematic review of technical and analytical challenges. Frontiers in Psychology, 8:817, 2017. (Cited on pages 11 and 31.)

[78] J.C. Wall and J. Crosbie. Accuracy and reliability of temporal gait measurement. Gait & Posture, 4(4):293 – 296, 1996. (Cited on page 10.)

[79] Darren ER Warburton, Crystal Whitney Nicol, and Shannon SD Bredin. Health benefits of physical activity: the evidence. Canadian medical association journal, 174(6):801–809, 2006. (Cited on page 9.)

[80] Michael W Whittle. Clinical gait analysis: A review. Human Movement Science, 15(3):369–387, 1996. (Cited on page 10.)

[81] R Williamson and B J Andrews. Gait event detection for FES using accelerometers and supervised machine learning. IEEE transactions on rehabilitation engineering : a publication of the IEEE Engineering in Medicine and Biology Society, 8(3):312–9, Sep 2000. (Cited on pages 3, 12, 13, and 15.)

[82] Oliver J Woodman. An introduction to inertial navigation. Technical report, University of Cambridge, Computer Laboratory, 2007. (Cited on page 11.)

[83] Marjorie Woollacott and Anne Shumway-Cook. Attention and the control of posture and gait: a review of an emerging area of research. Gait & posture, 16(1):1–14, Aug 2002. (Cited on page 3.)

[84] Tishya AL Wren, George E Gorton, Sylvia Ounpuu, and Carole A Tucker. Efficacy of clinical gait analysis: A systematic review. Gait & posture, 34(2):149–153, 2011. (Cited on page 3.)

[85] Mitsuru Yoneyama, Yosuke Kurihara, Kajiro Watanabe, and Hiroshi Mitoma. Accelerometry-based gait analysis and its application to parkinson's disease assessment part 1: Detection of stride event. Neural Systems and Rehabilitation Engineering, IEEE Transactions on, 22(3):613–622, 2014. (Cited on pages 12, 15, and 25.)

[86] JA Zeni, JG Richards, and JS Higginson. Two simple methods for determining gait events during treadmill and overground walking using kinematic data. Gait & posture, 27(4):710–714, 2008. (Cited on page 10.)

[87] Yuting Zhang, Gang Pan, Kui Jia, Minlong Lu, Yueming Wang, and Zhaohui Wu. Accelerometer-based gait recognition by sparse representation of signature points with clusters. IEEE transactions on cybernetics, 45(9):1864–1875, 2015. (Cited on pages 12 and 34.)

[88] Wiebren Zijlstra and At L Hof. Assessment of spatio-temporal gait parameters from trunk accelerations during human walking. Gait & posture, 18(2):1–10, Oct 2003. (Cited on pages 12 and 25.)

Appendix I

Paper I - Gait Event Detection in Real-World Environment for Long-Term Applications: Incorporating Domain Knowledge Into Time-Frequency Analysis

Gait Event Detection in Real-World Environment for Long-Term Applications: Incorporating Domain Knowledge Into Time-Frequency Analysis

Siddhartha Khandelwal and Nicholas Wickström, *Member, IEEE*

***Abstract*—Detecting gait events is the key to many gait analysis applications that would benefit from continuous monitoring or long-term analysis. Most gait event detection algorithms using wearable sensors that offer a potential for use in daily living have been developed from data collected in controlled indoor experiments. However, for real-word applications, it is essential that the analysis is carried out in humans' natural environment; that involves different gait speeds, changing walking terrains, varying surface inclinations and regular turns among other factors. Existing domain knowledge in the form of principles or underlying fundamental gait relationships can be utilized to drive and support the data analysis in order to develop robust algorithms that can tackle real-world challenges in gait analysis. This paper presents a novel approach that exhibits how domain knowledge about human gait can be incorporated into time-frequency analysis to detect gait events from long-term accelerometer signals. The accuracy and robustness of the proposed algorithm are validated by experiments done in indoor and outdoor environments with approximately 93 600 gait events in total. The proposed algorithm exhibits consistently high performance scores across all datasets in both, indoor and outdoor environments.**

***Index Terms*—Accelerometer, gait analysis, inertial sensors, morlet, principles of gait, stride parameters, wavelet transform.**

I. Introduction

NORMAL gait consists of three primary components: locomotion, balance and ability to adapt to the environment [1]. This requires a balance between various interacting neuronal and musculoskeletal systems. Dysfunction in one or more of these systems can disturb gait, which elucidates the importance of gait analysis. In the temporal domain, the two most relevant events in a normal gait cycle are heel strike (HS) and toe off (TO); other parameters such as swing, stance and stride duration can be computed from them. Thus, identifying these events is the key to many gait analysis applications [2]–[9] that would benefit from long-term, continuous monitoring in humans' natural environment, enabling gait assessment and interventions that have not previously been possible [10]. The present state of practice is to perform clinical gait analysis in controlled gait labs equipped with stationary sensor systems such as motion capture systems and force plates [11]. Although these systems provide rich and accurate information, they are inadequate for use in daily life as they are immobile, expensive, require high operational competence and provide information that is restricted to only a couple of steps. Foot switches such as force sensitive resistors (FSRs) provide contact timing information and are often used as the reference method in determining the accuracy of gait event detection in other systems [2], [12]–[14]. However, they do not provide any kinematic data or spatial information during swing phase, which are important aspects in pathological gait assessment [15]. Alternatively, inertial sensors such as accelerometers and gyroscopes can be used for gait assessment as they provide spatio-temporal information and can be used in combination to estimate parameters such as the trajectory of foot during gait [16]. Technological advancements have made them miniature, low-powered, durable, inexpensive and highly mobile, thus making it possible to collect long-term data from daily life. While some researchers have developed gait event detection algorithms from gyroscope data, others have developed from accelerometer signals [17]. In either of these situations, researchers could potentially benefit by applying improved algorithms to existing gait databases and utilizing them for future applications and further gait analysis. In the context of gyro-based algorithms, many methods have been developed from angular velocity signals obtained from shank-attached gyroscopes. For example, the approach in [18] uses adaptive thresholds while [13], [19] use peak detection to identify HS and TO from angular velocity signals. Other approaches include [20], where the gait cycle is divided into four gait phases represented in the form of a state machine and the transitions are governed by a knowledge-based algorithm, and [21], where an online Hidden Markov Model based method is presented. In [12], a wavelet based method is used to search for peaks associated with HS and TO which is modified in [22], such that the method can be used with minimal time delay. On the other hand, accelerometers are also being increasingly used as they are low powered devices, in the range of few microamperes, and have been shown to provide reliable measures of gait parameters [17], [23]. Most algorithms analyze signals obtained from individual accelerometer axis by positioning the sensor in a specific pre-defined orientation [2], [3], [13], [24]–[28] with the assumption that the accelerometer shall stay statically positioned throughout the experiment. However, it is quite likely that external factors might disturb the original configuration during long-term analysis [28], and thus either the axis alignment should be checked and readjusted fre-

Manuscript received June 04, 2015; revised October 29, 2015; accepted February 07, 2016. Date of publication March 02, 2016; date of current version December 06, 2016.

The authors are with the School of Information Technology, Halmstad University, 301 18 Halmstad, Sweden (e-mail: siddhartha.khandelwal@hh.se; nicholas.wickstrom@hh.se).

Color versions of one or more of the figures in this paper are available online at http://ieeexplore.ieee.org.

Digital Object Identifier 10.1109/TNSRE.2016.2536278

quently or the exact orientation of the accelerometer must be known throughout, to compensate for the misalignment of the axes. An alternative is to analyze the magnitude of the resultant accelerometer signal instead which makes it invariant to individual axis alignment, as done in [4], [29]. While some methodologies instruct subjects to walk in a straight line or a given path at a self-selected pace [4], [13], [27], [29], others either pre-define a set of walking speeds or ask the subjects to walk slowly, normal and fast, in order to test the algorithmic robustness to different velocities [3], [14], [24]–[26], [28]. A number of algorithms apply thresholds either to filtered accelerometer signals or use them at some intermediate stage after signal transformation, to perform peak detection for identifying events [25], [28], [29]. The performance of such algorithms is usually dependent on choosing the optimum values of these thresholds and tuning other parameters associated with them. Another approach is the use of machine learning techniques that depend strongly on labelled training data [2], [27]. Since they are data-driven approaches that resemble a black-box model [26], not only might they be difficult to interpret by clinicians [30] but it also remains unclear whether and how often such a system would need to be retrained with changing scenarios. Other approaches include [4], where a rule-based state machine is realized with four gait states, namely, mid-stance, pre-swing, swing and loading response; and the state transitions are determined by five reference signals derived from tri-axial accelerometer signals. In recent years, wavelet transforms are being increasingly used for gait analysis [31] and in particular to detect gait events [12], [27], [32]–[35]. In [27], wavelet transform is used to express the raw acceleration signals in time-frequency space which gives high dimensionality features. Then dimensionality reduction is done using a manifold embedding algorithm to project the data to a smaller dimensional subspace in order to obtain a minimal subset of features that contain salient signal information. Finally, a Gaussian mixture model (GMM) is applied to classify each time sample as HS, TO or no-event.

The existing gait event detection algorithms that offer potential for use in daily living have been developed from data collected in controlled indoor experiments placing a number of assumptions on the experimental design itself. On the other hand, human gait in the real-world is quite dynamic, and frequently involves different gait speeds, changing walking terrains, varying surface inclinations and regular turns among other things. Although some recent attempts have been made [27], it is highly challenging to imitate these scenarios in labs or corridors. However, portable wearable systems can be used to carry out long-term experiments directly in natural human environments. Moreover, it is essential to distinguish between walking and non-walking tasks prior to applying the event detection algorithms [36] unless such a feature is included in the algorithm itself. Instead of relying only on data-driven approaches, existing domain knowledge about the fundamental principles of gait and other prior auxiliary information could be used to help guide the data analysis in order to achieve greater robustness and accuracy. This paper proposes a novel approach that exhibits how domain knowledge about human gait can be incorporated into time-frequency analysis in order to detect gait events from walking and running segments of long-term accelerometer signals. The performance of the proposed method is validated by experiments done in indoor and outdoor environments, and the results are compared with two state of the art algorithms. The rest of this paper is organized as follows. Section II describes the proposed approach and Section III outlines the data collection procedure. Section IV presents the results of applying the algorithm in indoor and outdoor environments. Finally, Section V discusses and concludes this paper. The Appendix provides relevant details required to implement a part of the proposed algorithm.

II. Proposed Algorithm

A. Domain Knowledge

To detect gait events from long-term accelerometer signals, the algorithm should be able to tackle real-world issues such as different gait speeds, changing environments and disturbances in sensor orientation. To achieve this goal, domain knowledge in the form of principles or underlying fundamental gait relationships between various governing gait parameters can be utilized to drive and support the analysis. One such underlying gait principle is the frequency relationship that is present between gait event and gait cycle, i.e., the frequency of the event (HS and TO) is twice that of the cycle. In the proposed algorithm, the use of this knowledge is two-fold. The first is to logically reason around choosing the appropriate mother wavelet for wavelet transform, as there are insufficient guidelines on the selection of wavelet basis function for gait signals [31]. The second involves incorporating this fundamental frequency relationship into the signal analysis procedure, which allows the algorithm to effectively tackle changes in gait speeds. Thus, the raw acceleration signal is first pre-processed, and this is followed by time-frequency analysis guided by domain knowledge.

B. Time-Frequency Analysis

As mentioned in Section I, it is quite likely that the original sensor orientation may be disturbed during long-term analysis. Hence, to avoid misalignment issues, the magnitude of the resultant accelerometer signal, Acc_r, henceforth referred to as the "composite acceleration signal," is computed as

$$Acc_r = \sqrt{acc_x^2 + acc_y^2 + acc_z^2} \tag{1}$$

where acc_x, acc_y, acc_z are the signals obtained from each individual axis of the 3-axes accelerometer, respectively. Fig. 1(a) shows the HS and TO events present in one gait cycle of the composite acceleration signal. To exemplify the time-frequency relationship between gait event and gait cycle, continuous wavelet transform (CWT) is used [37]. It produces a time-frequency decomposition where both, short-duration high frequency and long-duration low frequency information can be captured simultaneously. Another key advantage of wavelet techniques is the variety of wavelet basis functions available for signal analysis [38]. Domain knowledge is used to select the appropriate wavelet based on the following criteria.

- It should highly correlate with both, the frequency of the events and the frequency of the cycle in Acc_r, in order to clearly distinguish these spectral components in time.

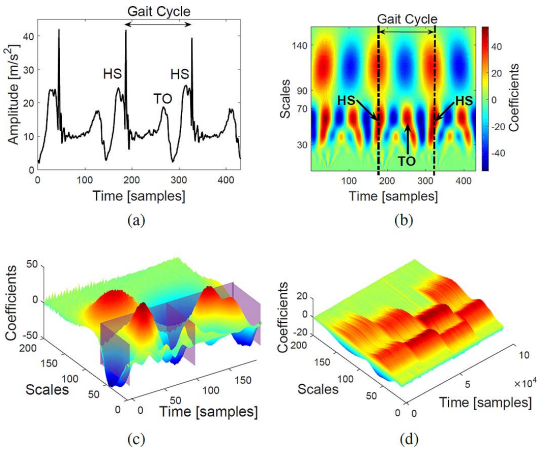

Fig. 1. (a) HS and TO events in one gait cycle of a composite acceleration signal, Acc_r, obtained from the 3-axis accelerometer attached to the right ankle. The amplitude of Acc_r is approx. 10 $\mathrm{m/s^2}$ during stance due to the effect of the gravitational component. (b) Time-frequency representation (top view) of the composite acceleration signal using CWT by the Morlet wavelet. HS and TO events exist in the finer scales (30–70) while the corresponding gait cycle exists along the coarser scales (90–140). Color bar presented in this subfigure is also applicable to subfigures Fig. 1(c) and (d). (c) Example of spectral-temporal boundary, shown as semi-transparent walls, around the HS and TO region in one gait cycle. (d) Example of CWT coefficients shifting along the spectral axis with changes in gait speed. With faster gait speeds, the event and cycle coefficients shift towards the finer scales and vice-versa.

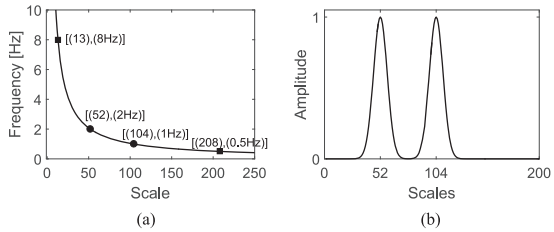

Fig. 2. (a) Frequency-scale relationship for Morlet wavelet. So, for example, if the minimum gait frequency is assumed to be 0.5 Hz, then the corresponding maximum scale to be considered for analysis is 208, denoted $s_{\max}$. (b) *A priori* energy density spectrum estimate E_s^- formulated by assuming the initial frequency of the event to be 2 Hz, i.e., $\mu_e^- = 52$ and $\sigma^- = 9$.

- It should be symmetric to avoid spectral domain skewness. Moreover, a wavelet with a high degree of symmetry leads to good performance for the analysis of periodic signals [39].

Thus, the Morlet wavelet is chosen, which is a complex sinusoid modulated by a Gaussian. It is defined as $\psi_0(\eta) = \pi^{-1/4} e^{i\omega_0 \eta} e^{-\eta^2/2}$ where ω_0 is the frequency and η is a nondimensional time parameter [40]. The CWT of a discrete time signal, x_n, with equal time spacing δ_t, is defined as the convolution of x_n with a scaled and translated mother wavelet $\psi_0(\eta)$

$$W_n(s) = \sum_{n'=0}^{N-1} x_{n'} \psi^* \left[\frac{(n'-n)\delta_t}{s} \right] \tag{2}$$

where the $(*)$ indicates the complex conjugate, s is the wavelet scaling factor and n is the localized time index. Fig. 1(b) shows the CWT of the Acc_r signal where the time-frequency relationship between the individual gait events of HS and TO and their corresponding gait cycle can be simultaneously observed. The event coefficients exist towards the finer scales that correspond to higher frequencies while the cycle coefficients exist towards the coarser scales corresponding to lower frequencies. As shown in Fig. 1(c), the event regions can be located by defining appropriate boundaries along the spectral and temporal axes and the position of the event can be derived by fitting a 2-D Gaussian distribution over this region. However, defining these boundaries is a challenging task as changes in gait speed cause the event and cycle coefficients to shift along the scales, as shown in Fig. 1(d), because of shifts in the local signal energy. Faster gait speeds mean higher gait frequency, and thus the event and cycle coefficients exist towards the finer scales and vice-versa. Hence, a tracking procedure is proposed that utilizes domain knowledge to detect these transitions along the scales such that the event regions can be determined.

Thus, as depicted in Fig. 4, the proposed algorithm consists of three major steps that are performed systematically. These steps are elaborated in the following subsections.

1) Pre-Processing: First, composite acceleration signal Acc_r is computed from the individual acceleration signals obtained from the 3-axes accelerometer using (1). Then, the CWT of this signal is computed using (2), by convoluting Acc_r with a scaled and translated real-valued Morlet wavelet to obtain $W_n(s)$. The range of scales to be considered for CWT can be estimated from the non-linear frequency-scale relationship of the Morlet [40], as shown in Fig. 2(a).

2) Tracking the Gait Speed Changes: As explained earlier, changes in gait speed cause transitions of the event and cycle coefficients along the scale or spectral axis and these transitions need to be detected in order to find appropriate event region boundaries. This is done by defining a tracking procedure that utilizes the domain knowledge about the frequency relationship between the gait event and cycle, i.e., the frequency of the event (HS and TO) is twice that of the cycle. The relative contribution of these two major frequencies to the total signal energy at a specific scale s can be measured by the scale-dependent energy density spectrum E_s, as

$$E_s = \sum_{n=0}^{N-1} |W_n(s)|^2, \quad s \in [1, s_{\max}] \tag{3}$$

where $|W_n(s)|^2$ is the 2-D wavelet energy density function known as the scalogram that measures the total energy distribution of the signal [37]. Peaks in E_s highlight the dominant energetic scales and it is the event and cycle peaks that contribute to most of the signal energy in the spectral domain. Thus, the energy density spectrum E_s, of the CWT coefficients can be approximated as a mixture of two 1-D Gaussian distributions,

where each Gaussian represents the spectral signal energy of the event and cycle, respectively as

$$E_s \approx \underbrace{a_e e^{-(s-\mu_e/\sigma_e)^2}}_{event} + \underbrace{a_c e^{-(s-\mu_c/\sigma_c)^2}}_{cycle}. \quad (4)$$

In addition, the event-cycle frequency relationship can be used to associate the two Gaussian means in E_s as

$$\mu_c = 2\mu_e \quad (5)$$

where μ_e and μ_c are the two most dominant scales representing event and cycle energy, respectively. Using this approximation, an *a priori* energy density spectrum estimate E_s^- is formulated which is used to start the tracking procedure. The value of Gaussian mean μ_e^- (in scale units) can be obtained from the frequency-scale relationship of the Morlet, shown in Fig. 2(a), by making an initial assumption of the frequency of the event. The corresponding μ_c^- is then computed using (5). Also for simplicity, both Gaussians are assumed to be of unit amplitude and equal standard deviation σ^-, well representing event and cycle energies. With these simplified initial parameters, E_s^- can be formulated [shown in Fig. 2(b)] as

$$E_s^- = e^{-(s-\mu_e^-/\sigma^-)^2} + e^{-(s-2\mu_e^-/\sigma^-)^2}, \quad s \in [1, s_{\max}]. \quad (6)$$

To track the transitions of event and cycle coefficients along the spectral axis, an overlapping running window is taken along the temporal axis of the CWT coefficients. Within each window, E_s is computed using (3) and is cross-correlated with the *a priori* estimate E_s^-, which helps in extracting event and cycle spectral information from E_s using the Gaussian approximation formulation given in (4). Based on the extracted information, the parameters in E_s^- are updated to form an *a posteriori* estimate $\hat{E}_s$, which serves as the prior for the next window. See the Appendix and Figs. 6 and 7 for details of the entire tracking procedure within a window.

3) Locating and Identifying the Gait Event: In order to set up appropriate boundaries to define spectral-temporal event regions as shown in Fig. 1(c), the information stored in the tracking procedure is utilized. The Gaussian means $\hat{\mu}_{e,r}$ and $\hat{\mu}_{c,r}$ that are stored in every window r hold information about the local frequency of the event and cycle for the time duration of that window. By successively compiling them from all windows and selecting the CWT coefficients at those particular scales, two distinct temporal signals are obtained that match the frequency of the event and cycle in the composite acceleration signal as shown in Fig. 3. The discrete time signal matching the frequency of the event, denoted x_n^e, is obtained as

$$x_n^e \triangleq W_n[(\hat{\mu}_{e,0}, \hat{\mu}_{e,1}, \ldots, \hat{\mu}_{e,r}, \ldots, \hat{\mu}_{e,N/M-1})^T] \quad (7)$$

where W_n is the CWT coefficients computed using (2), r is the window index, M is the window step, n is the discrete time sample and N is the total number of samples in the composite acceleration signal. Similarly, the discrete time signal matching the frequency of the cycle, denoted x_n^c, is obtained as

$$x_n^c \triangleq W_n[(\hat{\mu}_{c,0}, \hat{\mu}_{c,1}, \ldots, \hat{\mu}_{c,r}, \ldots, \hat{\mu}_{c,N/M-1})^T]. \quad (8)$$

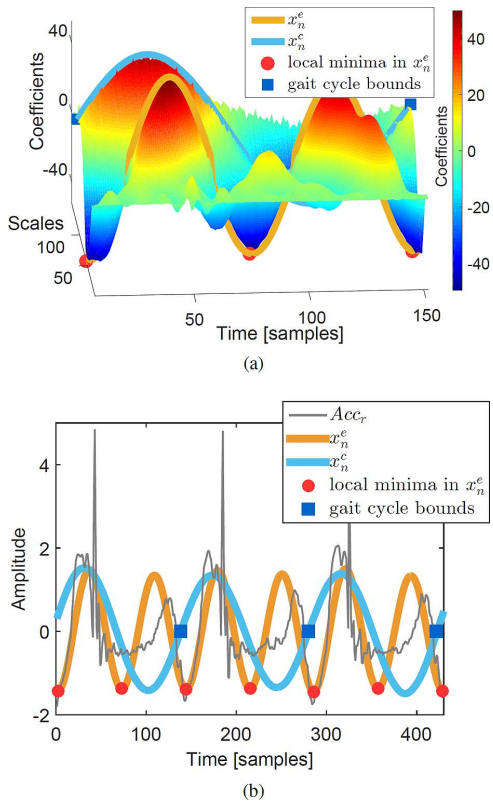

Fig. 3. (a) Figure shows CWT coefficients from one gait cycle. Two temporal signals, x_n^e and x_n^c, are obtained by selecting the CWT coefficients from scales corresponding to Gaussian means $\hat{\mu}_{e,r}$ and $\hat{\mu}_{c,r}$ that are stored in every window r. As shown, x_n^e and x_n^c hold information about the local frequency of the event and cycle. Local minima points (m_i) in x_n^e give the temporal bounds for individual event regions. Positions where the signal x_n^c changes sign from negative to positive mark the beginning and end of consecutive gait cycles. (b) Example of the two temporal signals, x_n^e and x_n^c, obtained after low-pass filtering, that match the frequency of the event and cycle in the composite acceleration signal, Acc_r, respectively. All signals have been standardized using zscore to scale them into the figure.

In order to remove high frequency noise and window edge effects, both signals, x_n^e and x_n^c, are low-pass filtered using a *zero-phase* FIR filter with a cut-off frequency that is higher than the maximum expected gait frequency, taken to be 8 Hz. The local minima points in x_n^e, defined by the set $\{m: m$ is the local minimum in $x_n^e\}$, provides the bounds for the individual event regions along the temporal axis (shown as circular dots in Fig. 3). To determine the corresponding spectral boundary for the event region, the scale $s_{\lambda,r}$ which distinguishes the event and cycle spectral energies, is successively compiled from all windows as

$$s_{\lambda,n}^e \triangleq [s_{\lambda,0}, s_{\lambda,1}, \ldots, s_{\lambda,r}, \ldots, s_{\lambda,N/M-1}]^T. \quad (9)$$

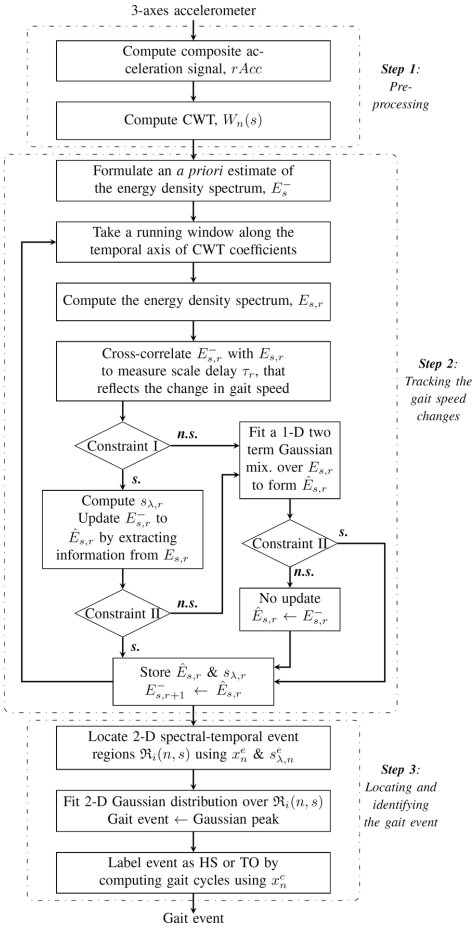

Fig. 4. Flow of the proposed gait event detection algorithm. The abbreviations "s." and "n.s." stand for "satisfied" and "not satisfied," respectively. $E_{s,r}^-$, $E_{s,r}$ and $\hat{E}_{s,r}$ represent the *a priori*, current and *a posteriori* energy density spectrum estimates in the current window index r, respectively. $E_{s,r+1}^-$ represents the *a priori* estimate in the next window with index $r+1$.

So for a given temporal bound $m_i(n)$, the corresponding spectral bound is given by the scale interval $[1, s_{\lambda,n}^e]$. Thus, a 2-D spectral-temporal event region $\Re(n,s)$ is located as

$$\Re_i(n,s) = W_{n\in[m_i,m_{i+1}]}(s \in [1, s_{\lambda,n}^e]). \tag{10}$$

The temporal position of the maximum CWT coefficient value in $\Re_i(n,s)$ could be simply used to estimate the event. However, highly noisy signal segments in Acc_r could lead to multiple local maxima in those CWT event regions and higher uncertainty in the precise location of the event. Thus, a 2-D Gaussian distribution fitting is done over each such spectral-temporal event region $\Re_i(n,s)$, such that the peak of the 2-D Gaussian fit gives the estimated location of the gait event in scale and time. Time signal x_n^c is then used to identify an event as an HS or TO. The positions where the signal x_n^c changes sign from negative to positive gives the temporal bounds for consecutive gait cycles (shown as squares in Fig. 3). Thus, within every gait cycle, the first event is labelled as an HS and the next as a TO.

C. Performance Assessment

Two state of the art algorithms, Rueterbories *et al.* ($\mathcal{A}_R$) [4] and Aung *et al.* ($\mathcal{A}_A$) [27], introduced earlier in Section I, were also implemented in order to compare them with the proposed method ($\mathcal{A}_{PM}$). The method of Hanlon *et al.* [41] was adopted to compute the ground truth (GT) gait events from the FSR measurements. A threshold value representing 39% of the maximum FSR value was used to identify the HSs on the rising edge of the FSR signal. The same procedure was repeated to identify the TOs after excluding the HS segments (HS $\pm$10 samples) from the signal. The matching between the actual gait events from the GT and the events detected by the proposed algorithm was based on a temporal tolerance of $\pm$5 samples or $\pm$0.039s. Any event missed by the FSR but detected by the algorithms implemented was automatically considered a false positive since the FSR was considered to be the GT. Statistical measures of sensitivity, specificity and F1 score were computed [42]. Conventionally, Mean Absolute Error (MAE) is used to present the temporal accuracy of a method in detecting gait events. The MAE was calculated (in samples) as the mean of the absolute temporal difference between the true positives of the algorithm and the corresponding GT events. Any constant bias was removed prior to the MAE calculation, for all algorithms. However, few true positives could lead to a low MAE value, indicating high accuracy even though many false positives might be detected by the method. Thus, the stride time was calculated and the Kolmogorov-Smirnov (KS) test was used to test the null hypothesis that the stride time samples from the algorithm and the GT came from the same empirical distribution [43]. If they did not, then the test rejected the null hypothesis at the 5% significance level. The KS test result provided an alternate perspective on the accuracy of a method as it took the entire stride time distribution into account, i.e., including both true positives and false positives. The data collected were divided into training and test data as the methodology in $\mathcal{A}_A$ required training of the model parameters. One third of the total number of subjects from the indoor and outdoor experiments were randomly selected to represent the hold-out test data. The purpose of this was to test the algorithmic performance in subjects that were not included in the training procedure. Sensitivity, specificity and the MAE of all algorithms were computed from the hold-out test data. However, the F1 score was computed by including the data from all subjects. Welch's t-test was used to find any significant differences between the F1 scores of any two sample groups.

III. Experiments

The study involved 20 healthy subjects (12 males and 8 females, average age: 33.4 $\pm$ 7 years, average weight: 73.2 $\pm$ 10.9 kg, average height: 172.6 $\pm$ 9.5 cm) with 11 subjects participating in indoor and 9 participating in outdoor experiments. Each subject had a 3-axes Shimmer3 accelerometer ($\pm$8g) attached to both ankles using Velcro straps. For the left ankle,

TABLE I
SUMMARY OF THE EXPERIMENTS CARRIED OUT IN INDOOR AND OUTDOOR ENVIRONMENTS

No. of subjects	Environment	Type of activity	Description	Speed	Approx. duration (minutes)	Total no. of gait events recorded
11	Indoor - Treadmill	Walk & run	Start walking and switch to running at any comfortable speed	4km/hr to 8km/hr; increasing in steps of 0.4km/hr every minute	10	30944
		Walk	Treadmill is set to (5°,0°,10°,0°,15°,0°) inclinations with 2 mins at each angle	Self-selected speed	12	25631
	Indoor - Flat space	Walk	Walking without any restrictions	Self-selected speed	3	7361
		Run	Steady running or jogging	Self-selected speed	3	10130
9	Outdoor - Street	Walk	Walking without any restrictions	Self-selected speed	3	10844
		Run	Steady running or jogging	Self-selected speed	3	8684*

* Two subjects did not complete the entire duration of the activity due to bad weather conditions.

the accelerometer axis was positioned with the y-axis pointing downward and the x-axis to the anterior direction while, for the right ankle, the accelerometer was casually attached without any planned orientation. The subjects were provided shoes that had force sensitive resistors (FSRs) fixed at the extreme ends of the sole in order to provide the ground truth values for HS and TO. Both, the accelerometer and the FSRs had a sampling frequency of 128 Hz, and the FSR output was stored locally on the Shimmer3 microSD card using an external expansion board. After every experiment, the data was transferred to a remote computer and the analysis was made offline using MATLAB v8.5 (MathWorks, Natick , MA, USA). Informed consent was obtained from all subjects prior to the experiments. The study was approved by and all procedures were conducted in accordance with the guidelines of the Ethical Review Board of Lund, Sweden. Table I summarizes the experiments carried out in different environments. The indoor experiments were conducted on the treadmill and in a large, empty flat space. The outdoor experiments were conducted in the form of a closed path on a street that was approximately 50% flat and the rest being equally uphill and downhill. The path included four turns, and the uphill and downhill inclination angles ranged between 5° and 10°. Except when on the treadmill, the subjects were free to select their pace and change directions during all other activities. Manual inspection revealed that, for some data sets, few events were missed due to extremely low FSR values. The percentage of the missed FSR events for indoor and outdoor data sets was 0.05% and 0.09%, respectively. Four subjects from the indoor and three subjects from the outdoor experiments were selected at random to act as the hold-out test data.

TABLE II
MEAN (AND STANDARD DEVIATION) OF THE PERFORMANCE SCORES COMPUTED FOR INDOOR (FLAT SPACE) WALKING TEST DATA. $\mathcal{A}_{\mathrm{PM}}$, $\mathcal{A}_{\mathrm{A}}$ AND $\mathcal{A}_{\mathrm{R}}$ STAND FOR PROPOSED METHOD, METHOD [27] AND METHOD [4]

Performance measures		Indoor walk: Flat space			
		LF		RF	
		HS	TO	HS	TO
Sensitivity	$\mathcal{A}_{\mathrm{PM}}$	**0.99** (0.00)	**0.98** (0.03)	**0.99** (0.00)	**0.99** (0.00)
	$\mathcal{A}_{\mathrm{A}}$	0.80 (0.36)	0.91 (0.10)	**0.99** (0.00)	0.97 (0.02)
	$\mathcal{A}_{\mathrm{R}}$	0.98 (0.00)	0.97 (0.03)	0.98 (0.00)	0.98 (0.01)
Specificity	$\mathcal{A}_{\mathrm{PM}}$	**0.99** (0.00)	**0.98** (0.03)	**0.99** (0.00)	**0.99** (0.00)
	$\mathcal{A}_{\mathrm{A}}$	0.96 (0.05)	0.00 (0.00)	0.95 (0.05)	0.07 (0.08)
	$\mathcal{A}_{\mathrm{R}}$	**0.99** (0.00)	0.97 (0.03)	**0.99** (0.00)	0.98 (0.01)
MAE (in samples)	$\mathcal{A}_{\mathrm{PM}}$	**0.55** (0.66)	**0.77** (0.94)	**0.66** (0.69)	**0.62** (0.73)
	$\mathcal{A}_{\mathrm{A}}$	0.85 (0.88)	0.90 (0.98)	0.74 (0.80)	0.88 (1.18)
	$\mathcal{A}_{\mathrm{R}}$	0.67 (0.74)	0.98 (0.98)	0.86 (0.85)	0.79 (0.77)
KS test ($\frac{\text{datasets not rejected}}{\text{total datasets tested}}$)	$\mathcal{A}_{\mathrm{PM}}$	$4/4$	$4/4$	$4/4$	$4/4$
	$\mathcal{A}_{\mathrm{A}}$	$2/4$	$0/4$	$3/4$	$0/4$
	$\mathcal{A}_{\mathrm{R}}$	$4/4$	$4/4$	$4/4$	$4/4$
No. of GT gait events		682	678	680	678

IV. RESULTS

Table II shows the mean and standard deviation of these performance scores for indoor (flat space) walking test data, which is the environment in which most gait event detection algorithms have been developed. Each cell in the table displays a distinct performance score for detecting HS or TO from the accelerometer signal obtained from the left (LF) or right foot (RF). The column under LF displays the score when the sensor is positioned at a fixed pre-defined axis while that under RF displays the score when the sensor is positioned arbitrarily, thus reflecting the influence to changes in axis orientation. The statistical measures of sensitivity and specificity display the true positive rate and the true negative rate of detecting HS and TO, respectively. The MAE, in sample units, gives the temporal accuracy of the algorithm for the correctly identified events. The KS test result is shown as a ratio of how many stride time data sets were not rejected by the null hypothesis compared to the total stride time data sets tested. The last row of the table shows the total number of GT gait events recorded from the test set data. The remaining rows present a comparison with the implemented methods in $\mathcal{A}_A$ and $\mathcal{A}_R$. Table III shows the mean and standard deviation of the performance scores for all indoor activities grouped together, only outdoor walking and all outdoor activities grouped together. The structure of Table III is similar to that of Table II, where each cell displays a score for detecting

TABLE III
MEAN (AND STANDARD DEVIATION) OF THE PERFORMANCE SCORES COMPUTED FOR ALL INDOOR ACTIVITIES GROUPED TOGETHER, ONLY OUTDOOR WALKING AND ALL OUTDOOR ACTIVITIES GROUPED TOGETHER. THE SCORES PRESENTED ARE COMPUTED FROM THE TEST DATA OF EACH ACTIVITY. $\mathcal{A}_{\mathrm{PM}}$, $\mathcal{A}_{\mathrm{A}}$ & $\mathcal{A}_{\mathrm{R}}$ STAND FOR PROPOSED METHOD, METHOD [27] AND METHOD [4], RESPECTIVELY

Performance measures		Indoor: Treadmill & Flat space				Outdoor							
		Walk & run				Walk				Walk & run			
		LF		RF		LF		RF		LF		RF	
		HS	TO	HS	TO	HS	TO	HS	TO	HS	TO	HS	TO
Sensitivity	$\mathcal{A}_{\mathrm{PM}}$	**0.99** (0.00)	**0.97** (0.02)	**0.99** (0.00)	**0.99** (0.00)	**0.99** (0.00)	**0.98** (0.00)	**0.99** (0.00)	0.98 (0.01)	**0.99** (0.00)	**0.99** (0.00)	**0.99** (0.00)	**0.99** (0.00)
	$\mathcal{A}_{\mathrm{A}}$	0.97 (0.05)	0.77 (0.16)	0.99 (0.01)	0.92 (0.10)	**0.99** (0.00)	0.94 (0.07)	0.45 (0.47)	**0.98** (0.00)	**0.99** (0.00)	0.89 (0.02)	0.70 (0.24)	0.54 (0.16)
	$\mathcal{A}_{\mathrm{R}}$	0.84 (0.12)	0.75 (0.23)	0.82 (0.12)	0.71 (0.23)	0.98 (0.00)	0.97 (0.02)	**0.99** (0.00)	**0.98** (0.00)	0.70 (0.02)	0.43 (0.04)	0.69 (0.02)	0.44 (0.03)
Specificity	$\mathcal{A}_{\mathrm{PM}}$	**0.99** (0.00)	**0.97** (0.03)	**0.99** (0.00)	**0.99** (0.00)	**0.99** (0.00)	**0.98** (0.01)	**0.99** (0.00)	0.98 (0.02)	**0.99** (0.00)	**0.99** (0.00)	**0.99** (0.00)	**0.99** (0.00)
	$\mathcal{A}_{\mathrm{A}}$	0.92 (0.12)	0.08 (0.12)	0.84 (0.21)	0.06 (0.11)	0.83 (0.21)	0.01 (0.02)	0.63 (0.53)	0.04 (0.07)	0.84 (0.07)	0.19 (0.24)	0.72 (0.20)	0.01 (0.02)
	$\mathcal{A}_{\mathrm{R}}$	0.95 (0.08)	0.85 (0.11)	0.94 (0.05)	0.82 (0.11)	**0.99** (0.00)	0.97 (0.02)	**0.99** (0.00)	**0.98** (0.00)	**0.99** (0.00)	0.71 (0.02)	0.96 (0.02)	0.71 (0.02)
MAE (in samples)	$\mathcal{A}_{\mathrm{PM}}$	**0.92** (0.93)	1.50 (1.28)	**1.02** (0.99)	**1.17** (1.12)	**0.78** (0.77)	**0.80** (0.99)	**0.66** (0.79)	**0.93** (1.13)	1.29 (1.08)	1.82 (1.32)	**1.08** (0.91)	1.50 (1.23)
	$\mathcal{A}_{\mathrm{A}}$	1.08 (1.06)	1.89 (1.52)	1.05 (0.97)	1.27 (1.21)	1.03 (0.88)	1.68 (1.68)	0.88 (0.93)	0.99 (1.12)	**1.13** (0.96)	2.50 (1.44)	1.64 (1.16)	1.51 (1.20)
	$\mathcal{A}_{\mathrm{R}}$	1.04 (1.05)	**1.28** (1.17)	1.27 (1.22)	1.30 (1.24)	0.98 (0.95)	1.02 (1.00)	0.75 (0.82)	1.21 (1.18)	1.23 (1.05)	**1.23** (1.08)	1.30 (1.19)	**1.22** (1.22)
KS test ($\frac{\text{datasets not rejected}}{\text{total datasets tested}}$)	$\mathcal{A}_{\mathrm{PM}}$	**12/12**	**12/12**	**12/12**	**12/12**	**3/3**	**3/3**	**3/3**	**3/3**	**3/3**	**3/3**	**3/3**	**3/3**
	$\mathcal{A}_{\mathrm{A}}$	6/12	0/12	5/12	0/12	1/3	0/3	0/3	0/3	1/3	0/3	0/3	0/3
	$\mathcal{A}_{\mathrm{R}}$	5/12	5/12	4/12	4/12	**3/3**	**3/3**	**3/3**	**3/3**	0/3	0/3	0/3	0/3
No. of GT gait events		6848	6837	6847	6842	566	562	565	562	1266	1264	1267	1264

HS or TO from LF or RF, for a particular environment and activity (listed at the top of the table). The best performance scores have been shown as bolded font in both tables. Fig. 5 shows the mean F1 score of all algorithms for detecting HS and TO in indoor and outdoor environments, obtained using all subjects' data.

V. DISCUSSION AND CONCLUSION

The experiments were specifically designed to test the performance of the algorithm on various aspects of robustness in a real-world setting. The objective of conducting experiments on a treadmill, in an indoor space and on an outdoor street was to assess the performance in a variety of environmental conditions consisting of different surfaces, varying inclinations and regular turns. The aim of having fixed and arbitrary sensor orientations on the left and right ankles was to evaluate the influence of changes in axis orientation on the method's performance in these environments. Similarly, the goal of defining walking and running activities was to evaluate the performance at different gait speeds. Most gait event detection algorithms, such as $\mathcal{A}_{\mathrm{A}}$ and $\mathcal{A}_{\mathrm{R}}$, have been developed from walking data collected in indoor settings. The proposed algorithm demonstrates good performance for detecting both HS and TO from indoor walking data, implied by the high sensitivity, specificity and F1 scores shown in Table II and Fig. 5. Moreover, it detects them with high temporal accuracy shown by the low MAE values that are below one sample and the KS test results that do not reject any of the four data sets tested. In comparison, $\mathcal{A}_{\mathrm{R}}$ also shows high performance scores for detecting both HS and TO, while $\mathcal{A}_{\mathrm{A}}$ detects HS significantly better than TO ($p < 0.05$). Although $\mathcal{A}_{\mathrm{A}}$ has an average MAE of below one sample, the low KS test result indicates the occurrence of excessive false positives, especially for detecting TO. All algorithms exhibit no influence to changes in axis orientation with no significant difference between the F1 scores of the left and right foot ($p > 0.05$). The proposed method also exhibits robustness to different gait speeds in indoor environments. It has high performance scores for all the indoor activities (walk and run) grouped together, as shown in Table III and Fig. 5. While $\mathcal{A}_{\mathrm{R}}$ had exhibited good performance for indoor walking, it underperforms when running is included, with a significantly lower F1 score as compared to walking ($p < 0.05$). Moreover, when running is included, $\mathcal{A}_{\mathrm{R}}$'s performance decreases even more for detecting TO as compared to HS ($p < 0.05$). In contrast to the controlled indoor experiments, the outdoor experiments were semi-controlled and representative of humans' natural environment in the real-world. The outdoor walking and running data grouped together plausibly represented the most diverse scenario, with unconstrained outdoor conditions and different gait speeds. The proposed method demonstrated good performance in this scenario, implied by the high performance scores shown in Table III and Fig. 5, with no significant difference between the indoor and outdoor F1 scores ($p > 0.05$). It also performed well in terms of temporal accuracy, with an average MAE of 1.42 samples and none of the datasets being rejected by the KS test. Both $\mathcal{A}_{\mathrm{A}}$ and $\mathcal{A}_{\mathrm{R}}$ had their lowest F1 scores for detecting events in this scenario as compared to all other environments in which they were tested. It was also significantly lower than their F1 scores for indoor activities grouped together ($p < 0.05$). This might be attributed

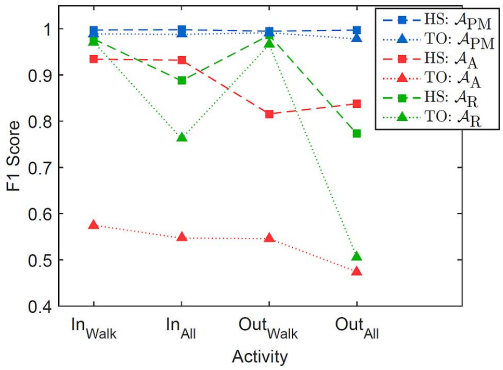

Fig. 5. Mean F1 scores of all algorithms for detecting HS and TO in indoor and outdoor environments. Mean values for each given activity on the x-axis were calculated by averaging the F1 score values obtained using data of all subjects. Activities labelled $\mathrm{In_{Walk}}$, $\mathrm{In_{All}}$, $\mathrm{Out_{Walk}}$ and $\mathrm{Out_{All}}$ represent only indoor (flat space) walking, all indoor activities grouped together, only outdoor walking and all outdoor activities grouped together, respectively. Mean F1 score of detecting HS for a particular activity is shown as a square while that for detecting TO is shown as a triangle. F1 score reaches its best value at 1 and worst at 0. $\mathcal{A}_{\mathrm{PM}}$, $\mathcal{A}_{\mathrm{A}}$ & $\mathcal{A}_{\mathrm{R}}$ stand for Proposed Method, method [27] and method [4], respectively.

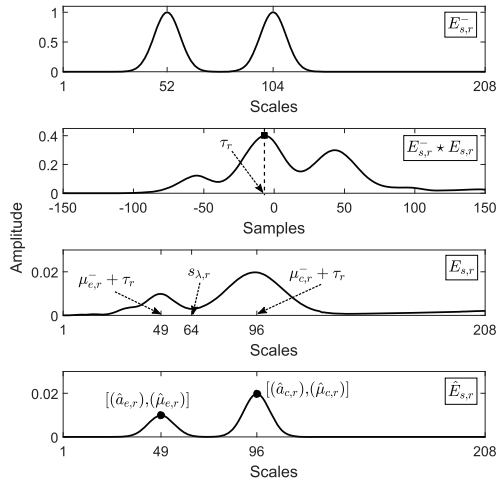

Fig. 6. Example of the steps involved in the tracking procedure of window index $r = 1$. First subfigure shows the *a priori* energy density spectrum estimate E^{-}_{s}, to start the tracking procedure. Second subfigure shows the scale delay, τ_r in the cross-correlation result of $(E^{-}_{s,r} \star E_{s,r})$. Third subfigure shows $s_{\lambda,r}$ which distinguishes the scales corresponding to event and cycle energies in $E_{s,r}$. Fourth subfigure shows the *a posteriori* estimate $\hat{E}_s$ whose parameters are stored after both constraints are satisfied.

to the fact that both $\mathcal{A}_{\mathrm{A}}$ and $\mathcal{A}_{\mathrm{R}}$ were designed using indoor walking data only and since activities in outdoor conditions are more uncontrolled and dynamic, they introduce more noise in the accelerometer signals. Moreover, it is difficult to make an objective comparison between algorithms that were designed using different datasets and protocols. However, the results exhibit that the proposed method could be directly applied in different environments for long-term applications.

The ability of the proposed method to effectively tackle real-world challenges is enabled by the use of domain knowledge to guide the time-frequency analysis. Knowledge about the event-cycle frequency relationship present in gait is utilized to logically reason around choosing the appropriate mother wavelet (Morlet), in order to gain a distinct separation between the event and cycle frequencies in time, as shown in Fig. 1(b) and (c). It is also utilized in the tracking procedure to tackle any gait speed speed changes, which is a substantial requirement for many real-world applications. In addition, the scale-frequency relationship of the Morlet is used to select the appropriate scales for analysis based on the frequency of the activity. While the proposed method was developed with the accelerometer placed around the ankle, it still remains to be investigated if and how the technique may be utilized to detect events from other parts of the body. With an arbitrary sensor placement on the body, it might be challenging to attribute the sensor information to the left or right foot, thus making it difficult to identify and label individual events. However, it would be possible to detect gait cycles using the tracking procedure presented in this method. Another limitation of the proposed method is that it has been validated only on healthy gait. Future work is needed to test the method on pathological gait and make any required adaptations to the algorithm. A service has been provided (http://islab.hh.se/mediawiki/Gait_events) to assist interested readers in making use of the proposed method with their data.

To conclude, this paper proposes a novel approach that exhibits how domain knowledge about human gait can be incorporated into time-frequency analysis in order to develop a robust algorithm that can detect gait events from long-term accelerometer signals. The ability of the algorithm to effectively adapt in real-world scenarios is validated by experiments done in indoor and outdoor environments that involve different gait speeds, changing walking terrains, varying surface inclinations and regular turns among other things. The proposed algorithm is shown be accurate and robust with consistently high performance scores across all datasets.

Appendix

This section elaborates on the details required to implement the tracking procedure to tackle changes in gait speeds. As explained earlier in Section II-B2, in order to track the transitions of the event and cycle coefficients, an overlapping running window is taken along the temporal axis of the CWT coefficients. In principle, a window size that captures the information about one gait cycle would be sufficient but it is practically desired to be large enough to account for signal noise and should thus include additional gait cycles. In this paper, the running window size is taken to be 3 or 6 s with a 50% overlap. The entire tracking procedure within a given window consists of the following steps (refer Fig. 6).

a) The energy density spectrum $E_{s,r}$ of the CWT coefficients selected from the current window is computed using (3) as $E_{s,r} = \sum_{n=rM}^{(r+1)M-1} |W_n(s)|^2$ where $s \in [1, s_{\max}]$, r is the window index and M is the window hop size, i.e., the number of samples by which each successive window is advanced in time. $E_{s,r}$ highlights

the dominant energetic scales of event and cycle in the current window r.

b) The *a priori* estimate $E^-_{s,r}$ is cross-correlated ($\star$) with $E_{s,r}$ in order to measure the scale delay τ_r between them, calculated as $\tau_r = \arg\max_{s\in[1,s_{\max}]}(E^-_{s,r} \star E_{s,r})$. For the first window ($r = 1$), the *a priori* estimate formulated in (6) is used. Scale delay τ_r reflects the change in gait speed from the previous window. However, very fast transitions in gait speeds would cause large shifts in the local signal energy. As such, the Gaussian mixture parameters in $E^-_{s,r}$ may be very different from that of $E_{s,r}$, resulting in an incorrect τ_r value due to poor alignment of the two signals. Thus, Constraint I is used to verify that τ_r lies within the expected scale bounds

$$\text{Constraint I}: \begin{cases} \mu^-_{e,r} + \tau_r > 1 \\ \mu^-_{c,r} + \tau_r < s_{\max} \end{cases}. \tag{11}$$

c) If Constraint I is satisfied, then the *a priori* estimate $E^-_{s,r}$ is updated to form an *a posteriori* estimate $\hat{E}_{s,r}$. This is done by first calculating a scale, $s_{\lambda,r} = \arg\min E_{s,r}$ where $s \in [\mu^-_{e,r} + \tau_r, \mu^-_{c,r} + \tau_r]$, that helps to distinguish the range of scales in which the event and cycle energies lie in $E_{s,r}$. The set of equations used to form the *a posteriori* estimate $\hat{E}_{s,r}$ are

$$\begin{aligned} \hat{\mu}_{e,r} &= \arg\max_{s\in[1,s_{\lambda,r}]} E_{s,r} \\ \hat{a}_{e,r} &= \max_{s\in[1,s_{\lambda,r}]} E_{s,r} \\ \hat{\sigma}_{e,r} &= \sigma^-_{e,r} \\ \hat{\mu}_{c,r} &= \arg\max_{s\in[s_{\lambda,r},s_{\max}]} E_{s,r} \\ \hat{a}_{c,r} &= \max_{s\in[s_{\lambda,r},s_{\max}]} E_{s,r} \\ \hat{\sigma}_{c,r} &= \sigma^-_{c,r}. \end{aligned} \tag{12}$$

To verify that the updated Gaussian means in $\hat{E}_{s,r}$ uphold the frequency relationship stated in (5), a constraint is applied as Constraint II: $1.9 \le \hat{\mu}_{c,r}/\hat{\mu}_{e,r} \le 2.1$. The relationship is relaxed by 5% to accommodate effects of signal noise and low frequency resolution in finer scales [44].

d) If either of the constraints are not satisfied, then curve fitting of a two term 1-D Gaussian mixture is performed over $E_{s,r}$ and the resulting fit parameters are used to constitute $\hat{E}_{s,r}$. Since curve fitting is sensitive to starting point declarations, the event-cycle frequency relationship can be utilized to define two sets of possible starting points for $\{a_e, \mu_e, \sigma_e, a_c, \mu_c, \sigma_c\}$, to guide the fitting procedure in order to obtain a good fit. These are $Set1 = \{a_\chi, \mu_\chi/2, s_{\max}/16, a_\chi, \mu_\chi, s_{\max}/8\}$ and $Set2 = \{a_\chi, \mu_\chi, s_{\max}/16, a_\chi, 2\mu_\chi, s_{\max}/8\}$ where μ_χ is the most energetic scale in $E_{s,r}$ i.e., $\arg\max_{s\in[1,s_{\max}]} E_{s,r}$ and a_χ is the corresponding energy value at that scale i.e., $\max_{s\in[1,s_{\max}]} E_{s,r}$. Thus, two fits over $E_{s,r}$ are obtained by using each set as the starting point. In order to decide the better fit, an initial check is made to verify whether the fit parameters lie within the expected bounds, i.e., $\{a_e, a_c\} > 0$ and $\{\mu_e, \mu_c, \sigma_e, \sigma_c\} \in [1, s_{\max}]$, and a fit that lies outside these bounds is rejected. If both fits lie within the expected bounds, then root mean square error (RMSE) is computed for both the fits. In the RMSE computation, only high energy density values are taken into account, and the lower 10% of $E_{s,r}$ is excluded to remove its influence on the RMSE calculation as it does not contribute to the event and cycle energies, as shown in Fig. 7. The better fit is chosen as the one with the lowest RMSE value, following which Constraint II is verified again to ensure that the fit is correct. In case of violation, the *a posteriori* estimate $\hat{E}_{s,r}$ is constituted directly from the existing parameters of the *a priori* estimate $E^-_{s,r}$ without any update from the current window, i.e., $\hat{E}_{s,r} \leftarrow E^-_{s,r}$.

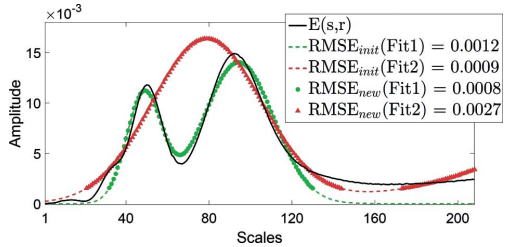

Fig. 7. Example of how RMSE computation is influenced by the lower energy values in $E_{s,r}$. Even though Fit1 is a better fit than Fit2, initially it gives a higher RMSE_{init} because it includes lower energy scales corresponding to the lower 10% values of $E_{s,r}$. However, if these lower energy scales are excluded, then Fit1 gives a lower RMSE_{new}, indicating that it is a better fit as compared to Fit2.

e) The Gaussian parameters in *a posteriori* estimate $\hat{E}_{s,r}$ and scale $s_{\lambda,r}$ computed in the current window are stored following which $\hat{E}_{s,r}$ serves as the prior for the next window, i.e., $E^-_{s,r+1} \leftarrow \hat{E}_{s,r}$.

ACKNOWLEDGMENT

The authors would like to thank T. Lithén for preparing the experimental setup. They would also like to thank Prof. J. Bigun for his valuable insights on wavelet transforms and Prof. E. Järpe for discussions on statistical inference.

REFERENCES

[1] A. H. Snijders, B. P. van de Warrenburg, N. Giladi, and B. R. Bloem, "Neurological gait disorders in elderly people: Clinical approach and classification," *Lancet Neurol.*, vol. 6, no. 1, pp. 63–74, 2007.

[2] R. Williamson and B. Andrews, "Gait event detection for FES using accelerometers and supervised machine learning," *IEEE Trans. Rehab. Eng.*, vol. 8, no. 3, pp. 312–319, Sep. 2000.

[3] A. Mansfield and G. M. Lyons, "The use of accelerometry to detect heel contact events for use as a sensor in FES assisted walking," *Med. Eng. Phys.*, vol. 25, no. 10, pp. 879–885, 2003.

[4] J. Rueterbories, E. G. Spaich, and O. K. Andersen, "Gait event detection for use in FES rehabilitation by radial and tangential foot accelerations," *Med. Eng. Phys.*, vol. 36, no. 4, pp. 502–508, 2014.

[5] T. A. Wren, G. E. Gorten III, S. Õunpuu, and C. A. Tucker, "Efficacy of clinical gait analysis: A systematic review," *Gait Posture*, vol. 34, no. 2, pp. 149–153, 2011.

[6] M. J. Socie, R. W. Motl, J. H. Pula, B. M. Sandroff, and J. J. Sosnoff, "Gait variability and disability in multiple sclerosis," *Gait Posture*, vol. 38, no. 1, pp. 51–55, 2013.

[7] V. Dietz, "Neurophysiology of gait disorders: Present and future applications," *Electroencephalogr. Clin. Neurophysiol.*, vol. 103, no. 3, pp. 333–355, 1997.

[8] M. Woollacott and A. Shumway-Cook, "Attention and the control of posture and gait: A review of an emerging area of research," *Gait Posture*, vol. 16, no. 1, pp. 1–14, 2002.
[9] T. IJmker and C. Lamoth, "Gait and cognition: The relationship between gait stability and variability with executive function in persons with and without dementia," *Gait Posture*, vol. 35, no. 1, pp. 126–130, 2012.
[10] P. B. Shull, W. Jirattigalachote, M. A. Hunt, M. R. Cutkosky, and S. L. Delp, "Quantified self and human movement: A review on the clinical impact of wearable sensing and feedback for gait analysis and intervention," *Gait Posture*, vol. 40, no. 1, pp. 11–19, 2014.
[11] D. A. Bruening and S. T. Ridge, "Automated event detection algorithms in pathological gait," *Gait Posture*, vol. 39, no. 1, pp. 472–477, 2014.
[12] K. Aminian, B. Najafi, and C. Büla, "Spatio-temporal parameters of gait measured by an ambulatory system using miniature gyroscopes," *J. Biomechan.*, vol. 35, no. 5, pp. 689–699, 2002.
[13] J. M. Jasiewicz *et al.*, "Gait event detection using linear accelerometers or angular velocity transducers in able-bodied and spinal-cord injured individuals," *Gait Posture*, vol. 24, no. 4, pp. 502–509, 2006.
[14] P. Lopez-Meyer, G. Fulk, and E. Sazonov, "Automatic detection of temporal gait parameters in poststroke individuals," *IEEE Trans. Inf. Tech. Biomed.*, vol. 15, no. 4, pp. 594–601, Jul. 2011.
[15] T. Everett and C. Kell, *Human Movement: an Introductory Text*. New York: Elsevier, 2010.
[16] J. R. Rebula, L. V. Ojeda, P. G. Adamczyk, and A. D. Kuo, "Measurement of foot placement and its variability with inertial sensors," *Gait Posture*, vol. 38, no. 4, pp. 974–980, 2013.
[17] J. Rueterbories, E. G. Spaich, B. Larsen, and O. K. Andersen, "Methods for gait event detection and analysis in ambulatory systems," *Med. Eng. Phys.*, vol. 32, no. 6, pp. 545–552, 2010.
[18] B. Greene *et al.*, "An adaptive gyroscope-based algorithm for temporal gait analysis," *Med. Bio. Eng. Comp.*, vol. 48, no. 12, 2010.
[19] A. Salarian *et al.*, "Gait assessment in Parkinson's disease: Toward an ambulatory system for long-term monitoring," *IEEE Trans. Biomed. Eng.*, vol. 51, no. 8, pp. 1434–1443, Aug. 2004.
[20] I. Pappas, M. Popovic, T. Keller, V. Dietz, and M. Morari, "A reliable gait phase detection system," *IEEE Trans. Neural Syst. Rehabil. Eng.*, vol. 9, no. 2, pp. 113–125, Jun. 2001.
[21] A. Mannini, V. Genovese, and A. Sabatin, "Online decoding of hidden Markov models for gait event detection using foot-mounted gyroscopes," *IEEE J. Biomed. Health Inf.*, vol. 18, no. 4, pp. 1122–1130, Jul. 2014.
[22] J. Lee and E. Park, "Quasi real-time gait event detection using shank-attached gyroscopes," *Med. Bio. Eng. Comp.*, vol. 49, no. 6, pp. 707–712, 2011.
[23] J. J. Kavanagh and H. B. Menz, "Accelerometry: A technique for quantifying movement patterns during walking," *Gait Posture*, vol. 28, no. 1, pp. 1–15, 2008.
[24] R. Selles, M. Formanoy, J. Bussmann, P. Janssens, and H. Stam, "Automated estimation of initial and terminal contact timing using accelerometers; development and validation in transtibial amputees and controls," *IEEE Trans. Neural Syst. Rehabil. Eng.*, vol. 13, no. 1, pp. 81–88, Mar. 2005.
[25] R. Torrealba, J. Cappelletto, L. Fermın-Leon, J. Grieco, and G. Fernández-López, "Statistics-based technique for automated detection of gait events from accelerometer signals," *Electron. Lett.*, vol. 46, no. 22, pp. 1483–1485, 2010.
[26] A. Sant'Anna and N. Wickström, "A symbol-based approach to gait analysis from acceleration signals: Identification and detection of gait events and a new measure of gait symmetry," *IEEE Trans. Inf. Tech. Biomed.*, vol. 14, no. 5, pp. 1180–1187, Sep. 2010.
[27] M. Aung *et al.*, "Automated detection of instantaneous gait events using time frequency analysis and manifold embedding," *IEEE Trans. Neural Syst. Rehabil. Eng.*, vol. 21, no. 6, pp. 908–916, Nov. 2013.
[28] M. Yoneyama, Y. Kurihara, K. Watanabe, and H. Mitoma, "Accelerometry-based gait analysis and its application to parkinson's disease assessment—Part 1: Detection of stride event," *IEEE Trans. Neural Sys. Rehabil. Eng.*, vol. 22, no. 3, pp. 613–622, May 2014.
[29] H.-K. Lee *et al.*, "Computational methods to detect step events for normal and pathological gait evaluation using accelerometer," *Electron. Lett.*, vol. 46, no. 17, pp. 1185–1187, 2010.
[30] D. Lai, R. Begg, and M. Palaniswami, "Computational intelligence in gait research: A perspective on current applications and future challenges," *IEEE Trans. Inf. Tech. Biomed.*, vol. 13, no. 5, pp. 687–702, Sep. 2009.
[31] T. Chau, "A review of analytical techniques for gait data. Part 2: Neural network and wavelet methods," *Gait Posture*, vol. 13, no. 2, pp. 102–120, 2001.
[32] D. Gouwanda and S. Senanayake, "Application of hybrid multi-resolution wavelet decomposition method in detecting human walking gait events," in *Proc. Int. Conf. Soft Comp. Pattern Recog.*, 2009, pp. 580–585.
[33] P. Forsman, E. Toppila, and E. Haeggstrom, "Wavelet analysis to detect gait events," in *Proc. Annu. Int. Conf. IEEE Eng. Med. Bio. Soc.*, 2009, pp. 424–427.
[34] J. McCamley, M. Donati, E. Grimpampi, and C. Mazzà, "An enhanced estimate of initial contact and final contact instants of time using lower trunk inertial sensor data," *Gait Posture*, vol. 36, no. 2, pp. 316–318, 2012.
[35] M. Yuwono, S. W. Su, Y. Guo, B. D. Moulton, and H. T. Nguyen, "Unsupervised nonparametric method for gait analysis using a waist-worn inertial sensor," *App. Soft Comp.*, vol. 14, pt. A, pp. 72–80, 2014.
[36] D. Novak *et al.*, "Automated detection of gait initiation and termination using wearable sensors," *Med. Eng. Phys.*, vol. 35, no. 12, pp. 1713–1720, 2013.
[37] P. Addison, J. Walker, and R. Guido, "Time-frequency analysis of biosignals," *IEEE Eng. Med. Biol. Mag.*, vol. 28, no. 5, pp. 14–29, Sep./Oct. 2009.
[38] J. Rafiee, M. Rafiee, N. Prause, and M. Schoen, "Wavelet basis functions in biomedical signal processing," *Expert Sys. App.*, vol. 38, no. 5, pp. 6190–6201, 2011.
[39] J. Lilly and S. Olhede, "Higher-order properties of analytic wavelets," *IEEE Trans. Signal Process.*, vol. 57, no. 1, pp. 146–160, Jan. 2009.
[40] C. Torrence and G. P. Compo, "A practical guide to wavelet analysis," *Bull. Am. Meteo. Soc.*, vol. 79, no. 1, pp. 61–78, 1998.
[41] M. Hanlon and R. Anderson, "Real-time gait event detection using wearable sensors," *Gait Posture*, vol. 30, no. 4, pp. 523–527, 2009.
[42] T. Fawcett, "An introduction to ROC analysis," *Pattern Recognit. Lett.*, vol. 27, no. 8, pp. 861–874, 2006.
[43] J. Massey and J. Frank, "The Kolmogorov-Smirnov test for goodness of fit," *J. Am. Stat. Assoc.*, vol. 46, no. 253, pp. 68–78, 1951.
[44] B. K. Alsberg, A. M. Woodward, and D. B. Kell, "An introduction to wavelet transforms for chemometricians: A time-frequency approach," *Chemometr. Intell. Lab. Syst.*, vol. 37, no. 2, pp. 215–239, 1997.

Siddhartha Khandelwal received the M.S. degree in robotics from WUT, Warsaw, Poland, and ECN, Nantes, France. He is currently working toward the Ph.D. degree at the School of Information Technology, Halmstad University, Halmstad, Sweden.

His current research interests are in wearable sensors and biomedical signal processing.

Nicholas Wickström (M'11) received the Ph.D. degree in computer engineering from Chalmers University of Technology, Gothenburg, Sweden, in 2004.

He is currently an Associate Professor at the School of Information Technology, Halmstad University, Halmstad, Sweden. His current research interests include biomedical sensing and signal processing.

Appendix II

Paper II - Evaluation of the performance of accelerometer-based gait event detection algorithms in different real-world scenarios using the MAREA gait database

Gait & Posture 51 (2017) 84–90

Contents lists available at ScienceDirect

Gait & Posture

journal homepage: www.elsevier.com/locate/gaitpost

Evaluation of the performance of accelerometer-based gait event detection algorithms in different real-world scenarios using the MAREA gait database

Siddhartha Khandelwal *, Nicholas Wickström

Center for Applied Intelligent Systems Research, Halmstad University, Sweden

ARTICLE INFO

Article history:
Received 11 May 2016
Received in revised form 22 September 2016
Accepted 25 September 2016

Keywords:
Gait events
Inertial sensors
Gait database
Heel-Strike
Toe-Off

ABSTRACT

Numerous gait event detection (GED) algorithms have been developed using accelerometers as they allow the possibility of long-term gait analysis in everyday life. However, almost all such existing algorithms have been developed and assessed using data collected in controlled indoor experiments with pre-defined paths and walking speeds. On the contrary, human gait is quite dynamic in the real-world, often involving varying gait speeds, changing surfaces and varying surface inclinations. Though portable wearable systems can be used to conduct experiments directly in the real-world, there is a lack of publicly available gait datasets or studies evaluating the performance of existing GED algorithms in various real-world settings.

This paper presents a new gait database called MAREA ($n = 20$ healthy subjects) that consists of walking and running in indoor and outdoor environments with accelerometers positioned on waist, wrist and both ankles. The study also evaluates the performance of six state-of-the-art accelerometer-based GED algorithms in different real-world scenarios, using the MAREA gait database. The results reveal that the performance of these algorithms is inconsistent and varies with changing environments and gait speeds. All algorithms demonstrated good performance for the scenario of steady walking in a controlled indoor environment with a combined median F1score of 0.98 for Heel-Strikes and 0.94 for Toe-Offs. However, they exhibited significantly decreased performance when evaluated in other lesser controlled scenarios such as walking and running in an outdoor street, with a combined median F1score of 0.82 for Heel-Strikes and 0.53 for Toe-Offs. Moreover, all GED algorithms displayed better performance for detecting Heel-Strikes as compared to Toe-Offs, when evaluated in different scenarios.

1. Introduction

The development of gait event detection (GED) algorithms using various sensing modalities has been an active area of research for many years [1]. In the past decade, several GED algorithms have been developed using motion capture systems, present in gait labs, and recent studies have compared and evaluated their performance [2–5]. Alternatively, inertial sensors are being used as they allow the possibility of long-term monitoring in everyday life and provide spatio-temporal information that can be fused to obtain the entire trajectory of the limb segment [6,7]. While many GED algorithms have been developed using gyroscopes, others have used accelerometers as they are miniature, inexpensive and low-powered devices [1,8]. However, as accelerometers suffer heavily from noise due to mechanical vibrations, they require robust algorithms for accurate event detection. Almost all existing accelerometer-based GED algorithms have been developed and assessed using data collected in controlled indoor experiments, that usually involves instructing the subjects to walk in a straight line or a given path at self-selected pace [9,10] or predefined walking speeds [11–13]. On the contrary, in the real-world, human gait is quite dynamic in different environments, often involving varying gait speeds, changing walking surfaces and varying surface inclinations, among others. Therefore, it needs to be assessed whether such dynamic and uncontrolled real-world scenarios have an impact on the performance of existing GED methods which have been developed from controlled protocols in laboratory settings. However, as almost all

* Corresponding author at: Center for Applied Intelligent Systems Research, School of Information Technology, Halmstad University, P.O. Box 823, SE-301 18 Halmstad, Sweden.
E-mail address: siddhartha.khandelwal@hh.se (S. Khandelwal).

http://dx.doi.org/10.1016/j.gaitpost.2016.09.023
0966-6362/

Table 1
Overview of the experiments carried out in different environments to create the MAREA gait database.

Subjects	Environment	Activity	Speed	Duration	Short description
11	Treadmill (flat)	Walk & run	4 km/h–8 km/h; increasing in steps of 0.4 km/h every minute	10 min	Start walking and switch to running at self-selected speed
	Treadmill (slope)	Walk	Self-selected	12 min	Treadmill is set to (5°, 0°, 10°, 0°, 15°, 0°) inclinations with 2 min at each angle
	Indoor flat space	Walk & run	Self-selected	6 min	Start walking and switch to running after 3 min
9	Outdoor street	Walk & run	Self-selected	6 min	Start walking and switch to running after 3 min

The database is made publicly available at http://islab.hh.se/mediawiki/Gait_database.

publicly available accelerometer-based gait databases [14,15] and recent comparative studies [16] also consist of only controlled indoor experiments, there is a lack of gait datasets or any studies that evaluate the performance of existing GED methods in various real-world settings; especially when portable wearable systems can be readily used to conduct experiments directly in humans' natural environment.

Consequently, a new gait database called **MAREA**: **M**ovement **A**nalysis in **R**eal-world **E**nvironments using **A**ccelerometers, was collected that comprises of various gait activities in different environments, both indoors and outdoors. The objective of this study is two-fold: (1) to introduce the MAREA database which is made publicly available for all readers, and (2) to assess the impact of different real-world scenarios on the performance of state-of-the-art GED algorithms, using the MAREA database. The database is made publicly available at http://islab.hh.se/mediawiki/Gait_database (Table 1).

2. Materials and methods

2.1. MAREA gait database

20 healthy adults (12 males and 8 females, average age: 33.4 ± 7 years, average mass: 73.2 ± 10.9 kg, average height: 172.6 ± 9.5 cm) participated in the study that was approved by the Ethical Review Board of Lund, Sweden. Each subject had a 3-axes Shimmer3 (Shimmer Research, Dublin, Ireland) accelerometer ($\pm 8\,g$) attached to their waist, left wrist and left and right ankles using elastic bands and velcro straps. Fig. 1 shows the position and orientation of the accelerometers at the beginning of each experiment. On the waist, the accelerometer X and Y axes were pointing to the lateral and downward direction, respectively. On the wrist and left ankle, the Z axis was pointing in the lateral direction while the Y axis was pointing downward and was aligned with the limb longitudinal axis. In order to simulate a lesser controlled scenario, the accelerometer on right ankle was positioned such that the Y axis was pointing downward but the Z axis was marginally disturbed such that it was not exactly perpendicular to the sagittal plane. The subjects were provided shoes that were instrumented with piezo-electric force sensitive resistors (FSRs), fixed at the extreme ends of the sole in order to provide the ground truth values for HS and TO. An external expansion board was used to synchronously collect the data from the FSRs on each foot and the respective ankle accelerometer, at a sampling frequency of 128 Hz, and stored locally on the Shimmer3 microSD card. However, as the waist and wrist accelerometers were not connected to the external expansion board, they were not in perfect synchronization with the ankle accelerometers and the FSRs.

11 subjects participated in the indoor experiments that were conducted on the treadmill and a flat surface (games court). Two separate trials were conducted on the treadmill. For the first trial, the treadmill speed was initially set to 4 km/h which was gradually incremented to 8 km/h, increasing in steps of 0.4 km/h every

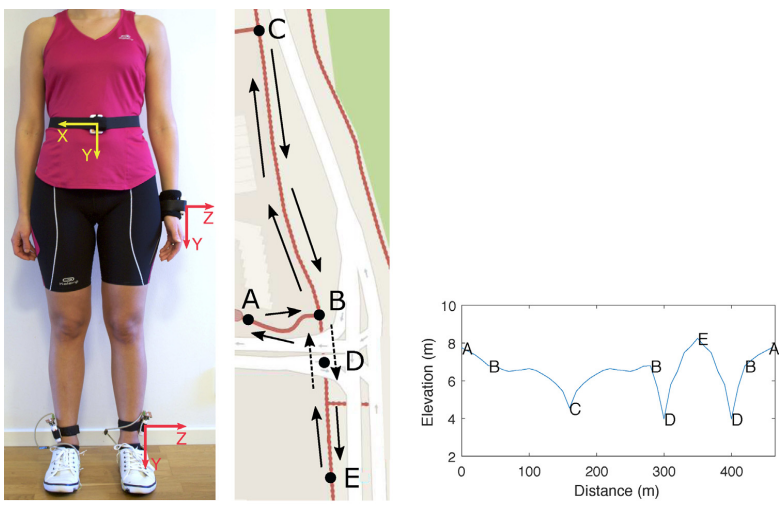

Fig. 1. (a) Position and orientation of each accelerometer at the beginning of every experiment. (b) The pedestrian street used for outdoor experiments is shown in red and the arrows show the closed-loop path defined for the experiments. Different path segments are annotated as A, B, C, D, E where segment BDE of the path, shown using dotted arrows, is an underpass. (c) The approximate elevation profile of the defined closed-loop outdoor path.

minute. The subjects were free to switch to running at any comfortable speed. For the second trial, the subjects were first asked to select their preferred walking speed (PWS) prior to the experiment. The experiment began by changing the treadmill inclinations to (5°, 0°, 10°, 0°, 15°, 0°), keeping each inclination angle for 2 min. For the flat surface experiment, the subjects were asked to walk for 3 min at self-selected pace and then run for 3 min at a steady pace. The subjects were free to change their directions at any time. For a given subject, all indoor experiments were conducted in one day with resting breaks in between each trial. 9 subjects participated in the outdoor experiments that were conducted in the form of a closed-loop path on a pedestrian street made of asphalt concrete, shown in Fig. 1b. The defined path consisted of turns and segments that were relatively flat, uphill and downhill, as shown in Fig. 1c. The subjects were asked to start at point A and walk for 3 min at self-selected pace and then switch to jogging or running for 3 min, at a steady pace.

After every experiment, the data was transferred to a remote computer and all analysis was done offline using MATLAB v8.5 (MathWorks, USA). Timings of the switch from walking to running were noted down during the experiments, in order to segregate the dataset into walking and running segments. The method of Hanlon and Anderson [17] was adopted to compute the ground truth (GT) gait events from the FSR signals. A threshold value representing 39% of the maximum FSR value was used to identify the HSs on the rising edge of the FSR signal. The same procedure was repeated to identify the TOs after excluding the HS segments (HS ± 10 samples) from the signal. Finally, all datasets were manually inspected to correct any false positives or false negatives that may have occurred.

In order to test the performance of GED algorithms in different environmental settings, five different scenarios were defined using the MAREA database, namely:

- **Indoor Walk:** Walking in an indoor flat space. This scenario represents the controlled experimental protocol of most GED methods as shown in Table 2.
- **Indoor Walk & Run:** Walking and running in an indoor flat space. This scenario involves variable gait speeds in a controlled environment.
- **Treadmill All:** All walking and running activities on the treadmill grouped together. This scenario involves a different surface with variable gait speeds and changing surface inclinations, in a controlled environment.
- **Outdoor Walk:** Walking on an outdoor street. This scenario represents walking on a different surface with varying surface inclinations, in a semi-controlled environment.
- **Outdoor Walk & Run:** Walking and running on an outdoor street. This scenario perhaps represents the most dynamic environment involving varying gait speeds and surface inclinations.

2.2. GED algorithms evaluated

Several methods have been developed to detect gait events from accelerometer positioned at the lower trunk as it requires only one sensor [18–22]. However, as the trunk accelerometer signal is composed of combined accelerations from both feet [8], the challenge is to distinguish and correctly attribute the detected events (both HS and TO) to the left and right foot in an automated way [20], using only the waist signal. Other authors have favored to use two accelerometers instead, positioning one on each lower leg [1], in order to be closer to the point of contact to measure maximal acceleration forces generated by each foot [16,23]. Six such state-of-the-art GED algorithms were selected that were developed from accelerometers positioned on the lower leg, such as forefoot [9], ankle [10,12,13,24] and shank [11]. A summary of the experimental protocol followed by each of these methods is given in Table 2. A brief description of the selected algorithms is given as follows:

***A_{JR}*:** In [9], a rule-based state machine is realized with four gait states, namely, mid-stance, pre-swing, swing and loading response. The state transitions are then determined by defining five reference signals derived from tri-axial accelerometer signals.

***A_{RT}*:** In [12], a statistics-based gait event detector algorithm is presented. The algorithm uses a sliding window and computes threshold values, based on local signal statistics, within every window. Then the thresholds are applied to isolate the peak and valley candidates from which gait events are detected.

***A_{RS}*:** In [11], strides are divided into faster and slower strides based on an approx. stride duration of 1.5 s and separate calculations are performed for each category. For the faster strides, the raw signal is low-pass filtered and the first and last peak within every approx. stride duration is labeled as approximate HS and approximate TO. Then temporal windows are defined to detect the final HS and TO. A similar approach is adopted for slower strides.

***A_{MA}*:** In [10], wavelet transform is used to express the 3-axis acceleration signals in time-frequency space. The high dimensionality is then reduced using a manifold embedding algorithm that projects the data to a smaller dimensional subspace and gives a minimal subset of features which contain

Table 2
An overview of the data collection protocol followed by the GED methods. The experimental protocol of most GED methods involves walking in an indoor flat space or treadmill.

Method	No. of subjects	Acc. type	Sampling freq. (Hz)	Activity (length/time)	Cadence/speed	Environment	Ground truth
A_{JR} [9]	10 healthy 10 hemiparetic	Tri-axial	160	Walk (30 m)	70 steps/min & self-selected speed	Indoor flat surface	Foot switches
A_{RT} [12]	1 above-knee amputee	Bi-axial	60	Walk	1.5–3 km/h	Treadmill (flat)	–
A_{RS} [11]	15 healthy 10 transtibial amputees	Two uni-axial	500	Walk (15 m)	60–100 steps/min & self-selected speed	Indoor flat surface	Force plates
A_{MA} [10]	8 healthy	Tri-axial	1500	Walk (8.4 m)	Self-selected speed	Indoor flat surface Platform (slope)	Mocap system
A_{AS} [13]	6 healthy	Tri-axial	50	Walk (6 m)	Self-selected speed & slow-paced speed	Indoor flat surface	Pressure mat
A_{SK} [24]	20 healthy[a]	Tri-axial	128	Walk & run (34 min)	4 km/h–8 km/h & self-selected speed	Treadmill (flat, slope) Indoor flat surface Outdoor street (flat, slope)	Foot switches

[a] MAREA gait database.

salient signal information. Finally, a Gaussian mixture model is applied to classify each time sample as HS, TO or no-event.

***A_{AS}*:** In [13], a symbol-based method is presented which uses piecewise linear segmentation followed by clustering to symbolize the 2-axis acceleration signal. Then the context and distribution of each symbol is analyzed based on expert knowledge, in order identify HS and TO.

***A_{SK}*:** In [24], domain knowledge about gait is incorporated into time-frequency analysis to detect gait events from 3-axis accelerometer signals. A tracking procedure is implemented using wavelet transform coefficients that extracts features from a running window to define spectral–temporal event regions. Finally, a 2-D Gaussian distribution fitting is done over each event region to estimate the corresponding gait event.

The above algorithms were implemented on the data obtained from left and right ankle accelerometers. Signals from all 3-axes were used to implement A_{SK}, A_{JR} and A_{MA}. The X and Y axis signals were used for methods A_{RT} and A_{RS}, as they utilize vertical and anterior–posterior axis information. Similarly, Y and Z axis signals were used for A_{AS} as it utilizes vertical and lateral axis information. The parameter values for all algorithms were used as reported by the respective authors except A_{RT} and A_{RS}, which explicitly set threshold values for the size of temporal windows utilized in their algorithms. As the window size is dependent on sampling frequency and gait speed, their values were empirically determined by varying the window size from 0% to 100% of the average gait cycle using the Treadmill All scenario, as it consisted of maximal variation in gait speeds.

2.3. Statistical analysis

A temporal tolerance of ±5 samples or ±0.039 s was used to match the GT gait events with those detected by the algorithms. Any constant bias was removed and the F1 score was computed in order to evaluate the overall performance, as:

$$F_1 = 2\frac{\text{Precision}\times\text{Recall}}{\text{Precision}+\text{Recall}}$$

where

$$\text{Precision} = \frac{\text{True positives}}{\text{True positives}+\text{False positives}}$$

and

$$\text{Recall} = \frac{\text{True positives}}{\text{True positives}+\text{False negatives}}$$

Welch's t-test was used to find any significant differences between the F1 scores of any two sample groups. In order to evaluate the accuracy, mean absolute error (MAE) was computed by finding the mean of the absolute difference (in time) between the true positives and the corresponding GT events. As an alternative approach, the stride time distributions resulting from the GED method and the corresponding GT were compared using non-parametric tests as similar distributions would indicate higher accuracy and vice-versa. The Kolmogorov–Smirnov (KS) test and the Mann–Whitney U (MWU) test were applied to test the null hypothesis that the two stride time distributions were identical and both tests rejected the null hypothesis at the 5% significance level [25].

3. Results

Fig. 2 shows the F1 scores for detecting HSs and TOs in five different scenarios, defined earlier in Section 2.2. Each colored boxplot consists of the F1 scores of applying a particular GED method on the data from all subjects collected for a given scenario.

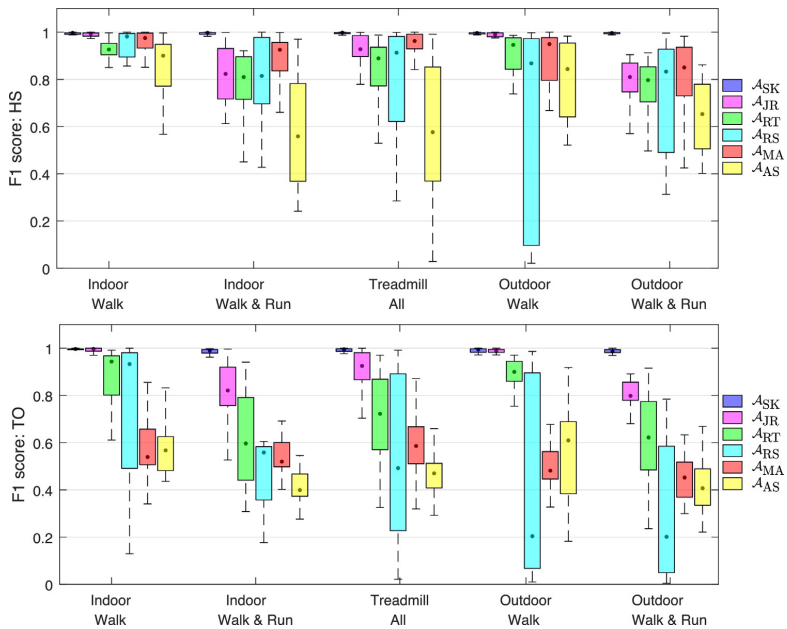

Fig. 2. F1 scores for detecting HSs and TOs by applying the GED methods in the five different scenarios consisting of a combination different environments and gait activities. Each boxplot represents the F1 scores of applying a particular GED method on data from all subjects collected for a given scenario. The median F1 score for each boxplot is shown as a black dot. The F1 score reaches its best value at 1 and worst at 0. The abbreviations A_{SK}, A_{JR}, A_{RT}, A_{RS}, A_{MA} and A_{AS} stand for methods [24], [9], [12], [11], [10] and [13], respectively.

The first two subfigures in Fig. 3 show the MAE in detecting HSs and TOs by various GED methods in different scenarios along with the number of true positives detected by the respective methods, for each scenario. The remaining subfigures in Fig. 3 show the KS test and MWU test results for comparing the stride time distributions, computed using HSs and TOs, of a particular GED method with that of the corresponding GT dataset, for a given scenario. Each bar shows the number of datasets not rejected by the KS test out of the total datasets tested, for a given algorithm. Similarly, each square point (connected by dotted lines) represents the MWU test result for the same datasets.

4. Discussion

The statistical results of applying GED methods in various real-world scenarios reveal that the performance of most GED methods for detecting HS and TO is not consistent across different environments and activities. As shown in Table 2, the experimental protocol of GED methods usually involves walking on a flat surface such as a corridor which is represented by the Indoor Walk scenario. In this setting, the best performance is exhibited by A_{SK} and A_{JR} with high median F1 scores of 0.99 for all subjects, for both HSs and TOs. Both algorithms demonstrate high temporal accuracy in detecting events, shown by the KS and MWU test results where none of the 22 stride time datasets were rejected with the exception of one dataset. Algorithms A_{RT} and A_{RS} exhibit high F1 scores for HSs but show comparatively larger variances in their F1 scores for TOs. Moreover, the rejection of few datasets by KS and MWU tests indicates that for those subjects, the methods have low temporal accuracy and diminished performance for detecting TOs. Algorithms A_{MA} and A_{AS} also exhibit good performance for detecting HSs for most subjects but not for TOs. This is indicated by the significantly lower F1 scores for TOs as compared to HSs ($p < 0.05$) and the rejection of all TO datasets by the KS and MWU tests. With the exception of A_{RT}, while all other algorithms have their highest median F1 scores for detecting HSs in the Indoor Walk

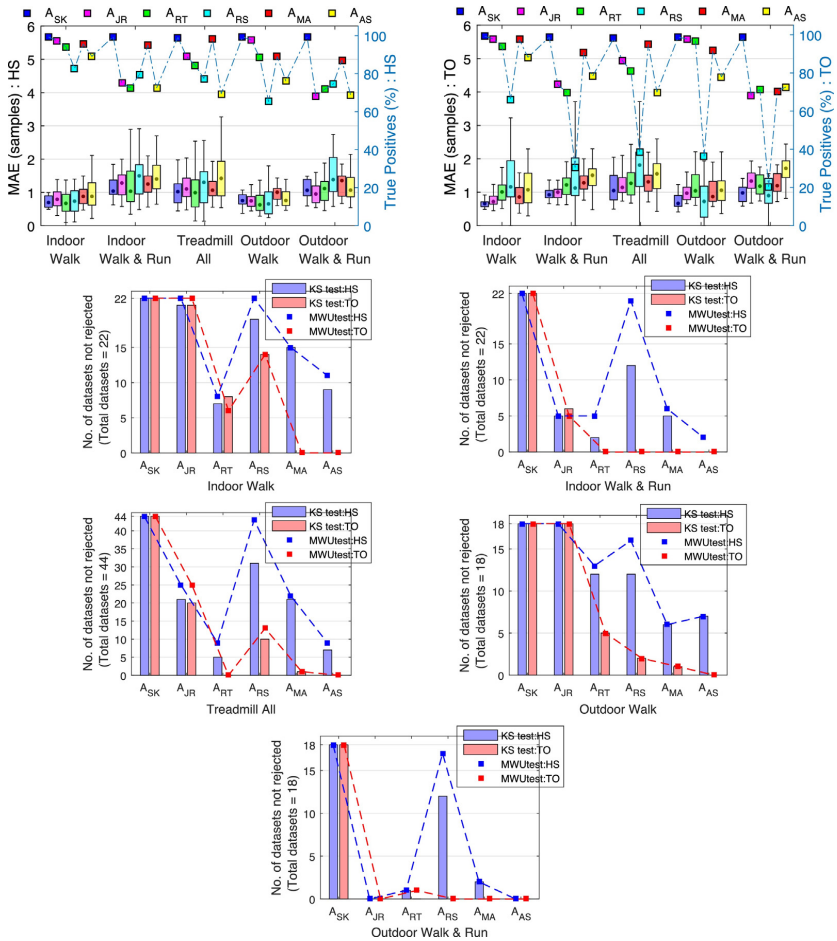

Fig. 3. The first two subfigures show the MAE (left y-axis) in detecting HSs and TOs along with the number of true positives (right y-axis) detected by various GED methods in different scenarios. The remaining five subfigures show the KS test and MWU test results for comparing the stride time distributions of a particular GED method with that of the corresponding GT dataset, for a given scenario. Each bar shows the number of datasets not rejected by the KS test out of the total datasets tested, for a given algorithm. Similarly, each square point (connected by dotted lines) represents the MWU test result for the same datasets. The total no. of datasets is computed as the product of: No. of subjects × Environment × Two ankles. For e.g. the total datasets for Treadmill All scenario = 11 × 2 × 2 (44 datasets). The abbreviations A_{SK}, A_{JR}, A_{RT}, A_{RS}, A_{MA} and A_{AS} stand for methods [24], [9], [12], [11], [10] and [13], respectively.

scenario, they exhibit larger variances in their F1 scores for Outdoor Walk suggesting decreased performance in a lesser controlled environment. In particular, A_{RS} exhibits the largest variance with significantly lower F1 score for TOs as compared to Indoor Walk scenario ($p < 0.05$). Additionally, for methods A_{RS} and A_{RT}, the ratio of TO datasets rejected by the KS and MWU test increases from Indoor Walk to Outdoor Walk, suggesting their decreased temporal accuracy with the change of environment. However, this change in accuracy with the change of environment is not distinctly observable in the conventional MAE results, as shown in Fig. 3. As MAE is computed using only the true positives, few true positives could result in a low MAE value indicating high accuracy although, in reality, the method might exhibit poor performance due to numerous false positives. In contrast, as the stride time distribution takes both, true positives and false positives into account; comparing the shape of this distribution with that of the GT, presents a better overview of the accuracy of a method.

Since most GED algorithms have been designed for walking with small speed variations, they are unable to adapt to large differences in gait speeds. This is illustrated in the results of all 'WalknRun' scenarios characterized by decreased F1 scores, for both HSs and TOs, as compared to the 'Walk' scenarios and large rejections of datasets by both KS and MWU tests. For example, when Indoor WalknRun is compared to Indoor Walk, methods A_{JR}, A_{RT} and A_{AS} have significantly lower F1 scores for HSs ($p < 0.05$) and all algorithms have significantly lower F1 scores for TOs ($p < 0.05$). Except A_{SK}, which is designed for variable gait speeds, all other algorithms show a large increase in the ratio of datasets being rejected by KS and MWU tests, especially for TOs, indicating reduced temporal accuracy for 'WalknRun' datasets. Moreover, almost all algorithms exhibit their lowest overall performance for Outdoor WalknRun scenario, which perhaps represents the most dynamic scenario. Though, it must be noted that it is difficult to make objective comparisons between various algorithms as they were developed using other datasets and protocols with different sensor positions, sampling frequencies and accelerometer specifications among others which may affect their performance scores. Nonetheless, the results indicate that their individual performance decreases in scenarios other than Indoor Walk, which is usually the laboratory setting in which they are designed and assessed.

This lower performance of GED methods in other, lesser controlled scenarios could be attributed to the fact that most GED algorithms are purely data-driven and hence find it challenging to adapt to larger variations in the accelerometer data collected from dynamic environments and activities. Moreover, the comparatively lower performance for detecting TOs as compared to HSs can be observed in algorithms that define spatial or temporal thresholds either explicitly, as A_{RS}, or use them at some intermediate stage after signal transformation, such as A_{RT} and A_{AS}. As mentioned earlier in Section 2.1, in contrast to the left ankle, the Z axis of the right ankle accelerometer was marginally disturbed. It was observed that methods A_{RT}, A_{RS}, A_{MA} and A_{AS} displayed significantly lower F1 scores for the right foot gait events as compared to the left foot, for all 'WalknRun' scenarios ($p < 0.05$). This may be attributed to the algorithmic design as methods A_{RT}, A_{RS} and A_{MA} process individual axis signals obtained from pre-defined axes alignment fixed relative to the limb, thus making it challenging to tackle larger deviations from original configuration likely to occur in dynamic and uncontrolled scenarios. Based on the presented study, it is suggested that incorporating gait data from different real-world settings, such as the MAREA database, during algorithmic development shall help in designing more robust and adaptive GED algorithms for use in everyday life. A current drawback of the database is that it lacks information from other inertial sensors such as gyroscopes, which shall be included in future additions to improve the database.

5. Conclusion

To conclude, a new gait database called MAREA is presented that consists of various gait activities in different environmental settings, both indoors and outdoors. The performance of existing GED methods is evaluated in various scenarios defined using the MAREA database. It is observed that while all GED methods exhibit good performance for the scenario of steady walking in a controlled indoor environment, they demonstrate decreased performance in other environments and more dynamic scenarios involving varying gait speeds and changing surface inclinations. Moreover, all GED algorithms displayed better performance for detecting Heel-Strikes as compared to Toe-Offs, when evaluated in different scenarios.

Acknowledgements

This study was supported in part by the Knowledge Foundation, Sweden.

Conflict of interest

There are no conflicts of interest.

References

[1] J. Rueterbories, E.G. Spaich, B. Larsen, O.K. Andersen, Methods for gait event detection and analysis in ambulatory systems, Med. Eng. Phys. 32 (6) (2010) 545–552, http://dx.doi.org/10.1016/j.medengphy.2010.03.007.
[2] J. Leitch, J. Stebbins, G. Paolini, A.B. Zavatsky, Identifying gait events without a force plate during running: a comparison of methods, Gait Posture 33 (1) (2011) 130–132, http://dx.doi.org/10.1016/j.gaitpost.2010.06.009.
[3] D.A. Bruening, S.T. Ridge, Automated event detection algorithms in pathological gait, Gait Posture 39 (1) (2014) 472–477, http://dx.doi.org/10.1016/j.gaitpost.2013.08.023.
[4] F. Alvim, L. Cerqueira, A. Netto, G. Leite, A. Muniz, Comparison of five kinematic-based identification methods of foot contact events during treadmill walking and running at different speeds, J. Appl. Biomech. 31 (5) (2015) 383–388, http://dx.doi.org/10.1123/jab.2014-0178.
[5] L. Smith, S. Preece, D. Mason, C. Bramah, A comparison of kinematic algorithms to estimate gait events during overground running, Gait Posture 41 (1) (2015) 39–43, http://dx.doi.org/10.1016/j.gaitpost.2014.08.009.
[6] R.E. Mayagoitia, A.V. Nene, P.H. Veltink, Accelerometer and rate gyroscope measurement of kinematics: an inexpensive alternative to optical motion analysis systems, J. Biomech. 35 (4) (2002) 537–542, http://dx.doi.org/10.1016/S0021-9290(01)00231-7.
[7] J.R. Rebula, L.V. Ojeda, P.G. Adamczyk, A.D. Kuo, Measurement of foot placement and its variability with inertial sensors, Gait Posture 38 (4) (2013) 974–980.
[8] J.J. Kavanagh, H.B. Menz, Accelerometry: a technique for quantifying movement patterns during walking, Gait Posture 28 (1) (2008) 1–15, http://dx.doi.org/10.1016/j.gaitpost.2007.10.010.
[9] J. Rueterbories, E.G. Spaich, O.K. Andersen, Gait event detection for use in FES rehabilitation by radial and tangential foot accelerations, Med. Eng. Phys. 36 (4) (2014) 502–508, http://dx.doi.org/10.1016/j.medengphy.2013.10.004.
[10] M.S.H. Aung, S.B. Thies, L.P.J. Kenney, D. Howard, R.W. Selles, A.H. Findlow, J.Y. Goulermas, Automated detection of instantaneous gait events using time frequency analysis and manifold embedding, IEEE Trans. Neural Syst. Rehabil. Eng. 21 (6) (2013) 908–916, http://dx.doi.org/10.1109/TNSRE.2013.2239313.
[11] R.W. Selles, M.A.G. Formanoy, J.B.J. Bussmann, P.J. Janssens, H.J. Stam, Automated estimation of initial and terminal contact timing using accelerometers; development and validation in transtibial amputees and controls, IEEE Trans. Neural Syst. Rehabil. Eng. 13 (1) (2005) 81–88, http://dx.doi.org/10.1109/TNSRE.2004.843176.
[12] R.R. Torrealba, J. Cappelletto, L. Fermin-Leon, J.C. Grieco, G. Fernandez-Lopez, Statistics-based technique for automated detection of gait events from accelerometer signals, Electron. Lett. 46 (22) (2010) 1483–1485, http://dx.doi.org/10.1049/el.2010.2118.
[13] A. Sant'Anna, N. Wickström, A symbol-based approach to gait analysis from acceleration signals: identification and detection of gait events and a new measure of gait symmetry, IEEE Trans. Inf. Technol. Biomed. 14 (5) (2010) 1180–1187, http://dx.doi.org/10.1109/TITB.2010.2047402.
[14] T.T. Ngo, Y. Makihara, H. Nagahara, Y. Mukaigawa, Y. Yagi, The largest inertial sensor-based gait database and performance evaluation of gait-based personal authentication, Pattern Recognit. 47 (1) (2014) 228–237, http://dx.doi.org/10.1016/j.patcog.2013.06.028.

[15] Y. Zhang, G. Pan, K. Jia, M. Lu, Y. Wang, Z. Wu, Accelerometer-based gait recognition by sparse representation of signature points with clusters, IEEE Trans. Cybern. 45 (9) (2015) 1864–1875, http://dx.doi.org/10.1109/TCYB.2014.2361287.
[16] D. Trojaniello, A. Cereatti, U.D. Croce, Accuracy, sensitivity and robustness of five different methods for the estimation of gait temporal parameters using a single inertial sensor mounted on the lower trunk, Gait Posture 40 (4) (2014) 487–492, http://dx.doi.org/10.1016/j.gaitpost.2014.07.007.
[17] M. Hanlon, R. Anderson, Real-time gait event detection using wearable sensors, Gait Posture 30 (4) (2009) 523–527, http://dx.doi.org/10.1016/j.gaitpost.2009.07.128.
[18] J. McCamley, M. Donati, E. Grimpampi, C. Mazzà, An enhanced estimate of initial contact and final contact instants of time using lower trunk inertial sensor data, Gait Posture 36 (2) (2012) 316–318, http://dx.doi.org/10.1016/j.gaitpost.2012.02.019.
[19] B. Auvinet, G. Berrut, C. Touzard, L. Moutel, N. Collet, D. Chaleil, E. Barrey, Reference data for normal subjects obtained with an accelerometric device, Gait Posture 16 (2) (2002) 124–134, http://dx.doi.org/10.1016/S0966-6362(01)00203-X.
[20] W. Zijlstra, A.L. Hof, Assessment of spatio-temporal gait parameters from trunk accelerations during human walking, Gait Posture 18 (2) (2003) 1–10, http://dx.doi.org/10.1016/S0966-6362(02)00190-X.
[21] K.B. Mansour, N. Rezzoug, P. Gorce, Analysis of several methods and inertial sensors locations to assess gait parameters in able-bodied subjects, Gait Posture 42 (4) (2015) 409–414, http://dx.doi.org/10.1016/j.gaitpost.2015.05.020.
[22] R.C. González, A.M. López, J. Rodriguez-Uría, D. Álvarez, J.C. Alvarez, Real-time gait event detection for normal subjects from lower trunk accelerations, Gait Posture 31 (3) (2010) 322–325, http://dx.doi.org/10.1016/j.gaitpost.2009.11.014.
[23] A. Godfrey, R. Conway, D. Meagher, G. ÓLaighin, Direct measurement of human movement by accelerometry, Med. Eng. Phys. 30 (10) (2008) 1364–1386, http://dx.doi.org/10.1016/j.medengphy.2008.09.005.
[24] S. Khandelwal, N. Wickström, Gait event detection in real-world environment for long-term applications: Incorporating domain knowledge into time-frequency analysis, IEEE Trans. Neural Syst. Rehabil. Eng. (2016), http://dx.doi.org/10.1109/TNSRE.2016.2536278.
[25] D.R. Cox, D.V. Hinkley, Theoretical Statistics, Chapman and Hall, London, 1974.

Appendix III

Paper III - Novel Methodology for Estimating Initial Contact Events from Accelerometers positioned at Different Body Locations

Gait & Posture 59 (2018) 278–285

Contents lists available at ScienceDirect

Gait & Posture

journal homepage: www.elsevier.com/locate/gaitpost

Novel methodology for estimating Initial Contact events from accelerometers positioned at different body locations

Siddhartha Khandelwal*, Nicholas Wickström

Center for Applied Intelligent Systems Research, Halmstad University, Sweden

ARTICLE INFO

Keywords:
Gait event
Inertial sensor
Sensor placement
Wavelet transform
Domain knowledge
Gait database

ABSTRACT

Identifying Initial Contact events (ICE) is essential in gait analysis as they segment the walking pattern into gait cycles and facilitate the computation of other gait parameters. As such, numerous algorithms have been developed to identify ICE by placing the accelerometer at a specific body location. Simultaneously, many researchers have studied the effects of device positioning for participant or patient compliance, which is an important factor to consider especially for long-term studies in real-life settings. With the adoption of accelerometery for long-term gait analysis in daily living, current and future applications will require robust algorithms that can either autonomously adapt to changes in sensor positioning or can detect ICE from multiple sensors locations.

This study presents a novel methodology that is capable of estimating ICE from accelerometers placed at different body locations. The proposed methodology, called DK-TiFA, is based on utilizing domain knowledge about the fundamental spectral relationships present between the movement of different body parts during gait to drive the time-frequency analysis of the acceleration signal. In order to assess the performance, DK-TiFA is benchmarked on four large publicly available gait databases, consisting of a total of 613 subjects and 7 unique body locations, namely, ankle, thigh, center waist, side waist, chest, upper arm and wrist. The DK-TiFA methodology is demonstrated to achieve high accuracy and robustness for estimating ICE from data consisting of different accelerometer specifications, varying gait speeds and different environments.

1. Introduction

Initial Contact events (ICE) segment the walking pattern into gait cycles and are essential in many gait analysis applications [1–3]. Consequently, numerous accelerometer-based algorithms have been developed to identify ICE from various body locations [4]. Usually, the accelerometer is positioned on the leg such as forefoot, ankle or shank [5–7]; or on the chest or lower trunk locations [8–11]. While choosing a position is application-dependent, researchers have studied the influence of device positioning for patient compliance, especially for long-term studies in real-life settings [12–14]. Overcoming non-compliance or self re-attachment of the sensor would cause changes in the original position and orientation of the device. This would alter features of the acceleration signal and affect most algorithms that are typically data-driven techniques reliant on signal characteristics of a particular body location [9,11,13]. Additionally, changes in sensor placement would require switching between various position-dependent algorithms designed with different methodologies and protocols. With the adoption of accelerometery for long-term gait analysis in daily living [15], current and future applications demand robust algorithms that can either autonomously adapt to changes in sensor positioning or can detect ICE from multiple sensors locations.

Recently, the authors had presented an algorithm that showed how domain knowledge about gait could be incorporated into time-frequency analysis to identify gait events [7]. However, it was limited to detecting heel-strikes and toe-offs from accelerometers positioned only on the ankles. Inspired by the prior approach, this study presents a novel methodology that is capable of estimating ICE from accelerometers placed at different body locations. The proposed methodology, called DK-TiFA: (Domain Knowledge in Time-Frequency Analysis), is based on utilizing domain knowledge about the fundamental spectral relationships present between the movement of different body parts during normal gait and incorporating it into time-frequency analysis of the acceleration signal. In order to assess the accuracy and robustness, DK-TiFA is benchmarked on four publicly available gait databases consisting of 7 unique body locations and varying data collection protocols.

* Corresponding author at: Center for Applied Intelligent Systems Research, School of Information Technology, Halmstad University, P.O. Box 823, SE-301 18 Halmstad, Sweden.
E-mail address: siddhartha.khandelwal@hh.se (S. Khandelwal).

http://dx.doi.org/10.1016/j.gaitpost.2017.07.030
Received 1 March 2017; Received in revised form 17 May 2017; Accepted 5 July 2017

2. Proposed DK-TiFA methodology

Normal gait consists of a series of co-ordinated periodic movements of various body parts such as arms, legs and trunk. The frequencies associated with these movements are captured in the measured acceleration signals and lead to distinct and consistent spectral characteristics in the frequency domain. Expert or domain knowledge is utilized to comprehend these spectral characteristics in order to drive the time-frequency analysis of the acceleration signal obtained from a given body location.

Firstly, to be orientation-invariant and avoid any misalignment issues, the magnitude of resultant accelerometer signal Acc_r is computed from the raw acceleration signals as:

$$\mathrm{Acc}_r = \sqrt{\mathrm{acc}_x{}^2 + \mathrm{acc}_y{}^2 + \mathrm{acc}_z{}^2} \tag{1}$$

where acc_x, acc_y, acc_z are obtained from each individual axis of the 3-axes accelerometer, respectively. As the objective is to capture spectral characteristics in the composite acceleration signal Acc_r, the continuous wavelet transform (CWT) is used as it provides a time-frequency representation that is appropriate for analyzing varying frequencies in time [16]. The CWT of a discrete time signal x_n with equal time spacing δ_t, is defined as the convolution of x_n with a scaled and translated mother wavelet $\psi_0(\eta)$:

$$W_n(s) = \sum_{n'=0}^{N-1} x_{n'}\ \psi^*\left[\frac{(n'-n)\delta_t}{s}\right] \tag{2}$$

where (*) indicates the complex conjugate, s is the wavelet scaling factor and n is the localized time index [17]. To avoid spectral domain skewness, the Morlet wavelet is chosen as it is symmetric and has been shown to effectively distinguish spectral characteristics in time [7,18]. Fig. 1 shows the CWT of composite acceleration signals obtained from different body locations, where finer scales correspond to high frequencies and vice-versa. To determine the relative contribution of a frequency to the total signal energy at a specific scale s, the scale-dependent energy density spectrum is computed from the CWT coefficients, as:

$$E_s = \sum_{n=0}^{N-1} |W_n(s)|^2, \qquad s \in [1, s_{\max}] \tag{3}$$

where $|W_n(s)|^2$ is the 2-D wavelet energy density function that measures the total energy distribution of the signal [16]. Peaks in E_s highlight the dominant energetic scales that contribute to most of the signal energy in the spectral domain. Fig. 1 shows the E_s profiles of the different body locations computed from the respective CWT coefficients.

2.1. Domain knowledge

An accelerometer placed at any body location captures accelerations from the local movement of the respective body part and the global movement of the body, in a given direction. As these co-ordinated body movements are periodic in nature during normal gait, the underlying frequencies associated with these movements are also co-related. These spectral relationships can be visualized in time by taking the CWT of the acceleration signal and the major frequencies get highlighted as dominant spectral peaks in their respective E_s profiles.

For example, an accelerometer located at the ankle of a leg, captures forces generated from two major events, Initial and Final Contact. As frequency of the events is twice that of the gait cycle, the CWT coefficients corresponding to the the gait cycle exist towards the coarser scales (or low frequency) while those corresponding to the Initial and Final Contact events exist towards the finer scales (or high frequency and twice that of the gait cycle). Thus, the resulting $E_{s(ankle)}$ profile is characterized by two distinct peaks corresponding to the event and cycle frequencies and the associated peak scales have a ratio of 2. Similarly, during normal gait, arm swing is a natural motion where each arm swings with the motion of the opposite leg. Thus, the wrist accelerometer captures a combination of the local acceleration forces due to the arm swing and the global acceleration forces due to the forward movement of the body. Peak scales in $E_{s(wrist)}$ show the underlying periodic frequencies which have a similar event-cycle spectral relationship as the ankle. An accelerometer positioned in the central body such as chest or waist captures a combination of forces generated periodically, consisting of the gait events from both legs and local movements of the body part such as pelvic movements in the transverse and frontal plane [19]. As such, the major frequency in the central body acceleration signal is a combination of the gait cycles of the two legs, which is twice the frequency of the gait cycle of an individual leg (e.g. refer subfigures 3 and 7 in the second and third column of Fig. 1).

However, in real-life settings, human gait is quite varied involving changing gait speeds and environmental factors. As such, these changes in movement patterns captured by the acceleration signal of a specific body position are reflected in the corresponding CWT coefficients. For example, increasing gait speeds would mean higher gait frequencies, and the resulting CWT coefficients would exist towards the finer scales (or high frequency) and vice-versa. Another example is shown in Fig. 4b, where a subject walks with no arm swing and then changes to swinging the arms, leading to varying peak amplitudes in $E_{s(wrist)}$. Hence, these changes during gait propagates to the corresponding E_s profiles as shift of dominant energy scales along the spectral axis and variations in their peak amplitudes. The challenge is to design an algorithm that can tackle these local spectral transitions in E_s and consistently track them, in time. Thus, DK-TiFA utilizes the aforementioned relative spectral relationships to define a two-step tracking procedure that tracks the most dominant scale in the E_s profile of a given body position. This spectral-temporal information is further used to estimate ICE from respective accelerometer signals.

2.2. Time-frequency analysis

As shown in Fig. 2, DK-TiFA consists of three major systematic steps elaborated in the following subsections.

2.2.1. Pre-processing

First, the composite acceleration signal Acc_r is computed from the 3-axis acceleration signals using (1). Then the CWT of Acc_r is computed using a real-valued Morlet wavelet, as shown in (2). The range of scales for analysis, i.e. $[1, s_{\max}]$ are chosen using the non-linear frequency-scale relationship of the Morlet wavelet such that $s_{\max} = \frac{F_c}{(\Delta F_a)}$, where Δ is the sampling period, F_a is the minimum gait frequency assumed to be around 0.5 Hz [20]; and $F_c = \frac{(\omega_o + \sqrt{2+\omega_o^2})}{4\pi}$ where ω_o is the center frequency of the Morlet, taken as 5.105 rad/s [17,21].

2.2.2. Tracking the most dominant spectral energy scale

Based on the accelerometer placement on central body or limb, this step tracks the most dominant spectral energy scale present in the E_s profile of that position.

As explained in Section 2.1, the E_s profile of a central body placement such as chest or waist is characterized by a dominant peak. For such placements, a running window is taken along the temporal axis of the CWT coefficients and within every window r, the peak scale μ_s^r is computed that corresponds to the maximum spectral energy in the local E_s^r profile, i.e.:

$$\mu_s^r = \arg\max_{s\in[1,s_{\max}]} E_s^r \tag{4}$$

$$\text{where,} \quad E_s^r = \sum_{n=rP}^{(r+1)P-1} |W_n(s)|^2,\ s \in [1, s_{\max}] \tag{5}$$

and P denotes the window hop size. In principle, a window size that captures the information of one gait cycle is sufficient but practically it is desired to be large enough to account for signal noise and thus it

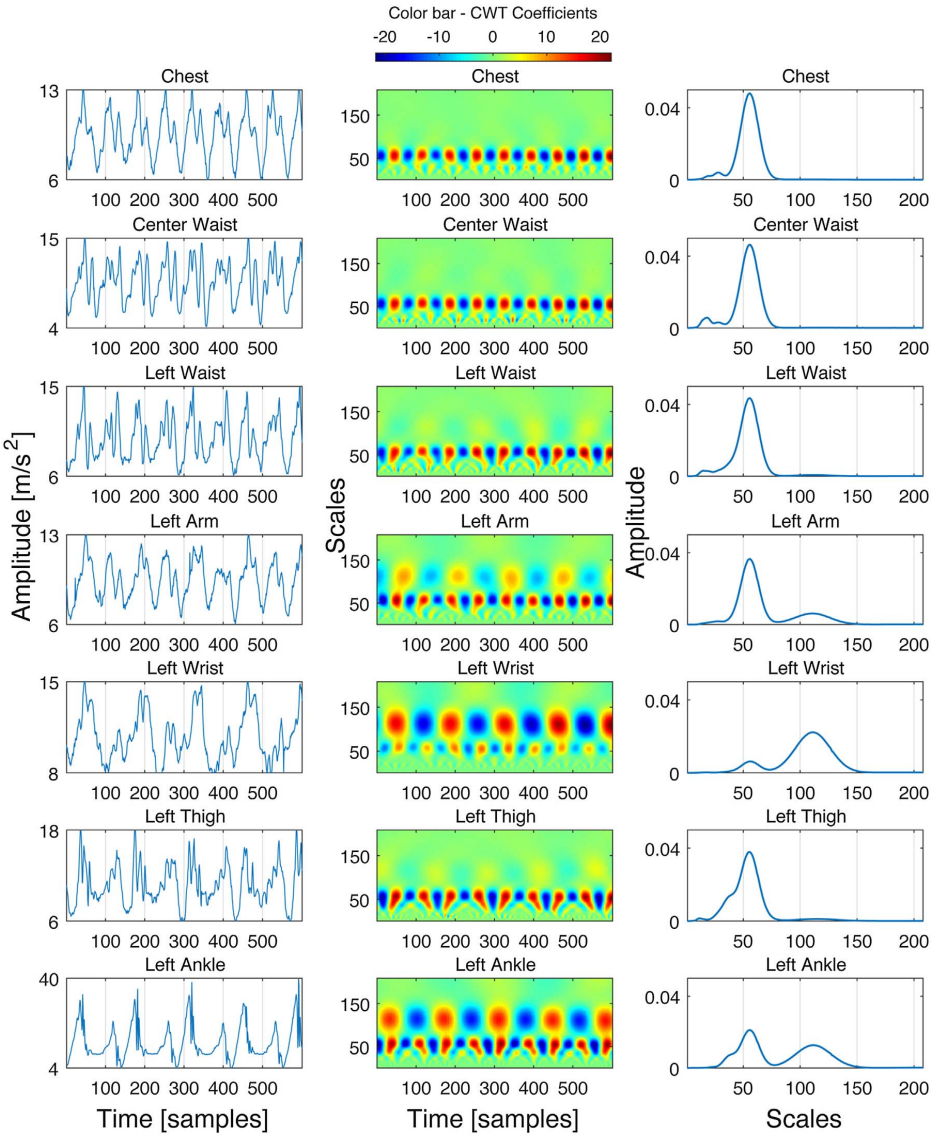

Fig. 1. The first column shows the different composite acceleration signals Acc_r obtained from accelerometers positioned at various body locations. The different Acc_r's are time-synchronized. The second column shows the top view of the corresponding CWT coefficients and the third column shows the energy density spectrum (E_s) profiles computed from the respective CWT coefficients. The E_s profiles are similar for accelerometer placements on the limbs, such as ankles and wrists, and are characterized by two distinct peak scales. Likewise, the E_s profiles are similar for accelerometer placements on the central body, such as chest and waist, and are characterized by one dominant peak scale. The E_s profiles have been normalized to scale them into the figure.

could be taken from 3 to 6 s to include additional gait cycles. The E_s profile of an accelerometer placed on the limbs such as ankle or wrist, is generally characterized by two distinct spectral energy peaks and the associated peak scales have a ratio of 2 due to the event-cycle spectral relationship. However, as explained in Section 2.1, changes in movement patterns would be reflected in the CWT coefficients and may lead to shift in peak scales and variations of the peak amplitudes in E_s^r profile. Thus, a two-step procedure is suggested: (1) determine which is the most dominant spectral energy scale (event or cycle) in the entire signal, and (2) consistently track the chosen peak scale in every window.

- **Step 1:** The E_s profile of the entire Acc_r is computed using (3). Then the possible candidates corresponding to the event and cycle peaks in E_s are computed as the set of local maxima points $\{(s_m, E_{s_m}), m \in [1, M]\}$; where s_m is the scale corresponding to a peak value E_{s_m} and M is the total number of maxima points. If only one local maxima is found ($M = 1$), it is determined that the event

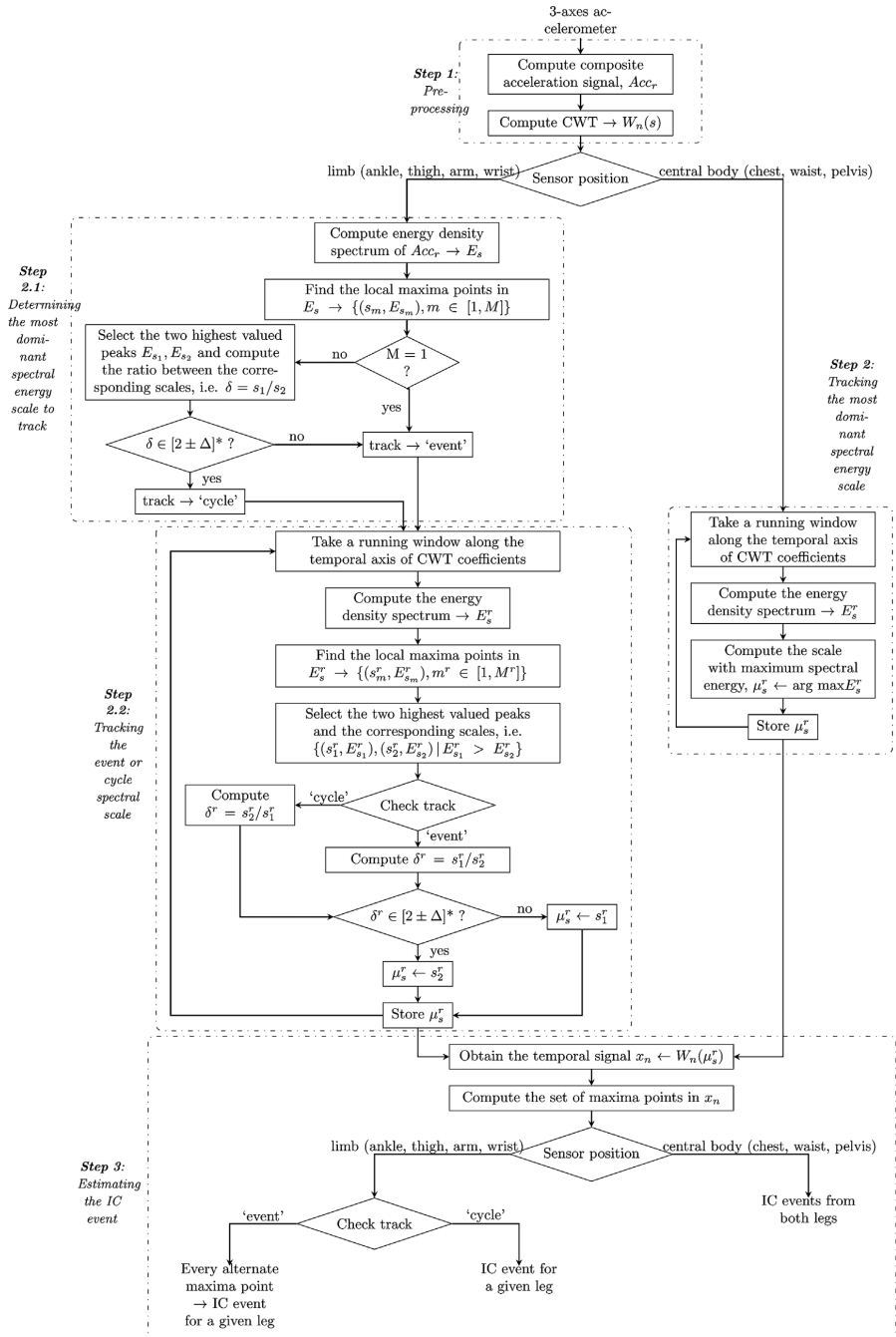

Fig. 2. An overview of the DK-TiFA methodology for detecting gait events from accelerometers positioned at various body locations. (*) In implementation, the event-cycle spectral relationship is relaxed by Δ (here taken to be 0.4) to accommodate effects of signal noise and low frequency resolution in finer scales.

peak scale is the most dominant spectral scale to track and the procedure goes to Step 2. Otherwise, in case of multiple local maxima points ($M \geq 2$), the two highest amplitude points are selected and the ratio between their corresponding scale values is computed as:

$$\delta = \frac{s_1}{s_2}, \quad \text{such that: } E_{s_1} > E_{s_2} \tag{6}$$

Utilizing the event-cycle spectral relationship, if $\delta = 2$, then the most dominant spectral scale s_1 corresponds to the cycle peak, otherwise s_1 corresponds to the event peak. In implementation, this spectral relationship is relaxed to accommodate effects of signal noise and low frequency resolution in finer scales [22].

- **Step 2:** Take a running window along the temporal axis of the CWT coefficients. Within every window r, select the two highest amplitude points and their corresponding scale values, i.e. $\{(s_1^r, E_{s_1}^r), (s_2^r, E_{s_2}^r) | E_{s_1}^r > E_{s_2}^r\}$ from the set of local maxima points in E_s^r. If Step 1 selects to track the cycle peak, then the spectral ratio δ^r is computed as:

$$\delta^r = \frac{s_2^r}{s_1^r} \tag{7}$$

and the following two cases are checked:

– Case I: If $\delta^r \neq 2$ then $s_1^r > s_2^r$ and the maximal peak $E_{s_1}^r$ corresponds to the cycle peak as expected. Accordingly, s_1^r is stored as the tracked scale μ_s^r.
– Case II: If $\delta^r = 2$ as $s_2^r = 2s_1^r$, then $E_{s_2}^r$ corresponds to the cycle peak instead due to locally varying peak amplitudes. Thus, s_2^r is stored as the tracked scale μ_s^r.

A similar procedure is adopted if Step 1 selects to track the event peak instead, as shown in Fig. 2.

2.2.3. Estimating the ICE

The tracked spectral scale μ_s^r stored in every window r represents the major underlying local frequency in Acc_r. By successively compiling them from all windows and selecting the CWT coefficients at those particular scales, a distinct temporal signal x_n is obtained as:

$$x_n \triangleq W_n(\mu_s^r), \quad r \in \left[1, \frac{N}{P-1}\right] \tag{8}$$

x_n is low-pass filtered using a zero-phase filter to remove any high frequency noise and window edge effects. Then the set of local maxima points in x_n is computed to estimate the desired ICE (refer Fig. 4a). If the accelerometer was positioned on the central body such as chest or waist, then the first point would correspond to the ICE from one leg and the second to the ICE from the other leg and so on. If the accelerometer was positioned on the limb such as ankle or wrist, then the corresponding ICE are estimated based on which spectral scale was tracked. If the event spectral scale was tracked then every alternate maxima point would correspond to the ICE while if the cycle spectral scale was tracked, the maxima points would correspond directly to the ICE of a given leg.

2.3. Benchmarking the DK-TiFA methodology

DK-TiFA was applied on four accelerometer-based gait databases, namely, MAREA Gait Database (MAREA-DB) [23], ZJU-GaitAcc Database (ZJU-GaitAcc-DB) [24], OU-ISIR Gait Database (OU-ISIR-DB) [3] and DaLiAc Database (DaLiAc-DB) [25]. Table 1 shows a summary of the walking datasets included in these databases. For each walking trial, the stride time distribution was computed from the estimated ICE of each body location. It was previously shown that non-parametric statistical tests could be used to assess the accuracy and consistency of a method by comparing the shape of the two stride time distributions obtained from the method and an external reference or ground truth [23]. If all ICE detected from a body location matched exactly the corresponding events from an external reference, then this would lead to identical stride time distributions and indicate high accuracy of the method. However, occurrence of any false positives or false negatives would lead to shorter or longer stride time durations, which in turn would be reflected in the shape of the resulting stride time distribution of the walking trial and would be dissimilar compared to the corresponding one obtained from the external reference. Thus, the Kolmogorov–Smirnov (KS) test and Mann–Whitney U (MWU) test were applied to test the null hypothesis that the two stride time distributions were identical and both tests rejected the null hypothesis at 5% significance level [26]. In case of lack of any external reference, the same approach was used to obtain insights into the consistency of the method by comparing the stride time distributions obtained from different parts of the body with the hypothesis that they must also be identical. Additionally, agreement between the two distributions was analyzed using the Bland–Altman plots [27]. None of the databases used motion capture system or force plates to collect gold standard reference. While MAREA-DB used force sensitive resistors as an external reference (XREF), the manually annotated gait cycles in ZJU-GaitAcc-DB was used as XREF for computing stride time distributions. MAREA-DB had 20 subjects but one dataset had no wrist data and was excluded from analysis. ZJU-GaitAcc-DB had 153 subjects with 2 walking sessions, 22 subjects with one session and 6 records/session, leading to 1968 datasets ($153 \times 2 \times 6 + 22 \times 1 \times 6$). As OU-ISIR-DB had very short durations of walking trials, the step time distribution was computed instead, to increase the statistical power of the test. Also, it was found that 12 datasets had no accelerometer data for either of the positions and 88 datasets had unequal number of samples (with more than 5% difference) for the same trial, and few datasets were in both categories. Thus, 95 out of 495 datasets were excluded from analysis.

3. Results

Table 1 shows the results of applying DK-TiFA on the gait databases. For MAREA-DB and ZJU-GaitAcc-DB, each cell in the first column shows the total number of datasets not rejected by KS and MWU test as a result of comparing the stride time distributions computed using the estimated ICE with that of the corresponding XREF datasets, for a particular sensor position. Each cell in all other columns shows the total number of datasets not rejected as a result of comparing the stride or step time distributions computed from the ICE of one sensor location with that of another location. Each row in Fig. 3 shows the Bland–Altman (BA) plot results for each database. The x-axis for each plot in the first two rows (MAREA-DB and ZJU-GaitAcc-DB) shows the arithmetic mean of the stride time computed from the estimated ICE and the corresponding XREF; while the y-axis shows their difference. As no XREF is available for OU-ISIR-DB and DaLiAc-DB, the last two rows show the BA plots of comparing the step or stride time computed from any two unique body locations. The dashed lines show the mean of the differences and the limits of agreement, i.e. $\pm 1.96\sigma$ (where σ is the standard deviation of the differences); such that 95% of the differences lie between the limits of agreement.

4. Discussion and conclusion

The results reveal that DK-TiFA performs excellently for the accelerometer placements on the legs such as ankle and thigh, and central body such as waist, side pelvis and chest. Table 1 shows that for MAREA-DB, none of the datasets were rejected by KS and MWU tests for ankle and waist placements when compared to the XREF datasets. Similarly for ZJU-GaitAcc-DB, only 0.39% of the datasets were rejected by KS test and 0.12% of the datasets were rejected by MWU test, for pelvis, thigh and ankle placements. For OU-ISIR-DB and DaLiAc-DB

Table 1
The KS and MWU test results of comparing the stride time or step time distributions of a given sensor position with the corresponding external reference dataset or another body location. The right column gives an overview of the walking datasets in each database. Numbers marked as (*) denote approximate estimations either reported by the respective authors or computed by manual inspection of the datasets.

	MAREA gait database [23]: total datasets tested = 19					
Sensor position	External reference	Right ankle	Waist	Wrist	Walking datasets	
Left ankle	KS test	19	19	19	14	Subjects: 20
	MWU test	19	19	19	16	Gender: 12 m, 8 f
Right ankle	KS test	19	–	19	15	Age: 33.4 ± 7
	MWU test	19		19	16	Acc. type 3-axis ± 8 g
Waist	KS test	19	–	–	13	Sampling rate: 128 Hz
	MWU test	19			16	Trial period: 3 min
Wrist	KS test	16	–	–	–	Steps/trial: 352*
	MWU test	16				Total steps: 7102*

	ZJU-GaitAcc database [24]: total datasets tested = 1968					
Sensor position	External reference	Thigh	Pelvis	Upper arm	Wrist	Walking datasets
Ankle	KS test	1961	1966	1963	1921	1830	
	MWU test	1965	1967	1960	1921	1825	Subjects: 175
Thigh	KS test	1962	–	1966	1920	1835	Gender: 2/3 m, 1/3 f*
	MWU test	1967		1963	1921	1824	Age: 16–40
Pelvis	KS test	1958	–	–	1919	1837	Acc. type: 3-axis ± 5 g
	MWU test	1965			1916	1815	Sampling rate: 100 Hz
Upper arm	KS test	1918	–	–	–	1821	Trial period: 7–15 s
	MWU test	1921				1807	Steps/trial: 22*
Wrist	KS test	1835	–	–	–	–	Total steps: 45,110*
	MWU test	1828					

	OU-ISIR gait database [3]: total datasets tested = 400			
Sensor position	Left waist	Right waist	Walking datasets	
Center waist	KS test	397	399	Subjects: 495
	MWU test	397	399	Gender: 1/2 m, 1/2 f*
Left waist	KS test	–	398	Age: 2–78
	MWU test			Acc. type: 3-axis ± 4 g
				Sampling rate: 100 Hz
				Steps/trial: 10*
				Total steps: 10,229

	DaLiAc database [25]: total datasets tested = 19				
Sensor position	Hip	Chest	Wrist	Walking datasets	
Ankle	KS test	19	19	18	Subjects: 19
	MWU test	19	19	18	Gender: 11 m, 8 f
Hip	KS test	–	19	18	Age: 26 ± 8
	MWU test		19	18	Acc. type: 3-axis ± 6 g
Chest	KS test	–	–	18	Sampling rate: 204.8 Hz
	MWU test			18	Steps/trial: 488*
					Total steps: 9416*

where XREF was unavailable, a comparison between the step or stride time distributions obtained from different positions show that with the exception of 3 datasets, none were rejected by KS and MWU test. These results are complemented by BA plots of the respective databases for accelerometer placements on the leg and central body. Fig. 3 shows that for these locations, mean of the differences in the corresponding stride or step time is very close to zero, indicating strong agreement between them. Moreover, almost all data points are concentrated in a cluster between the small limits of agreement with few outliers corresponding to the false positives (below -1.96σ) and false negatives (above $+1.96\sigma$).

However, it was observed that estimating ICE from accelerometer placements on the arm such as wrist and upper arm was more challenging as more datasets were rejected for these positions. For MAREA-DB, 3 datasets were rejected by the KS test while for ZJU-GaitAcc-DB, 4.65% of the total datasets were rejected by the KS test. This was also observed in the BA plots of upper arm and wrist, where two distinct clusters of data points exist outside the limits of agreement ($\pm 1.96\sigma$). The data points in the lower left corner of the graph appear due to the occurrence of false positives in estimating ICE as the resulting stride time values are lower in comparison to the external reference; leading to lower mean and negative difference between them. Similarly, those in the upper right corner appear due to the occurrence of false negatives leading to a larger mean and positive difference between them. This decrease in the performance is due to the fact that the tracking procedure is unable to effectively tackle rapid changes in arm swing behaviour of the subjects. Although, arm swing motion is generated naturally during bipedal walking, it is not a necessary criteria for stable walking and often humans change their arm motions during everyday walking [28]. An example is depicted in Fig. 4b which shows the variations in the CWT of a wrist accelerometer during standing and walking with successive movements of no swing, normal swing and

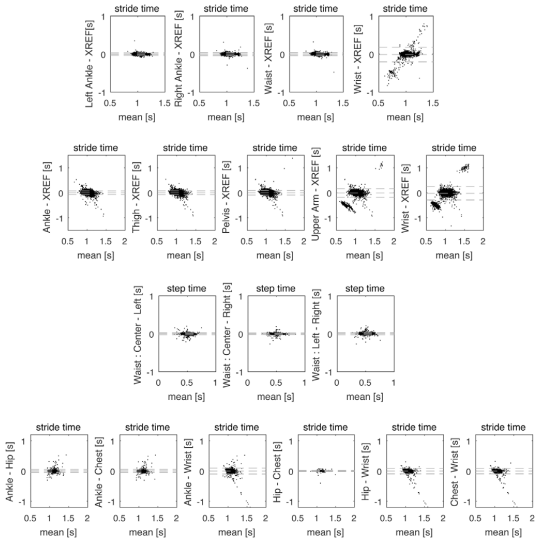

Fig. 3. This figure shows the Bland–Altman (BA) plot results of the MAREA-DB [23] (first row), ZJU-GaitAcc-DB [24] (second row), OU-ISIR-DB [3] (third row) and DaLiAc-DB [25] (fourth row), respectively. The *x*-axis for each plot in the first two rows (MAREA-DB and ZJU-GaitAcc-DB) shows the arithmetic mean of the stride time computed from the estimated ICE using the DK-TiFA methodology and the corresponding external reference (XREF); while the *y*-axis shows their difference. The dashed lines show the mean of the differences and the limits of agreement, i.e. $\pm$ 1.96σ (where σ is the standard deviation of the differences); such that 95% of the differences lie between the limits of agreement. As no XREF is available for OU-ISIR-DB and DaLiAc-DB, the last two rows show the BA plots of comparing the step or stride time computed from any two unique body locations.

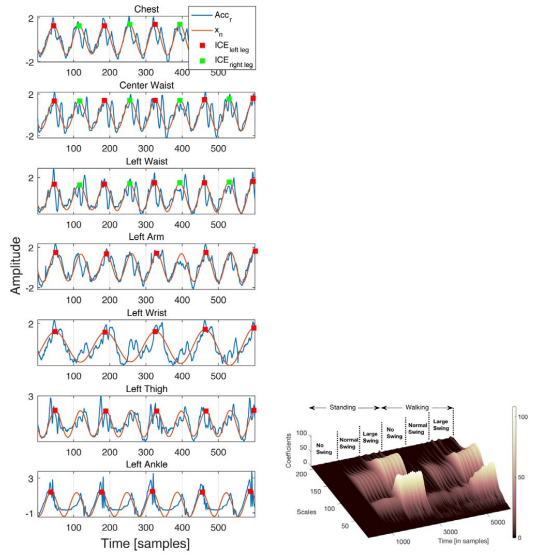

Fig. 4. (a) Examples of the low-pass filtered temporal signal x_n, for each sensor location, that matches the frequency of the event or cycle in the corresponding composite acceleration signal. All signals have been normalized to scale them into the figure. The estimated ICE for a given leg are marked as red or green square points. It is observed that the ICE estimated from other body locations are marginally delayed when compared to the ankle. (b) The CWT coefficients of the composite acceleration signal collected from the wrist during standing and walking with successive movements of no arm swing, normal arm swing and large arm swing. Only positive-valued coefficients are shown. (For interpretation of the references to color in this figure legend, the reader is referred to the web version of this article.)

large arm swings.

The high robustness of DK-TiFA is due to the adept use of domain knowledge about various body movements which can be easily extended to any body location and guide the signal analysis procedure. This is contrary to purely data-driven techniques that are often dependent on thresholds and tuning parameters and are unable to adapt to new sensor placements or different protocols [23]. Though non-parametric tests such as KS and MWU tests can be effectively applied to assess the accuracy of a method, the test results are dependent on the sample size and chosen level of significance which influences power of the test; thus making it difficult to make objective assessments for very small datasets, especially without any XREF. Further investigation is required to extend the methodology to estimate Final Contact (FC) or toe-off events from any location as it enables the computation of further gait parameters. However, this is much more challenging as an accelerometer positioned at upper body parts captures much lesser of the FC forces as compared to the combination of IC and the periodic forces generated due to the local movement of the body part during gait. Furthermore, there is an overlap between the IC of one foot and the FC of the other during double support. These factors not only make it very difficult to discern the frequency of FC from other periodic motions in the CWT of the acceleration signal but also correctly attribute the estimated event to either the right or left leg automatically. This is further compounded by the poor frequency resolution of the CWT in the finer scales. Additionally, future work is required to adapt DK-TiFA to pathological gait.

This paper presents a novel methodology that incorporates domain knowledge about fundamental spectral relationships present between co-ordinated body movements during normal gait, into time-frequency analysis. The DK-TiFA methodology is demonstrated to achieve high accuracy and robustness for estimating ICE from accelerometers positioned at various body locations and data consisting of different accelerometer specifications, varying gait speeds and different environments.

Conflict of interest

There are no conflicts of interest.

Acknowledgement

This study was supported in part by the Knowledge Foundation, Sweden and Promobilia Foundation, Sweden.

References

[1] A.H. Snijders, B.P. van de Warrenburg, N. Giladi, B.R. Bloem, Neurological gait disorders in elderly people: clinical approach and classification, Lancet Neurol. 6 (1) (2007) 63–74.
[2] T. IJmker, C. Lamoth, Gait and cognition: the relationship between gait stability and variability with executive function in persons with and without dementia, Gait Posture 35 (1) (2012) 126–130.
[3] T.T. Ngo, Y. Makihara, H. Nagahara, Y. Mukaigawa, Y. Yagi, The largest inertial sensor-based gait database and performance evaluation of gait-based personal authentication, Pattern Recognit. 47 (1) (2014) 228–237.
[4] J. Rueterbories, E.G. Spaich, B. Larsen, O.K. Andersen, Methods for gait event detection and analysis in ambulatory systems, Med. Eng. Phys. 32 (6) (2010) 545–552.
[5] J. Rueterbories, E.G. Spaich, O.K. Andersen, Gait event detection for use in FES rehabilitation by radial and tangential foot accelerations, Med. Eng. Phys. 36 (4) (2014) 502–508.
[6] J.M. Jasiewicz, J.H. Allum, J.W. Middleton, A. Barriskill, P. Condie, B. Purcell, R.C.T. Li, Gait event detection using linear accelerometers or angular velocity transducers in able-bodied and spinal-cord injured individuals, Gait Posture 24 (4) (2006) 502–509.
[7] S. Khandelwal, N. Wickström, Gait event detection in real-world environment for

long-term applications: incorporating domain knowledge into time-frequency analysis, IEEE Trans. Neural Syst. Rehabil. Eng. 24 (12) (2016) 1363–1372.
[8] J. McCamley, M. Donati, E. Grimpampi, C. Mazzà, An enhanced estimate of initial contact and final contact instants of time using lower trunk inertial sensor data, Gait Posture 36 (2) (2012) 316–318.
[9] W. Zijlstra, A.L. Hof, Assessment of spatio-temporal gait parameters from trunk accelerations during human walking, Gait Posture 18 (2) (2003) 1–10.
[10] R.C. González, A.M. López, J. Rodriguez-Uría, D. Álvarez, J.C. Alvarez, Real-time gait event detection for normal subjects from lower trunk accelerations, Gait Posture 31 (3) (2010) 322–325.
[11] M. Yoneyama, Y. Kurihara, K. Watanabe, H. Mitoma, Accelerometry-based gait analysis and its application to Parkinson's disease assessment – Part 1: Detection of stride event, IEEE Trans. Neural Syst. Rehabil. Eng. 22 (3) (2014) 613–622.
[12] C. Lützner, H. Voigt, I. Roeder, S. Kirschner, J. Lützner, Placement makes a difference: accuracy of an accelerometer in measuring step number and stair climbing, Gait Posture 39 (4) (2014) 1126–1132.
[13] S.D. Din, A. Hickey, N. Hurwitz, J.C. Mathers, L. Rochester, A. Godfrey, Measuring gait with an accelerometer-based wearable: influence of device location, testing protocol and age, Physiol. Meas. 37 (10) (2016) 1785.
[14] S.M. Rispens, M. Pijnappels, K.S. van Schooten, P.J. Beek, A. Daffertshofer, J.H. van Dieën, Consistency of gait characteristics as determined from acceleration data collected at different trunk locations, Gait Posture 40 (1) (2014) 187–192.
[15] J.J. Kavanagh, H.B. Menz, Accelerometry: a technique for quantifying movement patterns during walking, Gait Posture 28 (1) (2008) 1–15.
[16] P. Addison, J. Walker, R. Guido, Time-frequency analysis of biosignals, IEEE Eng. Med. Biol. Mag. 28 (5) (2009) 14–29.
[17] C. Torrence, G.P. Compo, A practical guide to wavelet analysis, Bull. Am. Meteorol. Soc. 79 (1) (1998) 61–78.
[18] J. Lilly, S. Olhede, Higher-order properties of analytic wavelets, IEEE Trans. Signal Process. 57 (1) (2009) 146–160.
[19] V.T. Inman, Human locomotion, Can. Med. Assoc. J. 94 (20) (1966) 1047–1054.
[20] T. Oberg, A. Karsznia, Basic gait parameters: reference data for normal subjects, 10–79 years of age, J. Rehabil. Res. Dev. 30 (2) (1993) 210.
[21] M. Farge, Wavelet transforms and their applications to turbulence, Ann. Rev. Fluid Mech. 24 (1) (1992) 395–458.
[22] B.K. Alsberg, A.M. Woodward, D.B. Kell, An introduction to wavelet transforms for chemometricians: a time-frequency approach, Chemom. Intell. Lab. Syst. 37 (2) (1997) 215–239.
[23] S. Khandelwal, N. Wickström, Evaluation of the performance of accelerometer-based gait event detection algorithms in different real-world scenarios using the MAREA gait database, Gait Posture 51 (2017) 84–90.
[24] Y. Zhang, G. Pan, K. Jia, M. Lu, Y. Wang, Z. Wu, Accelerometer-based gait recognition by sparse representation of signature points with clusters, IEEE Trans. Cybern. 45 (9) (2015) 1864–1875.
[25] H. Leutheuser, D. Schuldhaus, B.M. Eskofier, Hierarchical, multi-sensor based classification of daily life activities: comparison with state-of-the-art algorithms using a benchmark dataset, PLOS ONE 8 (10) (2013) 1–11.
[26] D.R. Cox, D.V. Hinkley, Theoretical Statistics, Chapman and Hall London, 1974.
[27] J.M. Bland, D. Altman, Statistical methods for assessing agreement between two methods of clinical measurement, Lancet 327 (8476) (1986) 307–310.
[28] J. Park, Synthesis of natural arm swing motion in human bipedal walking, J. Biomech. 41 (7) (2008) 1417–1426.